

Supplemental Information

# High-throughput computational screening for solid-state Li-ion conductors

Leonid Kahle,\* Aris Marcolongo,‡ and Nicola Marzari

## 1 Bandgaps

In our screening funnel, we calculate the band gap at the experimental volume. Here, using data for 717 Li-containing structures, we estimate how the bandgap at the relaxed volume  $V_{rel}$  correlates with the band gap at the experimental volume  $V_{exp}$ . We note that these structures are not necessarily the same as in the manuscript: since we did not relax metallic structures in the screening study, we would not be able to compare the bandgaps of metallic or small-bandgap compounds. Therefore, we took the data from another screening study that uses the same protocols as our work, including ICSD and COD entries. On the right (Fig. S1) we plot the PBE bandgap in the experimental configuration (before the variable-cell relaxation) against the PBE bandgap in the variable-cell relaxed configuration. In the same plot, the color encodes the relative change of volume during relaxation given by  $\frac{V_{rel}}{V_{exp}}$ . We observe very good correlation in those two values, indicating that we can take the bandgap in the experimental configuration as an estimate for the bandgap at the variable-cell relaxed configuration. There is no evidence that the relative volume change, indicated by the color, affects the quality of the estimate in any significant way. We also observe that a few structures with no bandgap at the experimental configuration display a bandgap at the variable-cell relaxed configuration, while the reverse does not happen. Therefore, we are confident that no structure that was estimated as an insulator turned metallic during the relaxation.

## 2 Estimate of the diffusion coefficient

In the following, we explain our method to extract diffusion coefficients from molecular dynamics simulations. In the literature, the following expression is most often employed (c.f. Eq (2) in the main manuscript):

$$D_{tr}^{\text{Li}} = \lim_{t \rightarrow \infty} \frac{1}{6t} \langle \text{MSD}(t) \rangle_{NVT} = \lim_{t \rightarrow \infty} \frac{1}{6t} \frac{1}{N_{\text{Li}}} \sum_I \left\langle |\mathbf{R}_I(t + \tau) - \mathbf{R}_I(\tau)|^2 \right\rangle_{\tau}, \quad (1)$$

where  $\mathbf{R}_I$  are the atomic positions and  $\langle \dots \rangle_{NVT}$  indicates the average over the canonical ensemble sampled ergodically by the molecular dynamics simulation, replacing thus the ensemble average with a time average  $\langle \dots \rangle_{\tau}$ . According to Eq. (1), one should calculate the MSD of the configuration at time  $t + \tau$  from a reference configuration at time  $\tau$  and divide by the time  $t$  that passed. However, this has the disadvantage that periodic atomic vibrations due to thermal motion are also contributing. By taking  $t \rightarrow \infty$ , it can be ensured that the effect of atomic vibrations becomes negligible. However, another approach is to estimate the derivative of  $\text{MSD}(t)$  with respect to  $t$ :

$$D_{tr}^{\text{Li}} = \lim_{t' \rightarrow \infty} \frac{1}{6} \frac{d}{dt} \langle \text{MSD}(t) \rangle_{NVT} \Big|_{t=t'}, \quad (2)$$

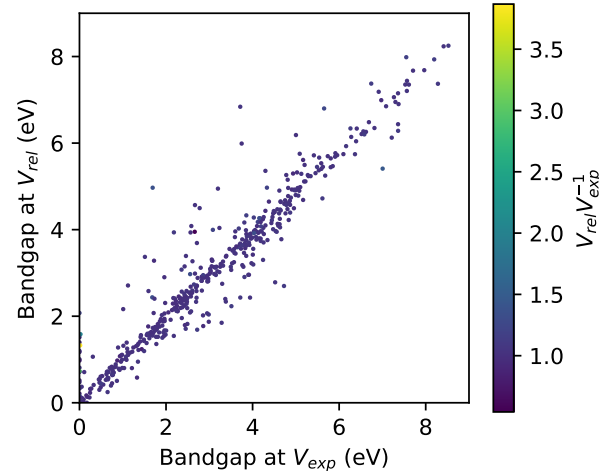


**Fig. S1** We plot the bandgap at  $V_{exp}$  on the  $x$ -axis against the bandgap at  $V_{rel}$  on the  $y$ -axis, with color encoding the relative volume change.

We also observe that a few structures with no bandgap at the experimental configuration display a bandgap at the variable-cell relaxed configuration, while the reverse does not happen. Therefore, we are confident that no structure that was estimated as an insulator turned metallic during the relaxation.

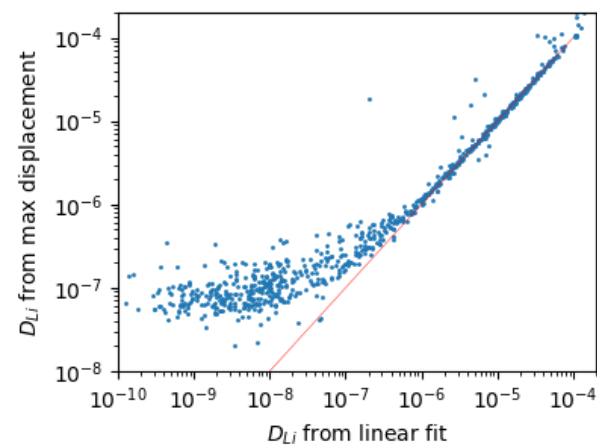


**Fig. S2** We plot the diffusion coefficient estimated from the total MSD at 50 ps on the  $y$ -axis against the diffusion coefficients estimate from the slope of the MSD between 8 ps and 10 ps.

Theory and Simulation of Materials (THEOS), and National Centre for Computational Design and Discovery of Novel Materials (MARVEL), École Polytechnique Fédérale de Lausanne, CH-1015 Lausanne, Switzerland. E-mail: leonid.kahle@epfl.ch

‡ Present address: IBM Research GmbH, Zürich Research Laboratory, CH-8803 Rüschlikon, Switzerland

which can be evaluated numerically by fitting a line to a segment around  $t'$ . Eq. (2) has the advantage, compared to Eq. (1), that the effect of periodic atomic motion at  $t \rightarrow 0$  can be dismissed as long as  $t'$  is in the diffusive regime. For fast diffusion and, equivalently, large times  $t$  where the MSD is taken or its slope fitted, the results should be equivalent. This is shown in Fig. S2, where we calculate the diffusion coefficients of Li in all pinball simulations presented in the main manuscript using Eqs. (1) and (2). For very diffusive systems, the two methods are equivalent, while for non-diffusive systems, the periodic contribution leads to an overestimate of the diffusion when using Eq. (1).

A further question is how small  $t$  can become in order to be in the diffusive regime for the systems of interest. As fitting at small times  $t$  is advantageous to increase the sampling of the MSD,  $t$  should ideally be as small as possible while giving the same results as larger times  $t$ . We take all simulations using the pinball model that showed a Li-ion diffusion above  $D_{Li} = 10^{-8} \text{ cm}^2 \text{ s}^{-1}$ , estimated as presented in the manuscript. Since we are not interested in structures with lower diffusion coefficients and therefore we do not need to consider the accuracy for those. To test how the slope of the MSD converges, we extract the slope at different times and compare these to the slope at 40 ps (see Fig. S3). If the slope is not in the diffusive regime and still capturing ballistic or cage motion, the diffusion coefficient should be overpredicted, as it happens if we fit the MSD at 5 ps (top left corner). However, the number of such false positives for diffusivity drops significantly when fitting at 10 ps (top right), which therefore is judged as an optimal choice, offering high statistical accuracy while lying in the diffusive regime for fast ionic conductors.

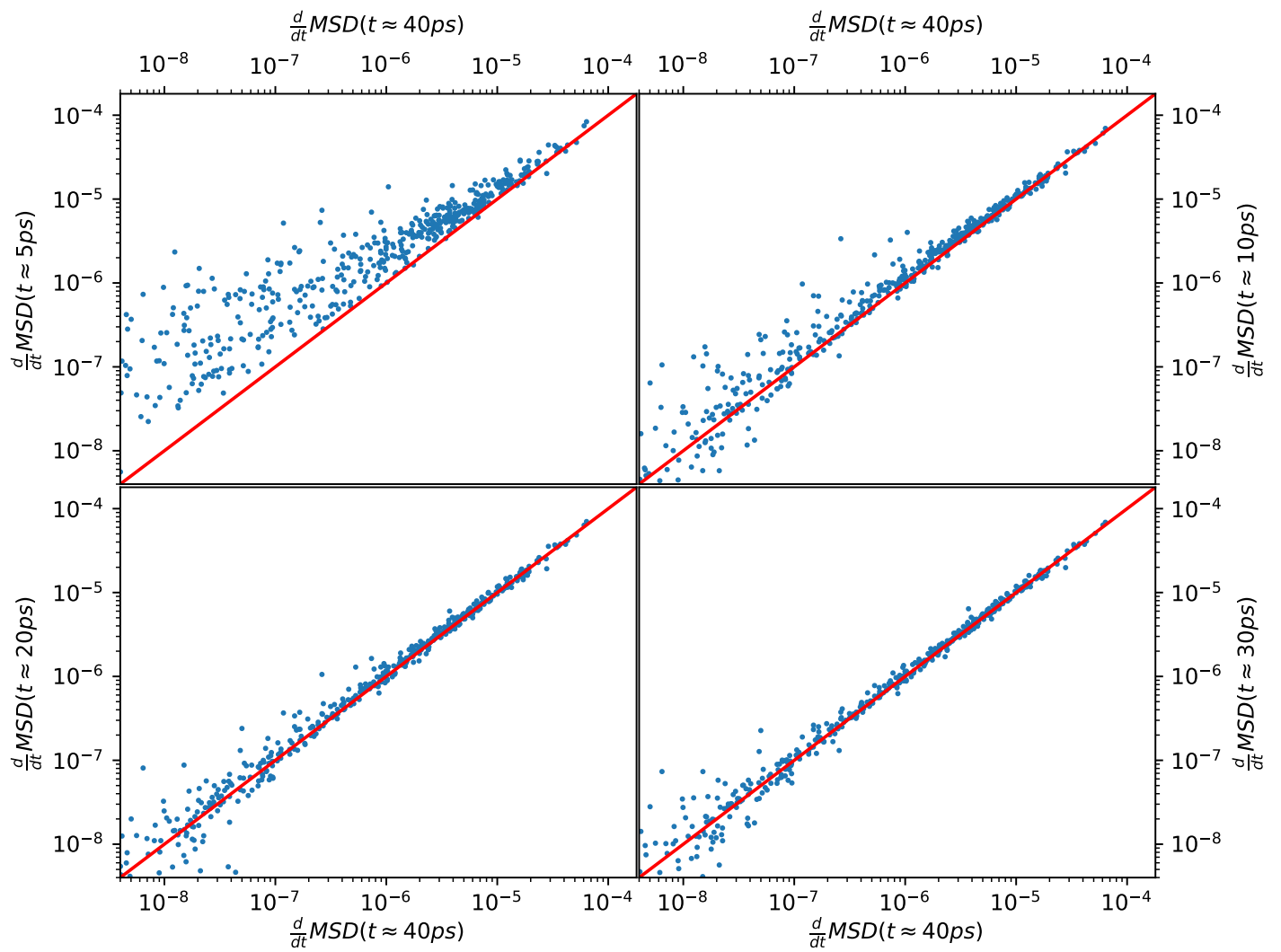


**Fig. S3** We plot the estimate from the slope of the MSD at  $t' = 40$  ps against the estimates at 5 ps, 10 ps, 20 ps, and 30 ps in the top left, top right, bottom left, and bottom right corner, respectively.

### 3 Fast-ion conductors (group A)

In the following, we plot the MSD for every species for the materials studied with FPMD (groups A, B, and C). The MSD is calculated as described in Secs. 2.5 and 2.6 of the manuscript. We split the trajectory into independent blocks and calculate for each the MSD (thin solid lines in subsequent blocks). The diffusion coefficient is extracted using Eq. (2), but with longer times than for the pinball simulations (at least 20 ps). A line is fitted to that regime using linear regression for every block; these are shown as thin dashed lines in the subsequent figures. The resulting diffusion coefficient is given in the legend, with the mean and standard error obtained from the independent estimates of the diffusion in every block.

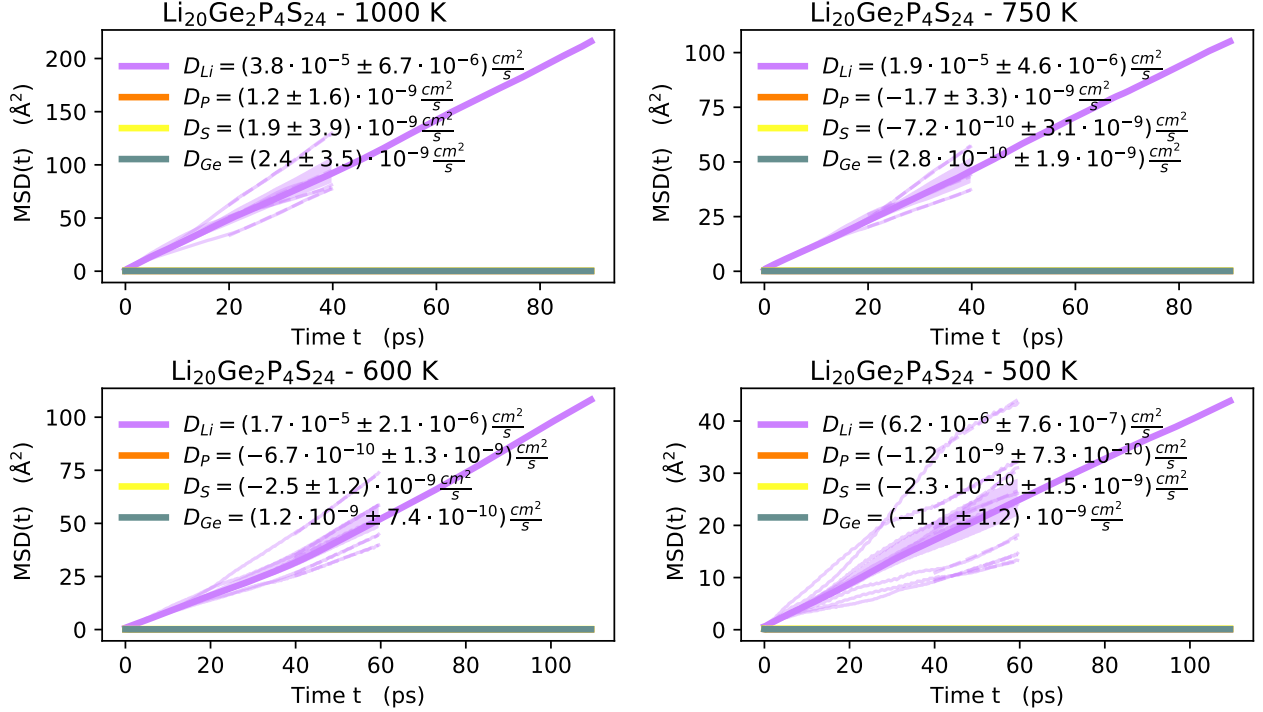


**Fig. S4** MSD(t) for  $\text{Li}_{20}\text{Ge}_2\text{P}_4\text{S}_{24}$  from FPMD for all temperatures studied.

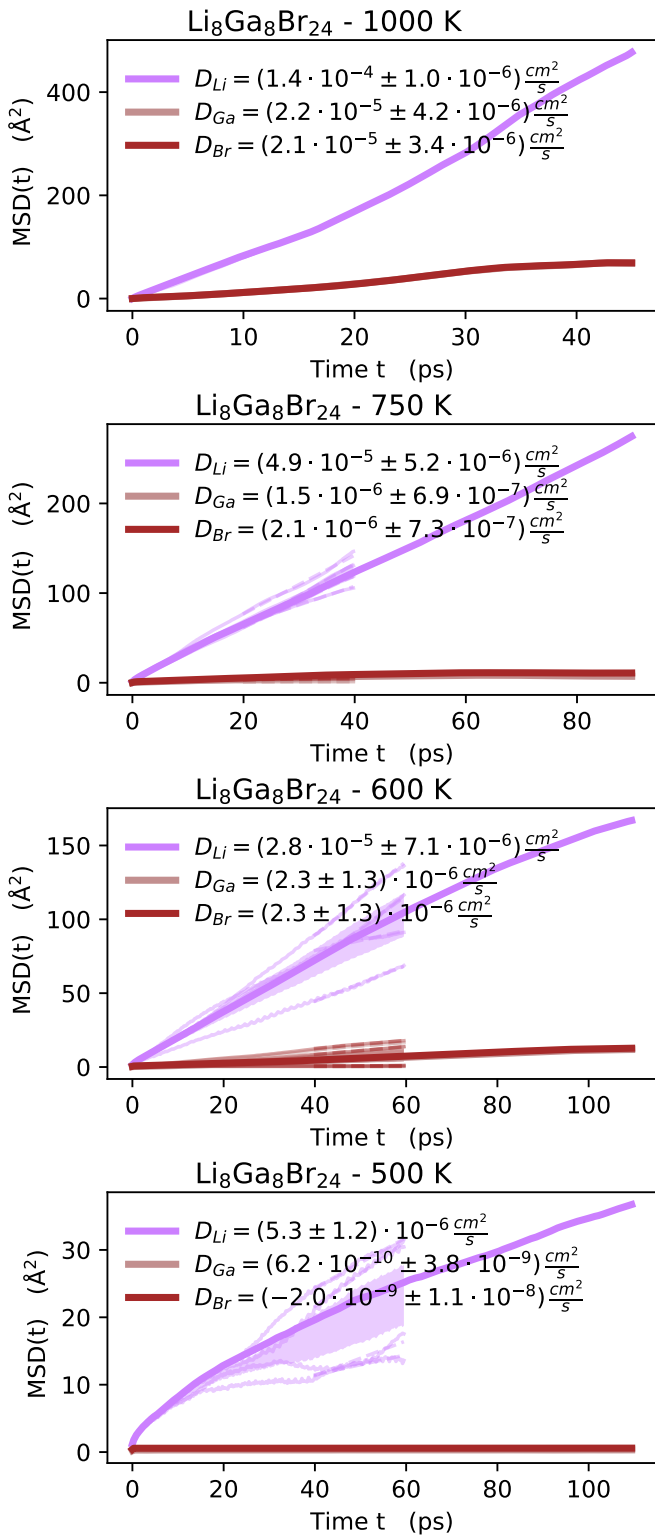


**Fig. S5** MSD(t) for Li<sub>8</sub>Ga<sub>8</sub>Br<sub>24</sub> from FPMD for all temperatures studied.

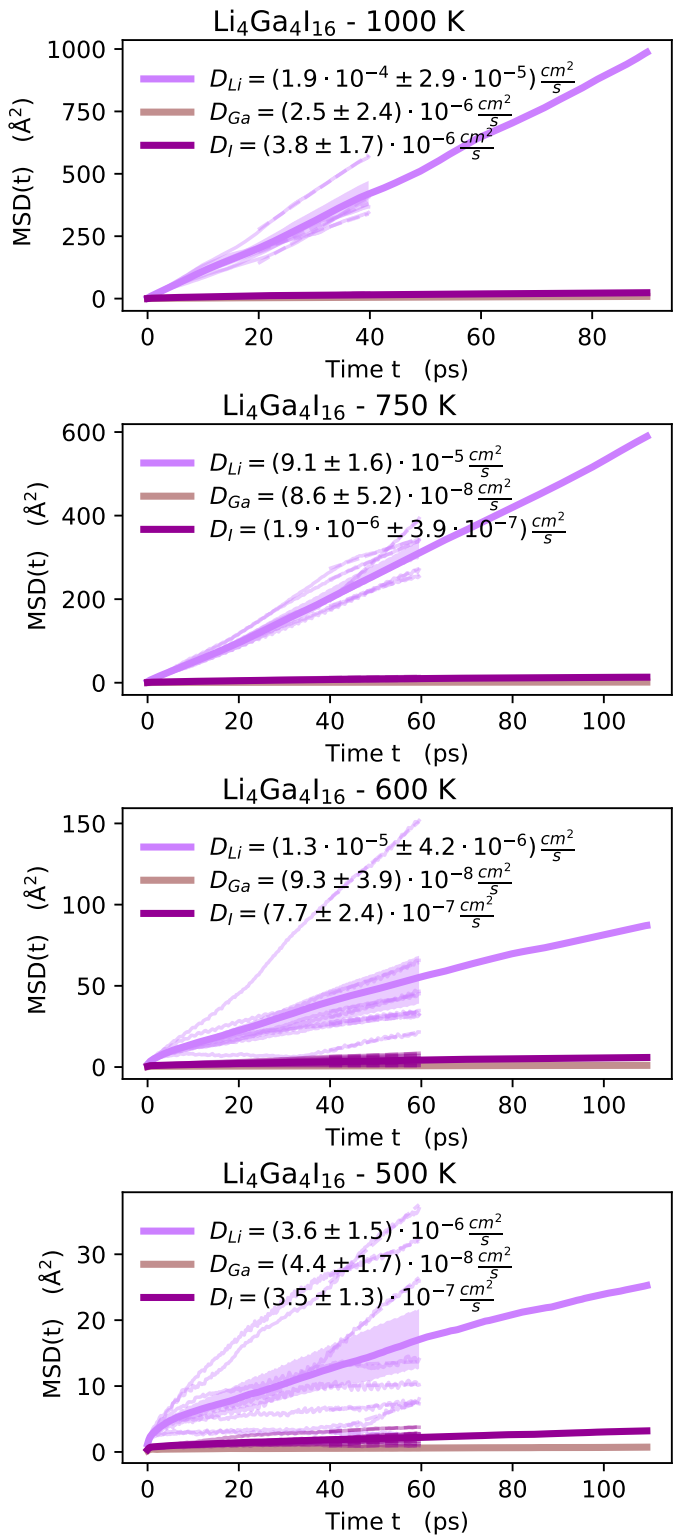


**Fig. S6** MSD(t) for Li<sub>4</sub>Ga<sub>4</sub>I<sub>16</sub> from FPMD for all temperatures studied.

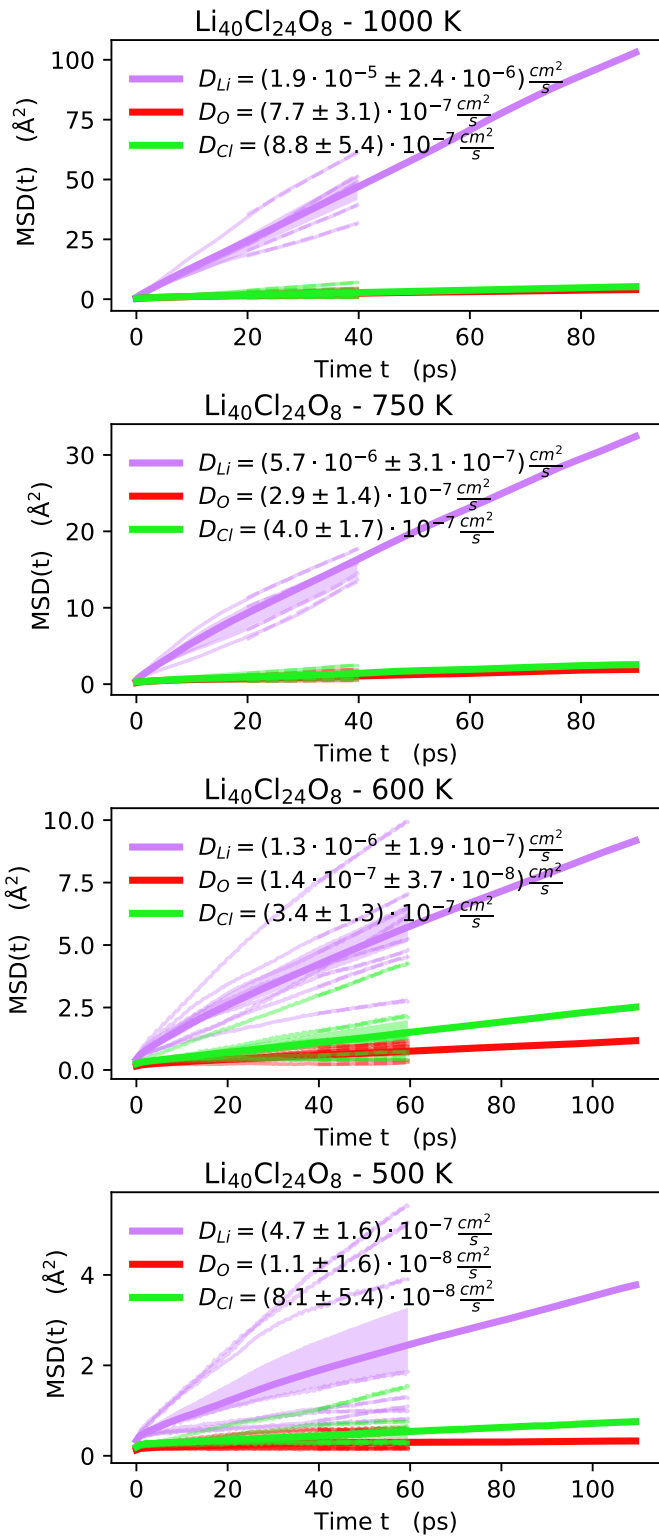


**Fig. S7** MSD(t) for Li<sub>40</sub>Cl<sub>24</sub>O<sub>8</sub> from FPMD for all temperatures studied.

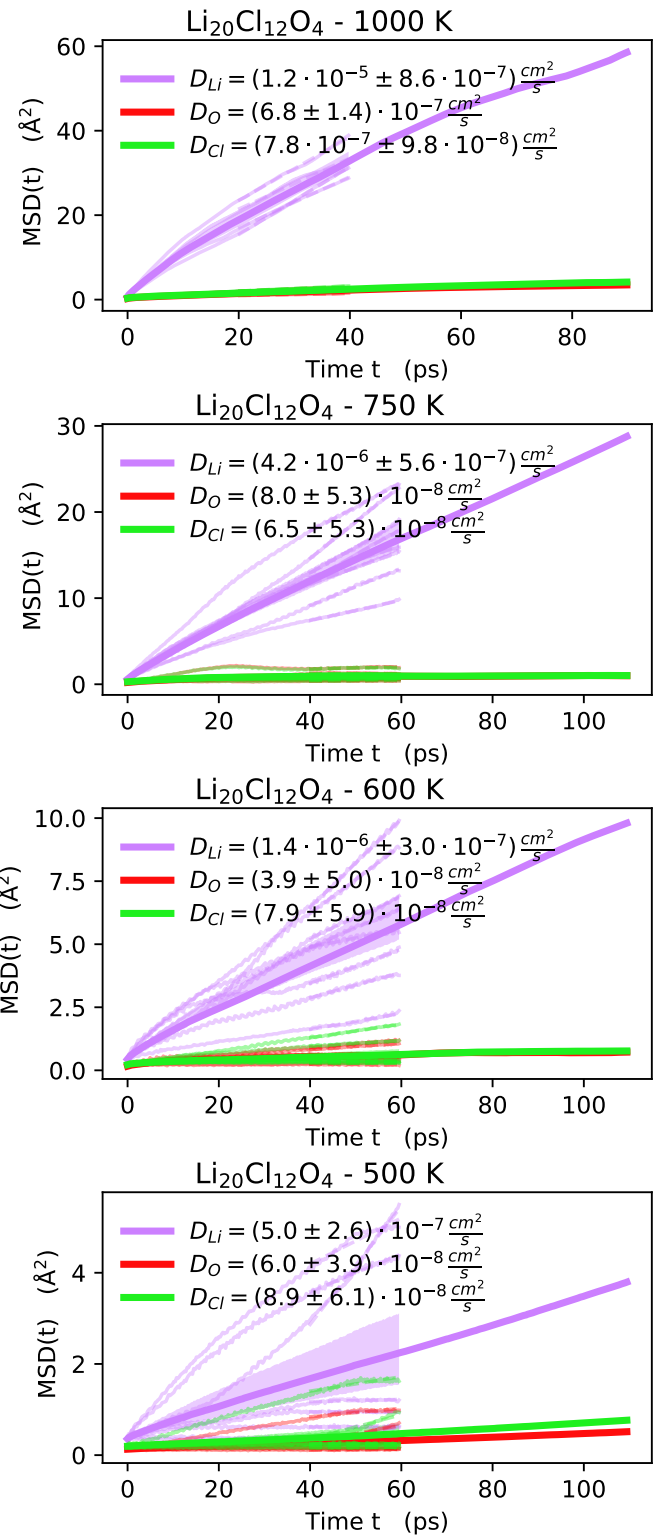


**Fig. S8** MSD(t) for Li<sub>20</sub>Cl<sub>12</sub>O<sub>4</sub> from FPMD for all temperatures studied.

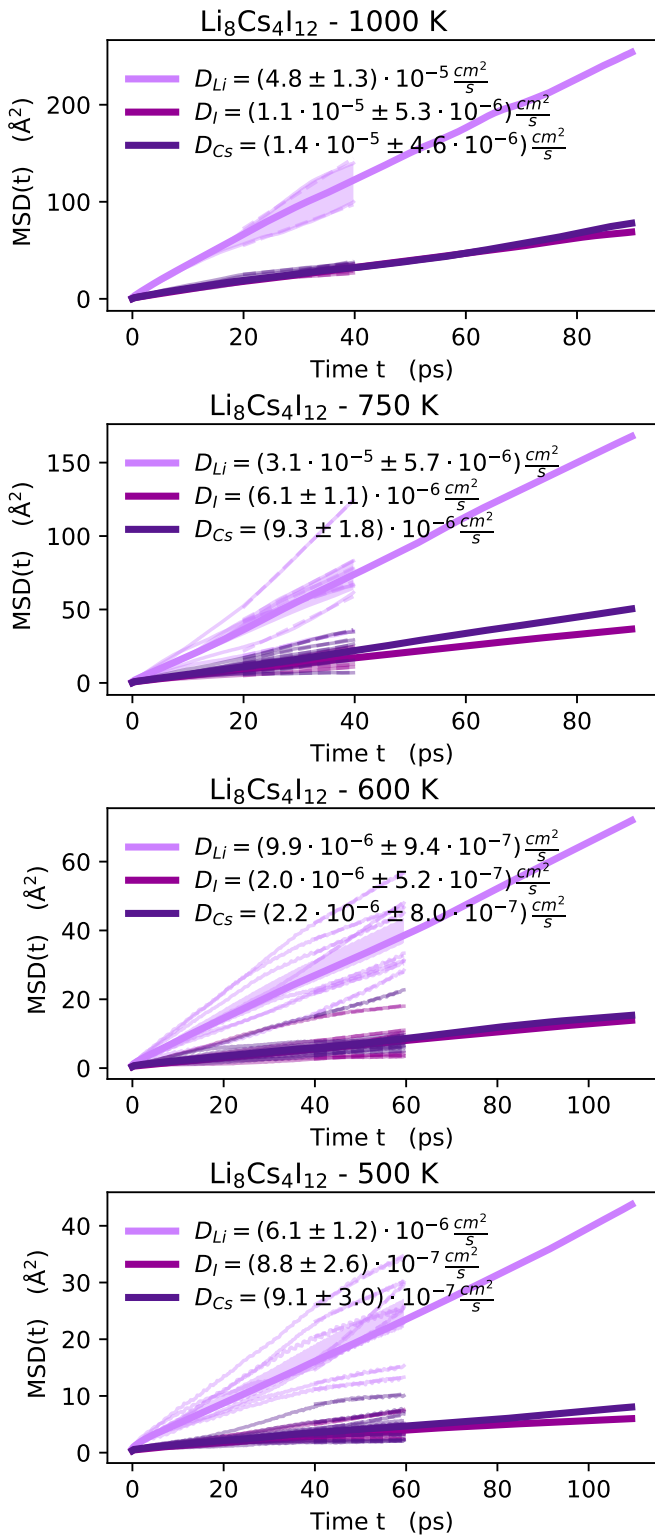


**Fig. S9** MSD(t) for Li<sub>8</sub>Cs<sub>4</sub>I<sub>12</sub> from FPMD for all temperatures studied.

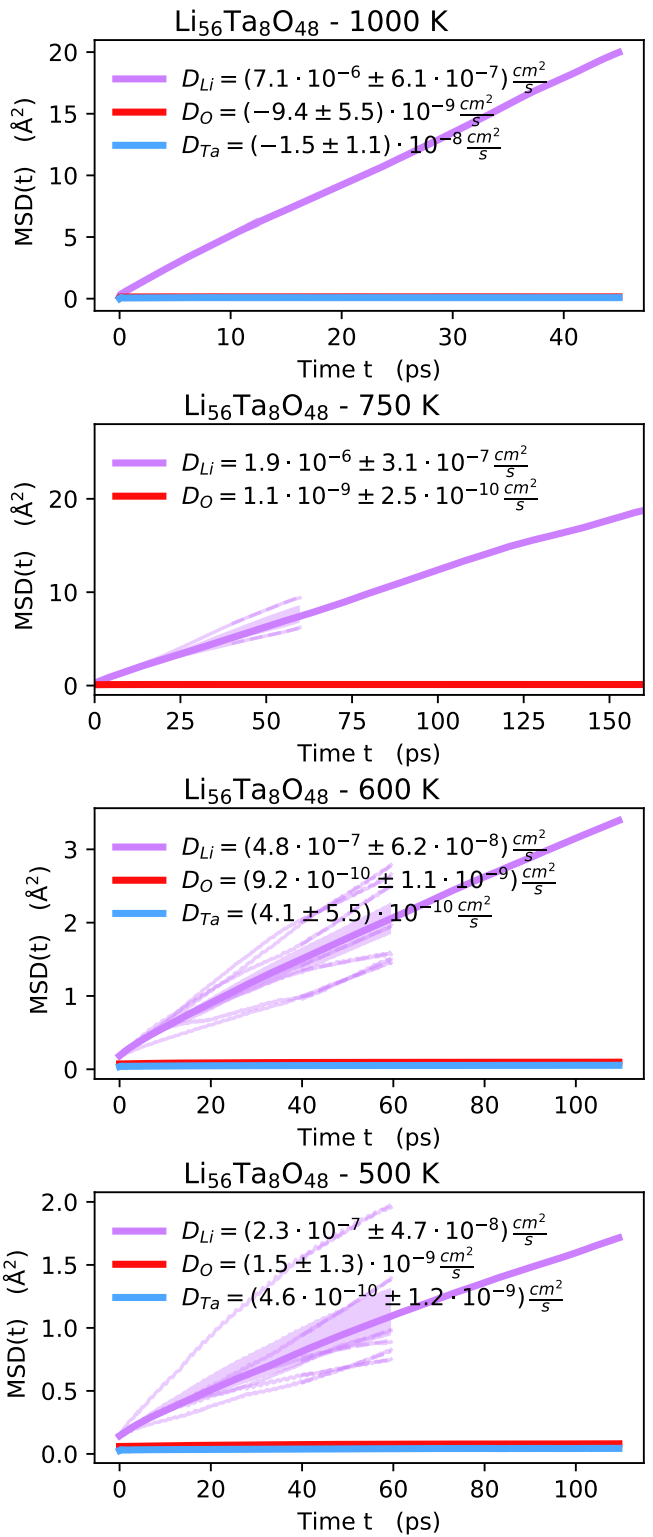


**Fig. S10** MSD(t) for Li<sub>56</sub>Ta<sub>8</sub>O<sub>48</sub> from FPMD for all temperatures studied.

#### 4 Potential fast-ionic conductors (group B)

**Table S1** The structures that are found as potential ionic conductors and studied at different temperatures (500 K – 1000 K). We give the stoichiometric formula, the database and identifier of the repository this structure originates from, the formula of the supercell used, the figure where the mean-square displacement is shown in this supplemental information, and the simulation times at 500 K, 600 K, 750 K, and 1000 K (in ps)

Structure	DB	DB-id	Supercell	Figure	Volume change	Tsim <sub>500</sub>	Tsim <sub>600</sub>	Tsim <sub>750</sub>	Tsim <sub>1000</sub>
Li <sub>4</sub> Re <sub>6</sub> S <sub>11</sub>	COD	1008693	Li <sub>16</sub> Re <sub>24</sub> S <sub>44</sub>	S11	2.6%	87.1	174.3	87.2	290.8
Li <sub>6</sub> P <sub>1</sub> S <sub>5</sub> I <sub>1</sub>	ICSD	421083	Li <sub>48</sub> P <sub>8</sub> S <sub>40</sub> I <sub>8</sub>	S14	2.9%	87.2	87.2	87.2	72.7
Li <sub>2</sub> B <sub>2</sub> S <sub>5</sub>	COD	1510745	Li <sub>8</sub> B <sub>8</sub> S <sub>20</sub>	S20	5.4%	203.4	203.4	348.7	145.4
Li <sub>1</sub> Ta <sub>1</sub> Ge <sub>1</sub> O <sub>5</sub>	ICSD	280992	Li <sub>4</sub> Ta <sub>4</sub> Ge <sub>4</sub> O <sub>20</sub>	S16	3.5%	145.3	523.0	319.6	218.1
Li <sub>2</sub> S <sub>2</sub> O <sub>7</sub>	ICSD	188009	Li <sub>16</sub> S <sub>16</sub> O <sub>56</sub>	S25	5.4%	232.4	145.3	174.3	203.6
Li <sub>1</sub> I <sub>1</sub> O <sub>3</sub>	ICSD	20032	Li <sub>16</sub> I <sub>16</sub> O <sub>48</sub>	S19	15.3%	145.3	726.4	523.0	72.7
Li <sub>1</sub> Al <sub>1</sub> Si <sub>1</sub> O <sub>4</sub>	COD	9000368	Li <sub>12</sub> Al <sub>12</sub> Si <sub>12</sub> O <sub>48</sub>	S17	3.6%	145.3	697.3	290.6	218.1
Li <sub>5</sub> B <sub>1</sub> S <sub>4</sub> O <sub>16</sub>	ICSD	428002	Li <sub>20</sub> B <sub>4</sub> S <sub>16</sub> O <sub>64</sub>	S15	6.3%	610.2	610.2	610.2	218.1
Li <sub>2</sub> Mg <sub>2</sub> S <sub>3</sub> O <sub>12</sub>	COD	2020217	Li <sub>8</sub> Mg <sub>8</sub> S <sub>12</sub> O <sub>48</sub>	S18	4.1%	145.3	726.4	406.8	218.1
Li <sub>1</sub> Ti <sub>1</sub> P <sub>1</sub> O <sub>5</sub>	ICSD	39761	Li <sub>16</sub> Ti <sub>16</sub> P <sub>16</sub> O <sub>80</sub>	S13	5.8%	232.4	232.4	261.5	218.1
Li <sub>3</sub> Cs <sub>1</sub> Cl <sub>4</sub>	ICSD	245975	Li <sub>24</sub> Cs <sub>8</sub> Cl <sub>32</sub>	S22	1.6%	726.4	726.4	726.4	218.1
Li <sub>6</sub> Y(BO <sub>3</sub> ) <sub>3</sub>	COD	1510933	Li <sub>24</sub> Y <sub>4</sub> B <sub>12</sub> O <sub>36</sub>	S21	2.8%	145.3	145.3	726.4	218.1
Li <sub>2</sub> Zn <sub>1</sub> Sn <sub>1</sub> Se <sub>4</sub>	COD	7035178	Li <sub>16</sub> Zn <sub>8</sub> Sn <sub>8</sub> Se <sub>32</sub>	S26	4.2%	145.3	145.3	145.3	218.1
Li <sub>2</sub> Ti <sub>3</sub> O <sub>7</sub>	ICSD	193803	Li <sub>8</sub> Ti <sub>12</sub> O <sub>28</sub>	S29	2.6%	145.3	145.3	145.3	218.1
Rb <sub>1</sub> Li <sub>7</sub> Si <sub>2</sub> O <sub>8</sub>	ICSD	33864	Rb <sub>4</sub> Li <sub>28</sub> Si <sub>8</sub> O <sub>32</sub>	S24	2.8%	145.3	145.3	726.4	218.1
Li <sub>3</sub> Ga <sub>1</sub> F <sub>6</sub>	COD	8101456	Li <sub>18</sub> Ga <sub>6</sub> F <sub>36</sub>	S27	4.8%	145.3	145.3	145.3	218.1
Li <sub>2</sub> In <sub>2</sub> Ge <sub>1</sub> S <sub>6</sub>	COD	4329224	Li <sub>16</sub> In <sub>16</sub> Ge <sub>8</sub> S <sub>48</sub>	S28	5.6%	145.3	261.5	145.3	218.1
Li <sub>1</sub> Mo <sub>1</sub> As <sub>1</sub> O <sub>6</sub>	COD	2014117	Li <sub>8</sub> Mo <sub>8</sub> As <sub>8</sub> O <sub>48</sub>	S30	8.2%	610.2	145.3	174.3	218.1
Li <sub>9</sub> Ga <sub>3</sub> P <sub>8</sub> O <sub>29</sub>	COD	2208797	Li <sub>18</sub> Ga <sub>6</sub> P <sub>16</sub> O <sub>58</sub>	S23	2.1%	145.3	145.3	261.5	218.1

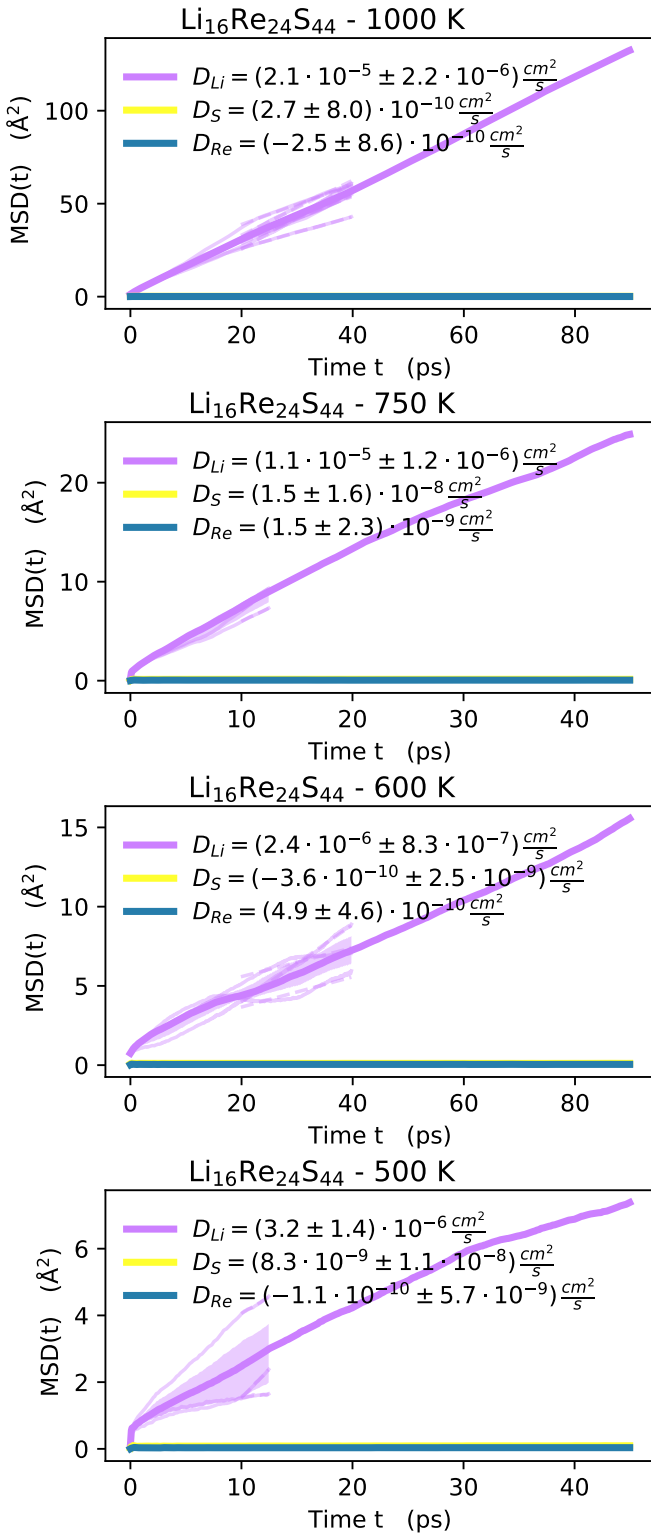


**Fig. S11** MSD(t) for Li<sub>16</sub>Re<sub>24</sub>S<sub>44</sub> from FPMD for all temperatures studied.

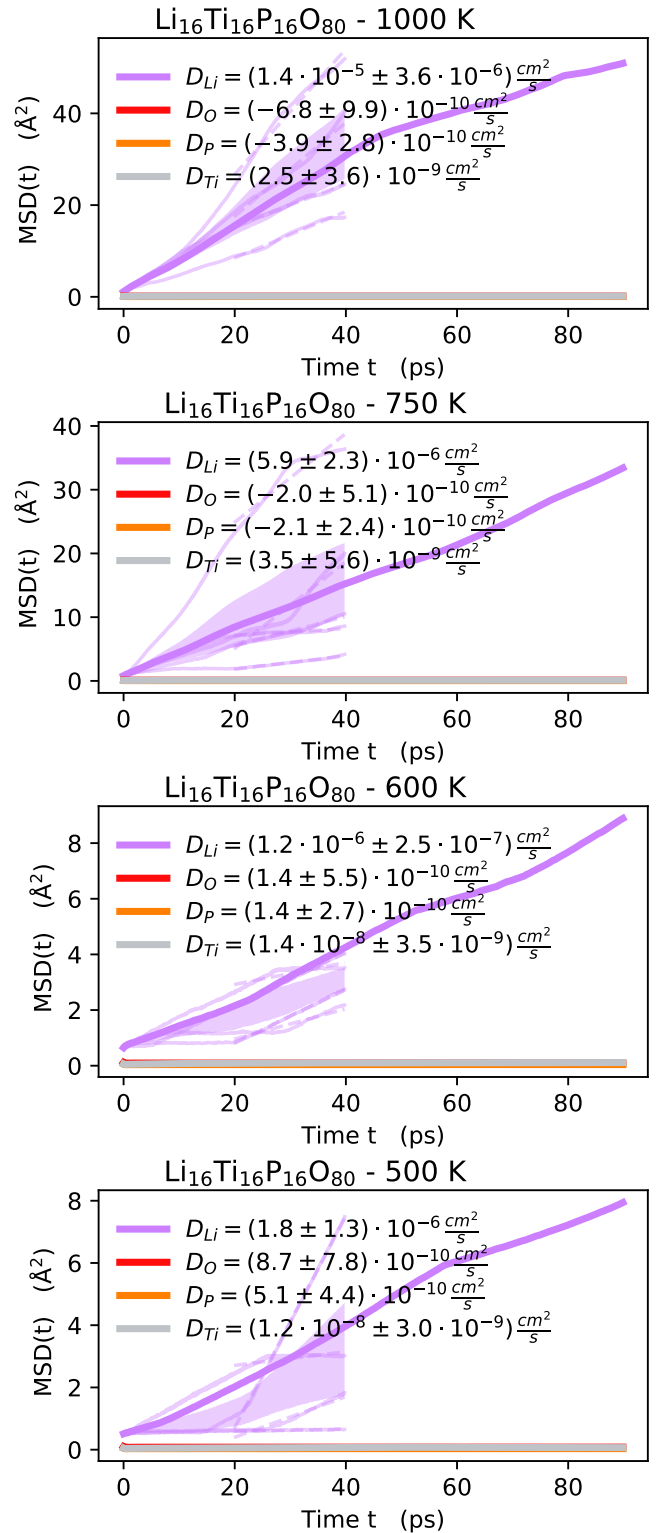


**Fig. S12** MSD(t) for Li<sub>16</sub>Ti<sub>16</sub>P<sub>16</sub>O<sub>80</sub> from FPMD for all temperatures studied.

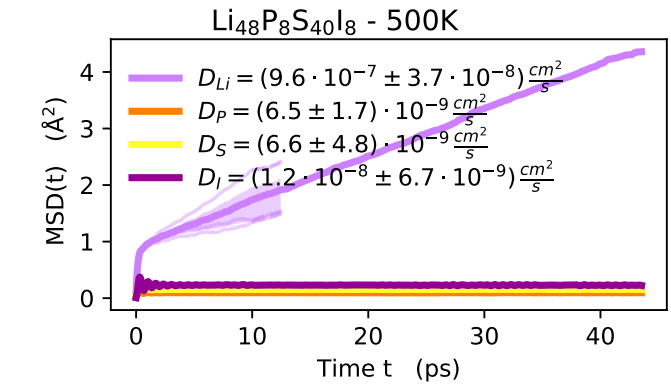
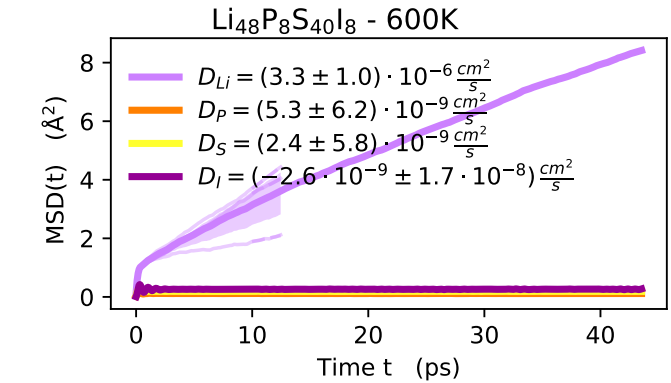
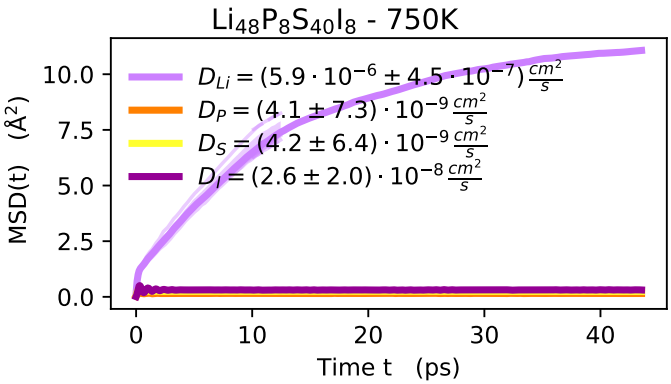
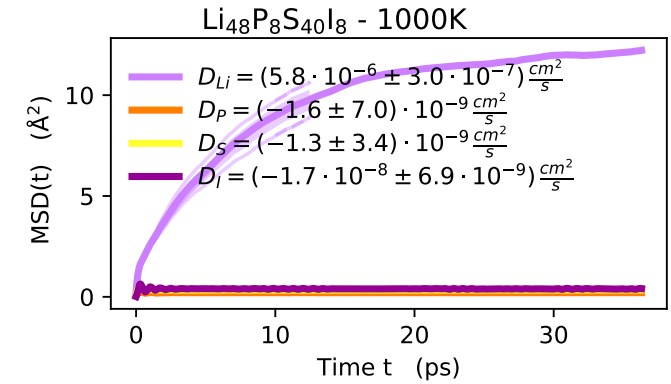
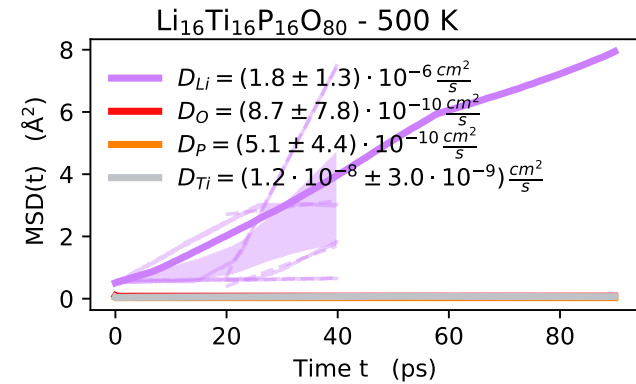
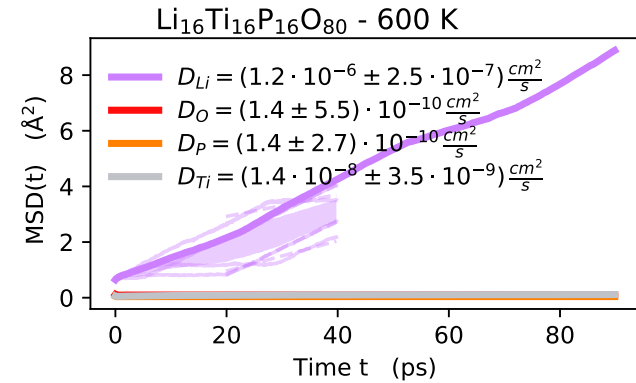
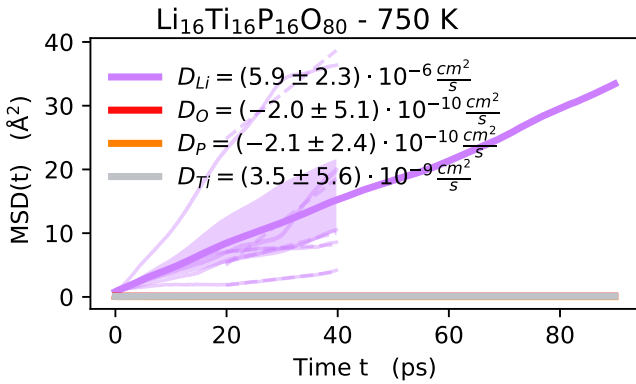
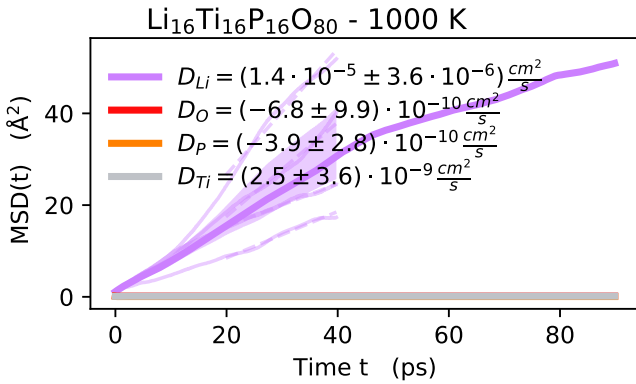


**Fig. S13** MSD(t) for Li<sub>16</sub>Ti<sub>16</sub>P<sub>16</sub>O<sub>80</sub> from FPMD for all temperatures studied.

**Fig. S14** MSD(t) for Li<sub>48</sub>P<sub>8</sub>S<sub>40</sub>I<sub>8</sub> from FPMD for all temperatures studied.

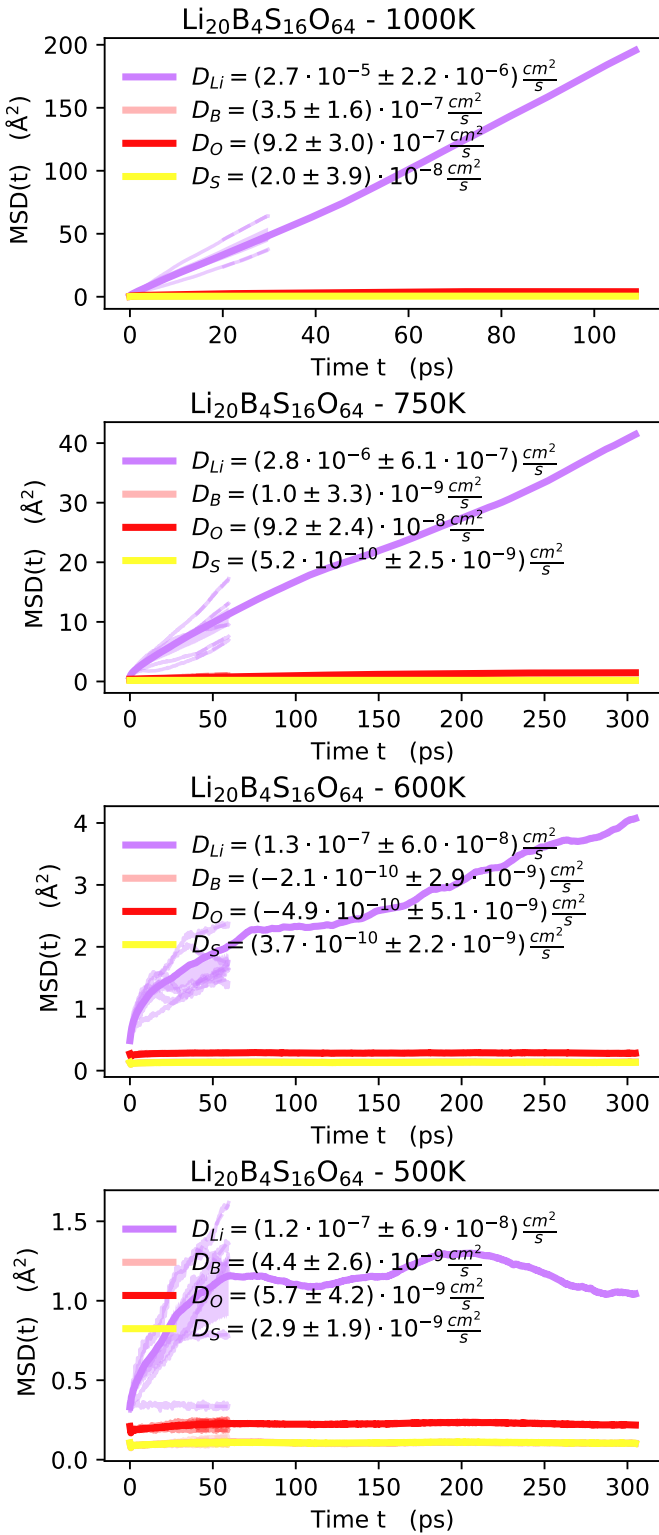


**Fig. S15** MSD(t) for Li<sub>20</sub>B<sub>4</sub>S<sub>16</sub>O<sub>64</sub> from FPMD for all temperatures studied.

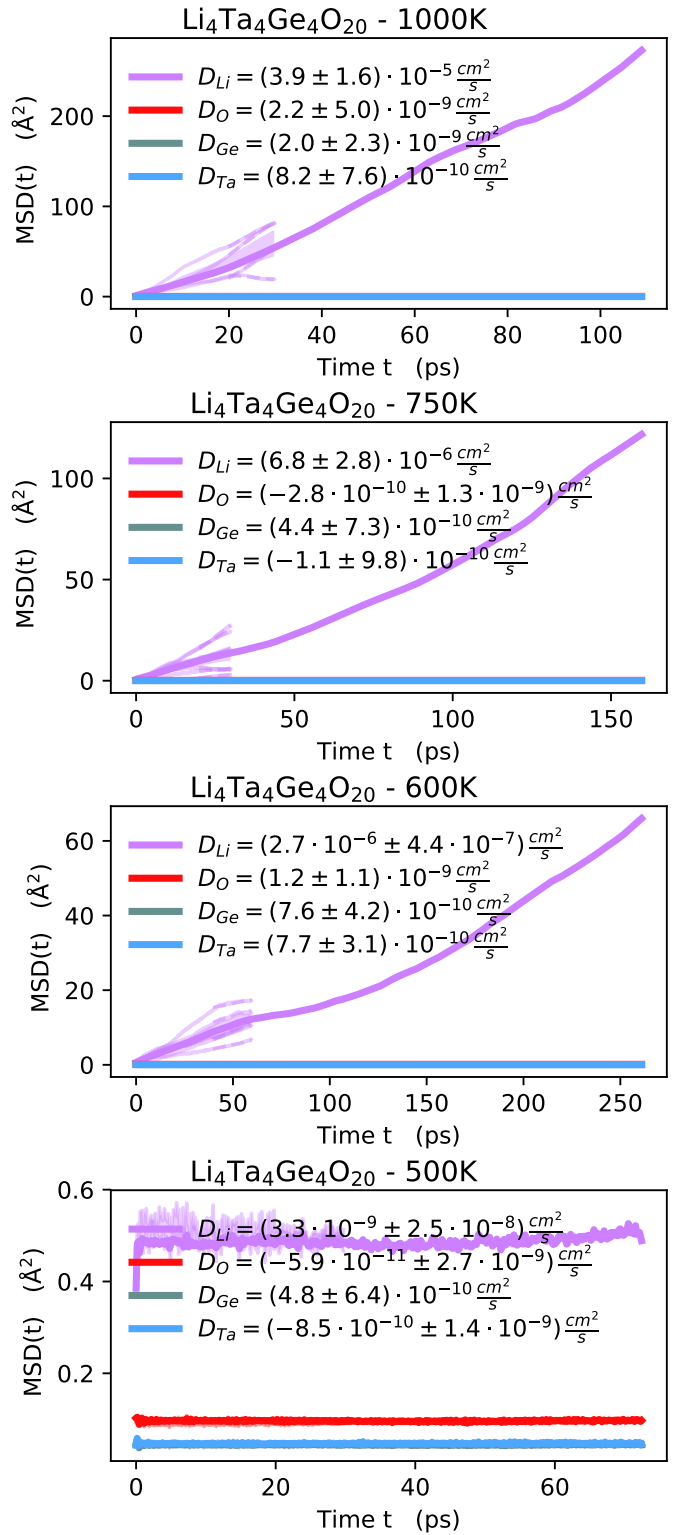


**Fig. S16** MSD(t) for Li<sub>4</sub>Ta<sub>4</sub>Ge<sub>4</sub>O<sub>20</sub> from FPMD for all temperatures studied.

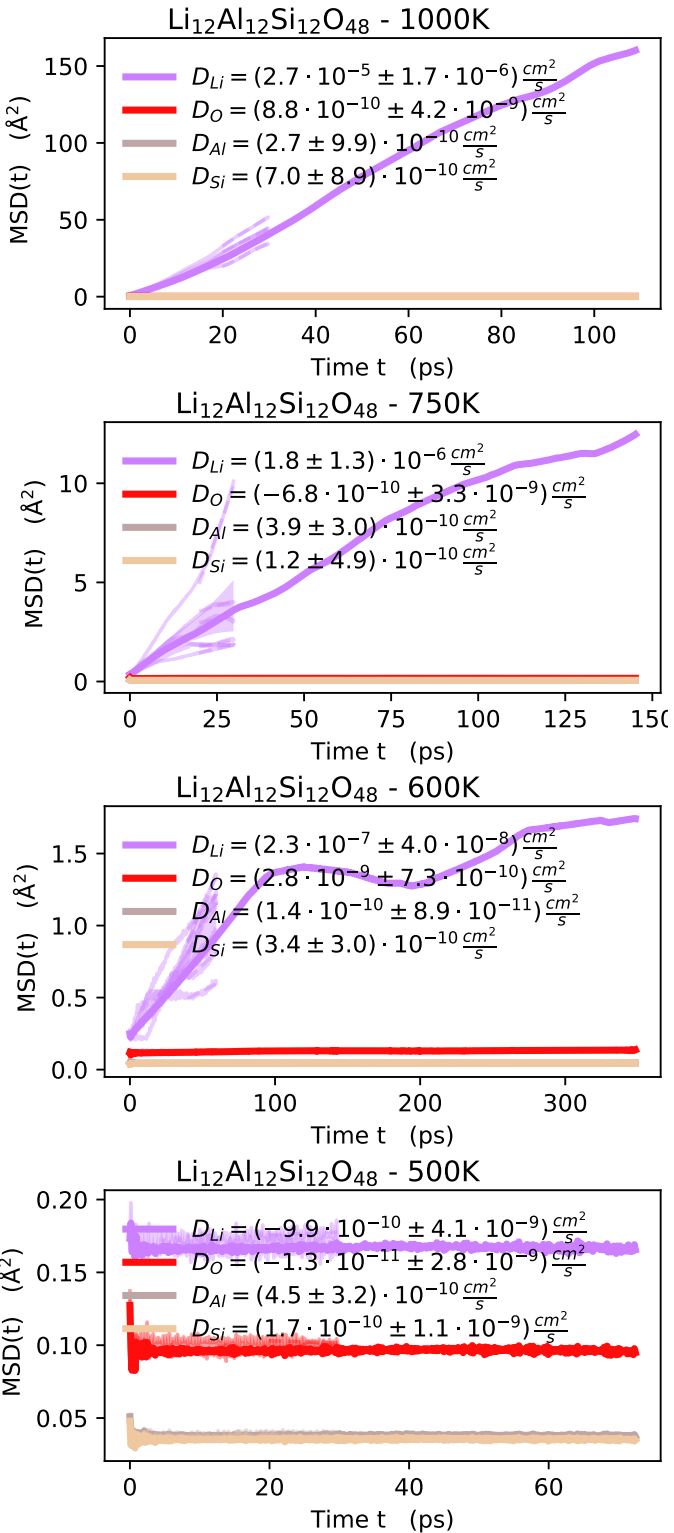


**Fig. S17** MSD(t) for Li<sub>12</sub>Al<sub>12</sub>Si<sub>12</sub>O<sub>48</sub> from FPMD for all temperatures studied.

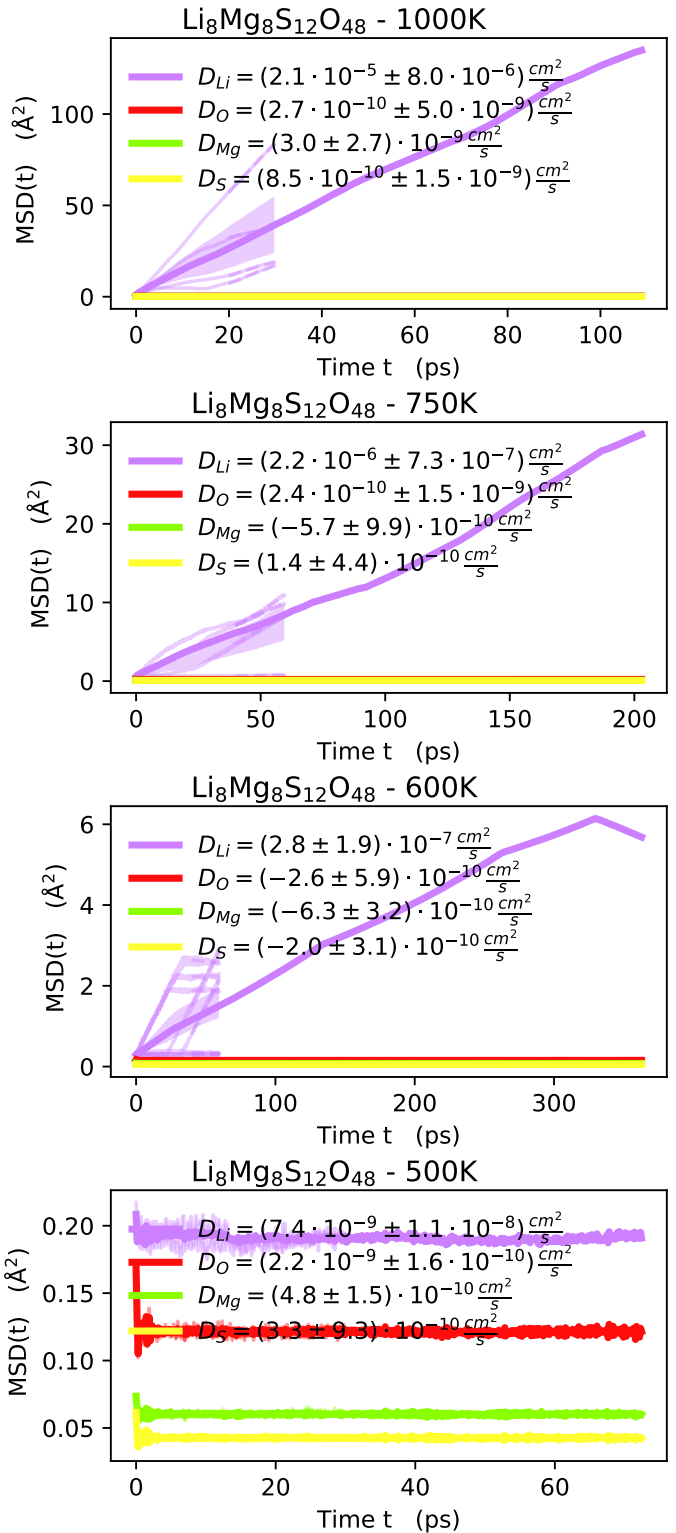


**Fig. S18** MSD(t) for Li<sub>8</sub>Mg<sub>8</sub>S<sub>12</sub>O<sub>48</sub> from FPMD for all temperatures studied.

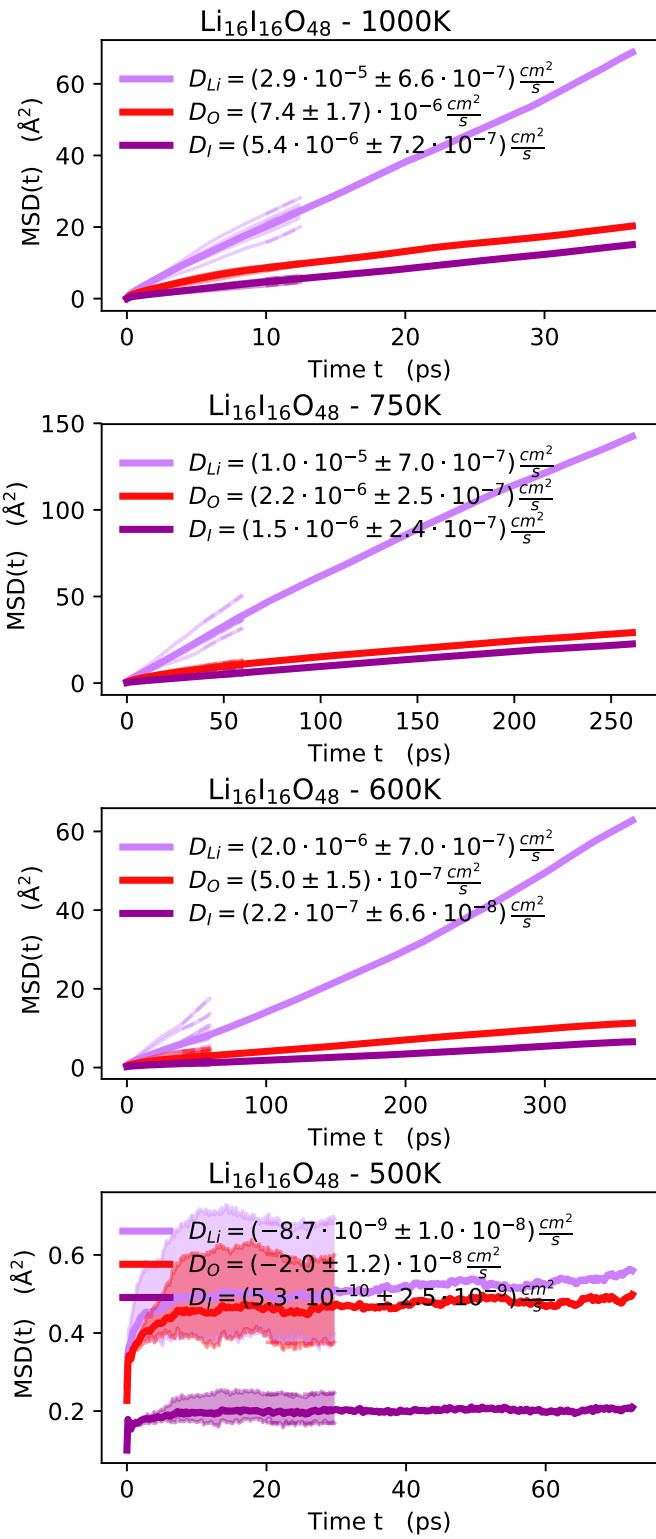


**Fig. S19** MSD(t) for Li<sub>16</sub>I<sub>16</sub>O<sub>48</sub> from FPMD for all temperatures studied.

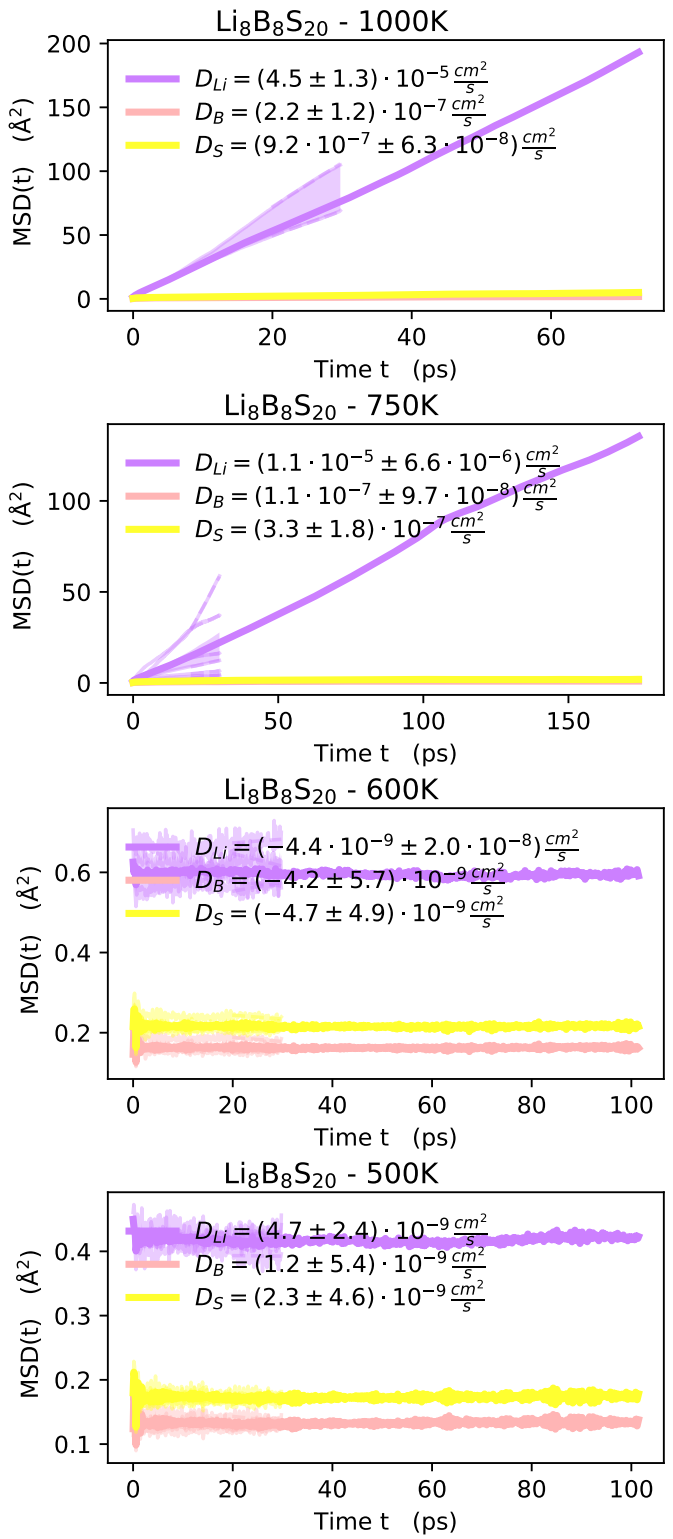


**Fig. S20** MSD(t) for Li<sub>8</sub>B<sub>8</sub>S<sub>20</sub> from FPMD for all temperatures studied.

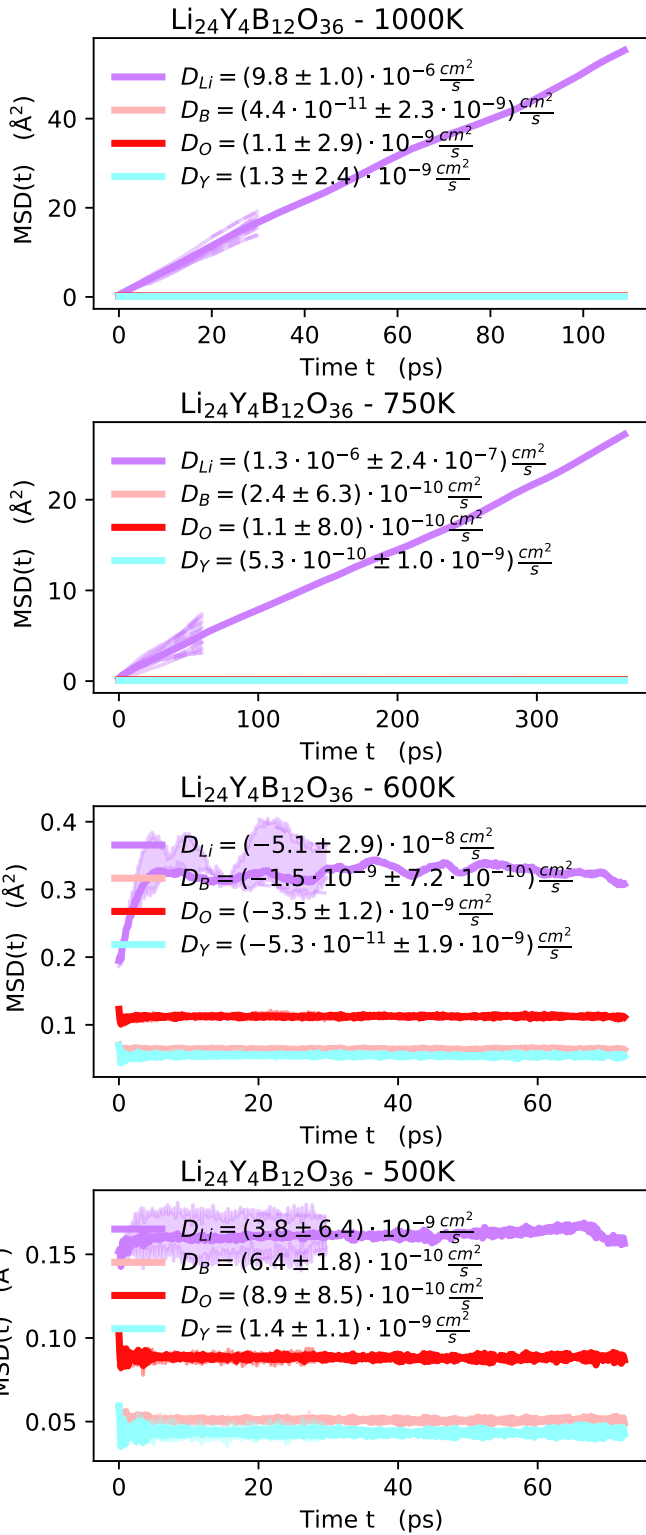


**Fig. S21** MSD(t) for Li<sub>24</sub>Y<sub>4</sub>B<sub>12</sub>O<sub>36</sub> from FPMD for all temperatures studied.

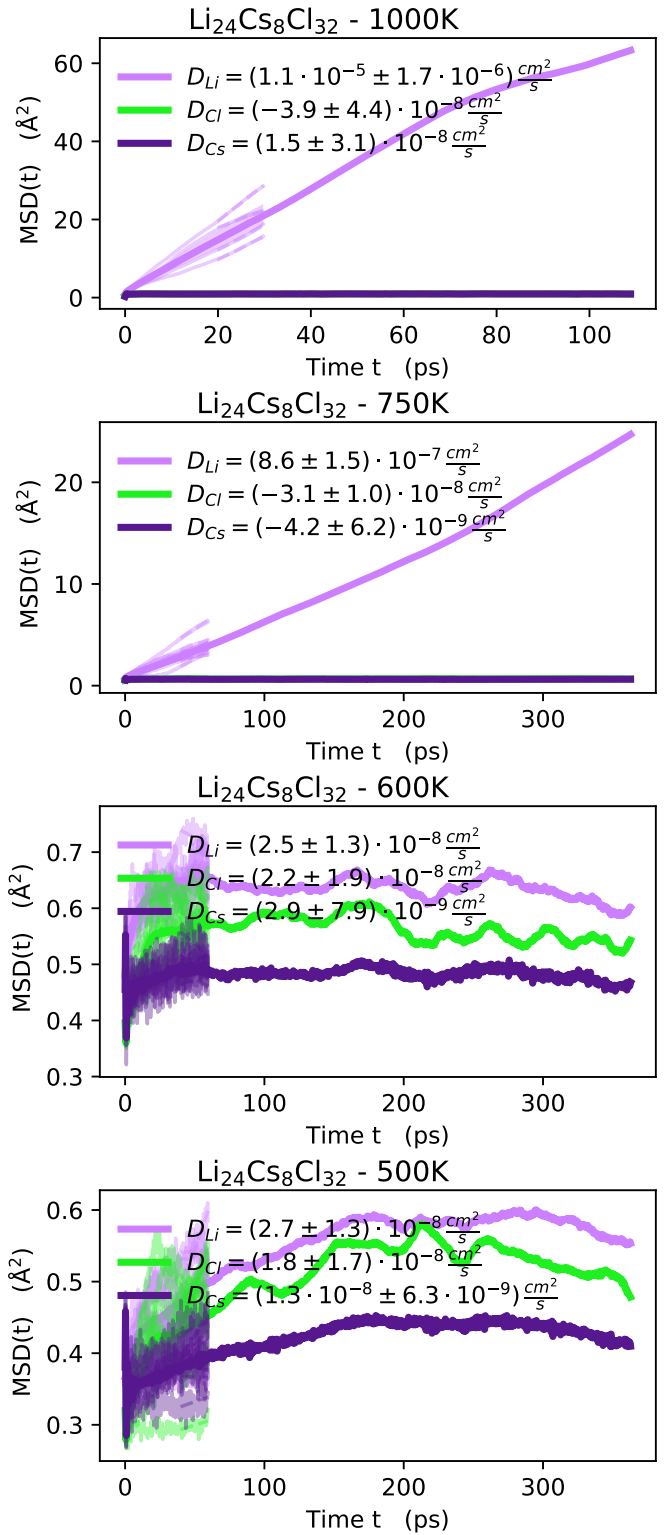


**Fig. S22** MSD(t) for Li<sub>24</sub>Cs<sub>8</sub>Cl<sub>32</sub> from FPMD for all temperatures studied.

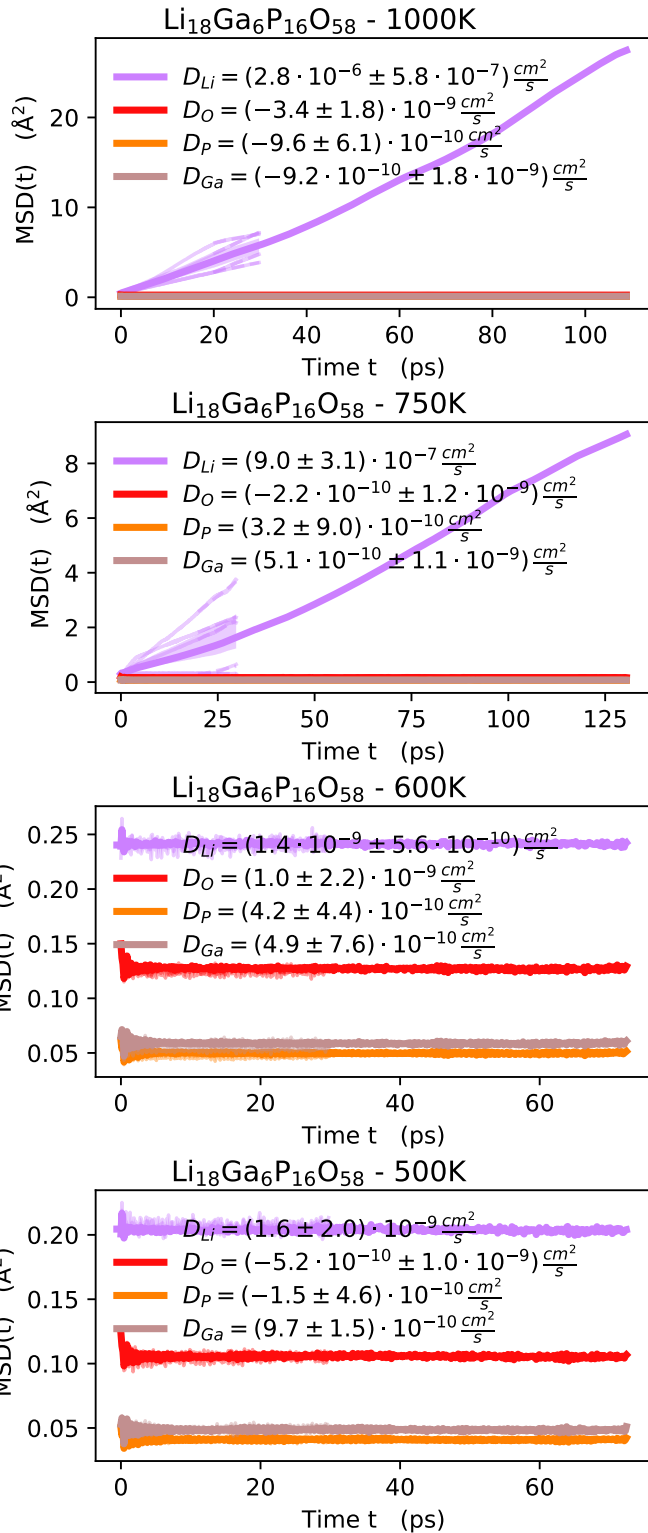


**Fig. S23** MSD(t) for Li<sub>18</sub>Ga<sub>6</sub>P<sub>16</sub>O<sub>58</sub> from FPMD for all temperatures studied.

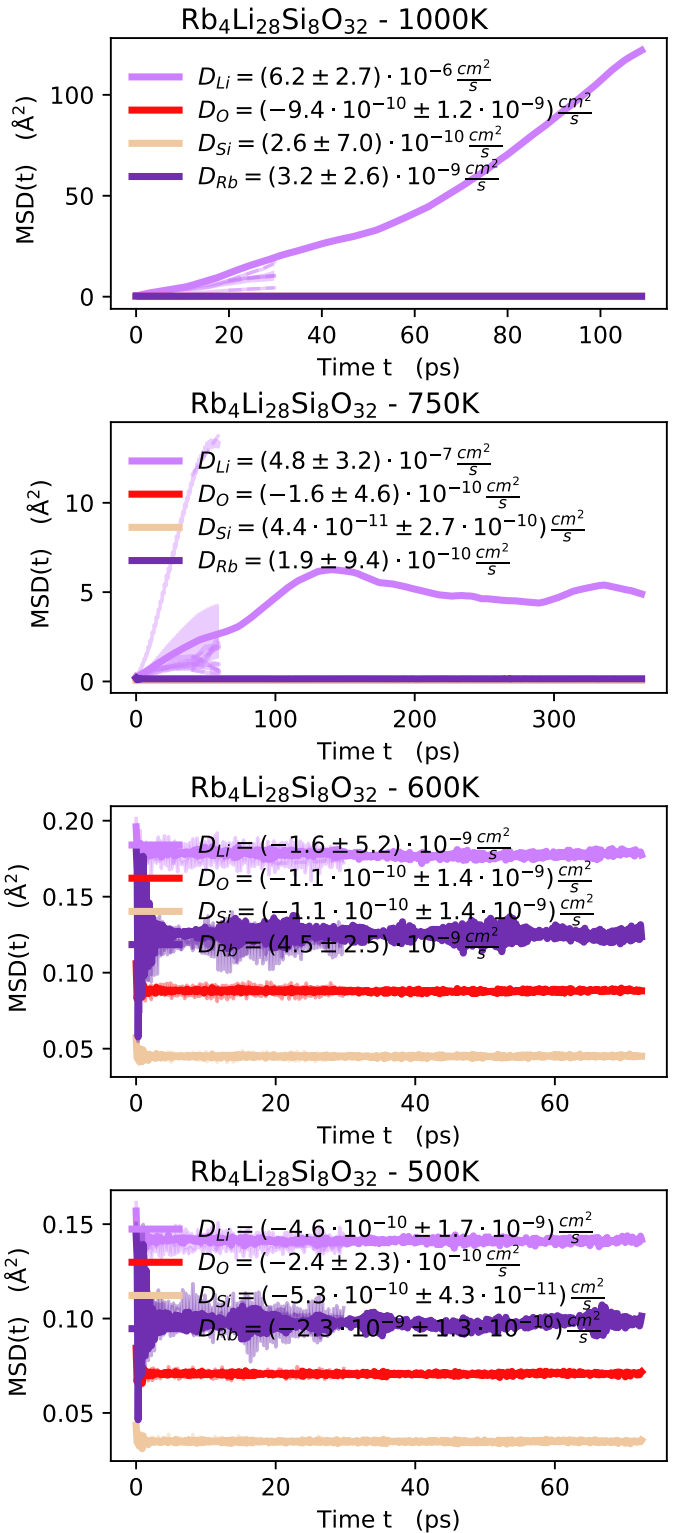


**Fig. S24** MSD(t) for Rb<sub>4</sub>Li<sub>28</sub>Si<sub>8</sub>O<sub>32</sub> from FPMD for all temperatures studied.

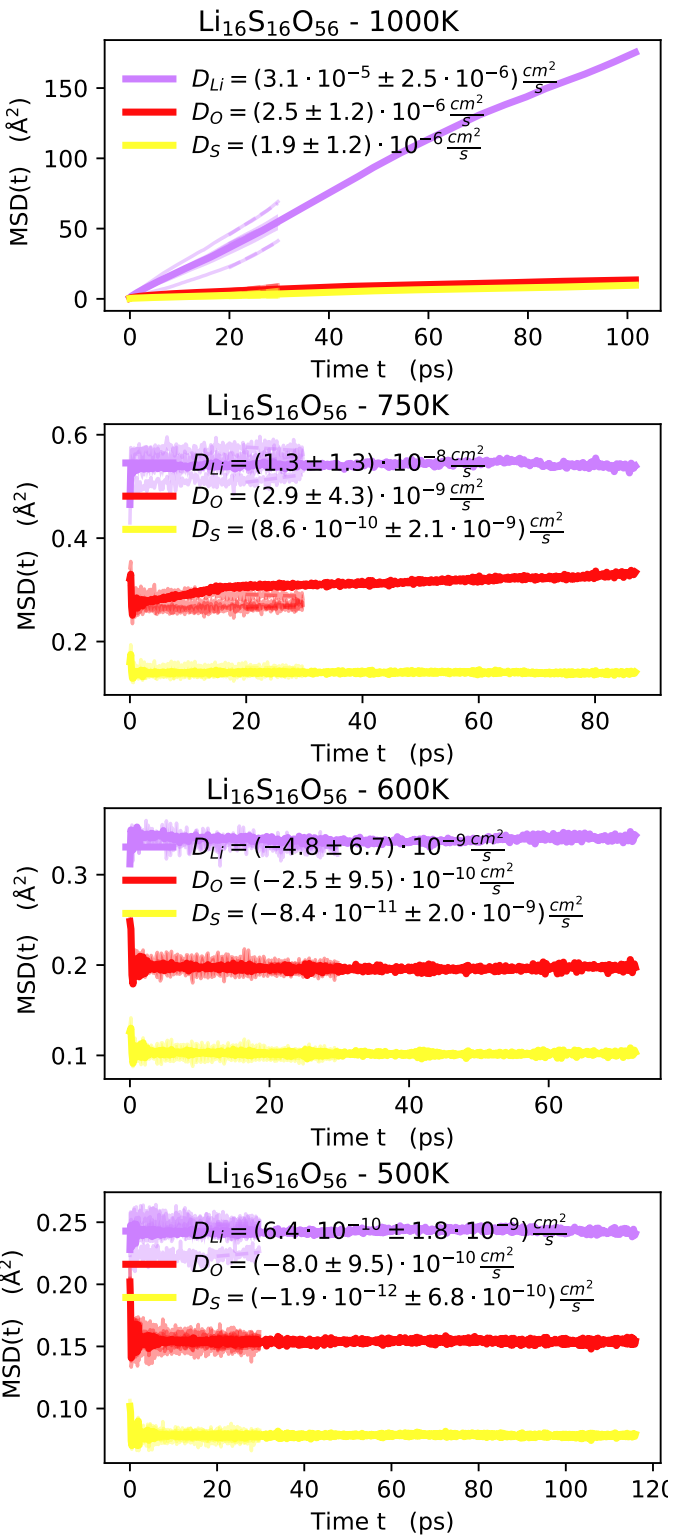


**Fig. S25** MSD(t) for Li<sub>16</sub>S<sub>16</sub>O<sub>56</sub> from FPMD for all temperatures studied.

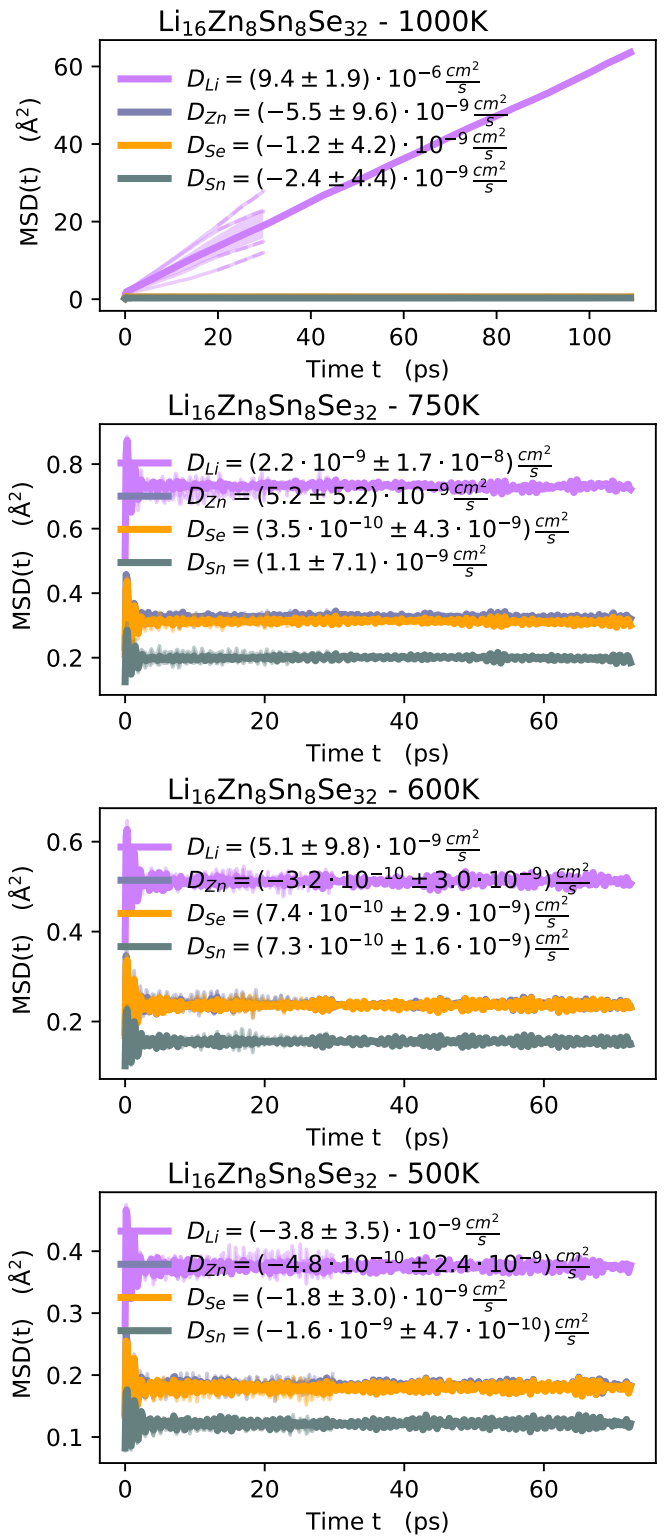


**Fig. S26** MSD(t) for Li<sub>16</sub>Zn<sub>8</sub>Sn<sub>8</sub>Se<sub>32</sub> from FPMD for all temperatures studied.

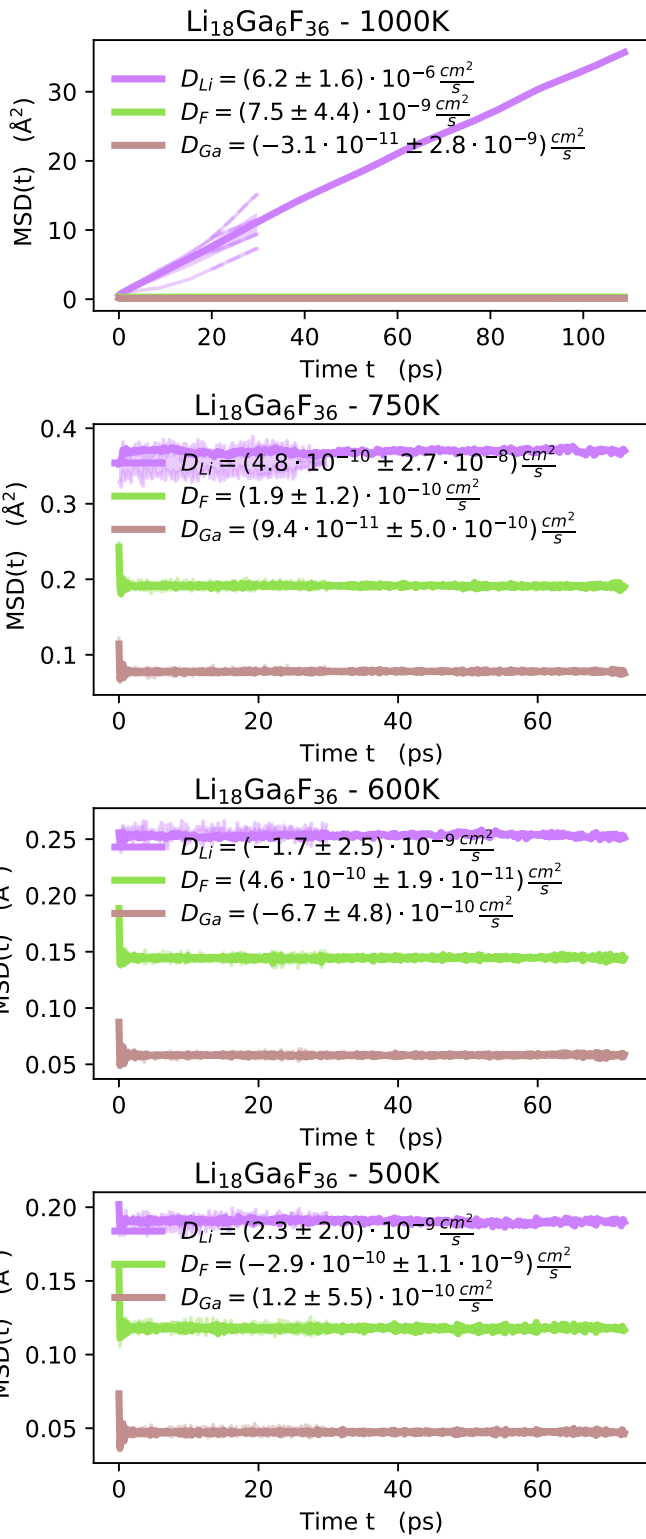


**Fig. S27** MSD(t) for Li<sub>18</sub>Ga<sub>6</sub>F<sub>36</sub> from FPMD for all temperatures studied.

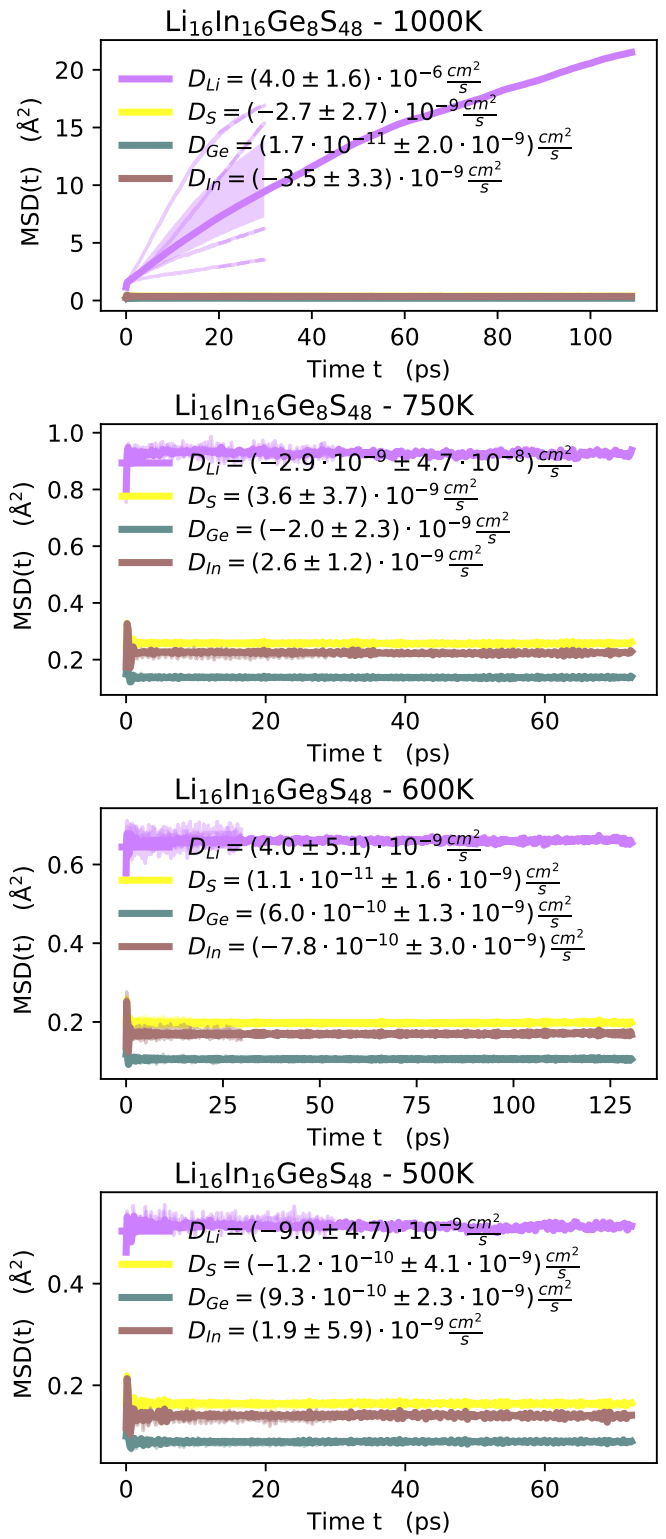


**Fig. S28** MSD(t) for Li<sub>16</sub>In<sub>16</sub>Ge<sub>8</sub>S<sub>48</sub> from FPMD for all temperatures studied.

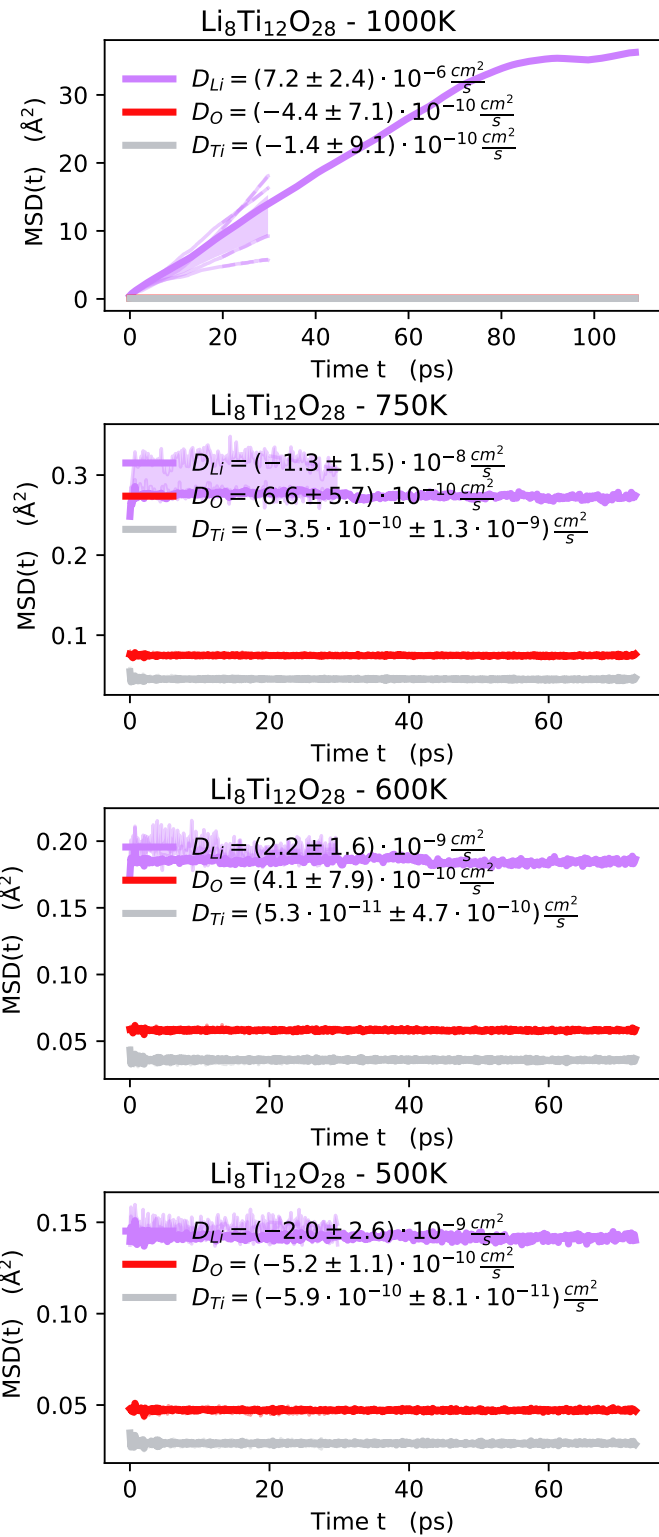


**Fig. S29** MSD(t) for Li<sub>8</sub>Ti<sub>12</sub>O<sub>28</sub> from FPMD for all temperatures studied.

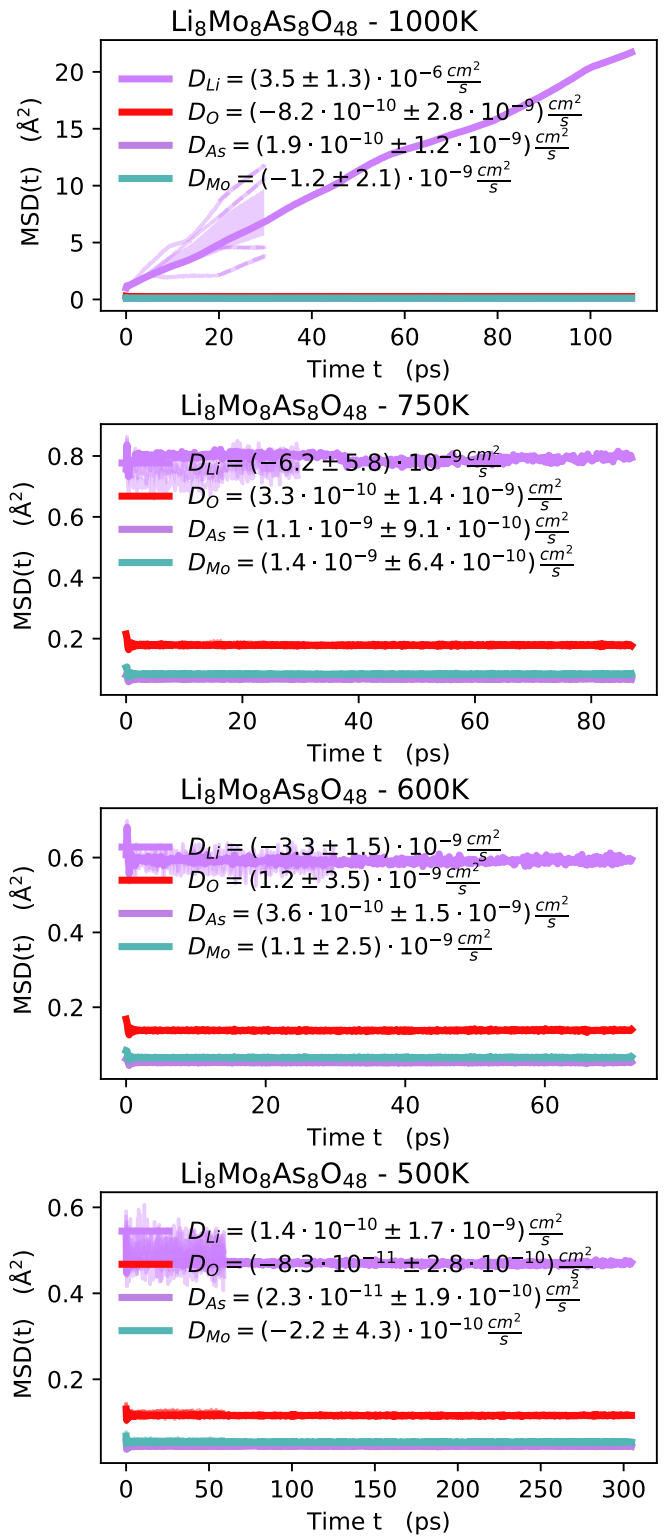


**Fig. S30** MSD(t) for Li<sub>8</sub>Mo<sub>8</sub>As<sub>8</sub>O<sub>48</sub> from FPMD for all temperatures studied.

**Table S2** We list all the structures that have been calculated only at 1000 K, and where we find diffusion of Li ions, although not high enough to warrant a calculation also at lower temperatures

Structure	DB	DB-id	Supercell	Fig.	Vol. $\Delta$	$T_{\text{sim}}^{1000}$
$\text{Li}_1\text{Ga}_1\text{Cl}_3$	COD	1530096	$\text{Li}_{16}\text{Ga}_{16}\text{Cl}_{48}$	S31	17.0%	58.2
$\text{Li}_1\text{Ga}_1\text{Br}_4$	ICSD	61337	$\text{Li}_{16}\text{Ga}_{16}\text{Br}_{64}$	S32	30.8%	72.7
$\text{Li}_6\text{Mg}_1\text{Br}_8$	ICSD	73275	$\text{Li}_{12}\text{Mg}_2\text{Br}_{16}$	S33	2.0%	72.7
$\text{Li}_3\text{P}_7$	ICSD	60774	$\text{Li}_{12}\text{P}_{28}$	S34	2.1%	174.5
$\text{Li}_3\text{As}_1\text{S}_3$	COD	2007413	$\text{Li}_{12}\text{As}_4\text{S}_{12}$	S35	2.9%	189.1
$\text{Li}_1\text{B}_1\text{S}_4\text{Cl}_4\text{O}_{12}$	COD	1004054	$\text{Li}_4\text{B}_4\text{S}_{16}\text{Cl}_{16}\text{O}_{48}$	S36	11.7%	218.1
$\text{Li}_1\text{Sn}_2\text{P}_3\text{O}_{12}$	ICSD	83831	$\text{Li}_2\text{Sn}_4\text{P}_6\text{O}_{24}$	S37	4.1%	87.3
$\text{Li}_4\text{Ge}_9\text{O}_{20}$	ICSD	34361	$\text{Li}_4\text{Ge}_9\text{O}_{20}$	S38	5.4%	58.2
$\text{Li}_1\text{I}_1\text{O}_4$	COD	1536985	$\text{Li}_8\text{I}_8\text{O}_{32}$	S39	10.4%	58.1
$\text{Rb}_2\text{Li}_1\text{Ta}_1\text{S}_4$	COD	1535645	$\text{Rb}_8\text{Li}_4\text{Ta}_4\text{S}_{16}$	S40	6.4%	436.3
$\text{Li}_1\text{P}_7$	ICSD	23621	$\text{Li}_8\text{P}_{56}$	S41	5.2%	436.3
$\text{Li}_4\text{P}_2\text{O}_7$	COD	2005920	$\text{Li}_{16}\text{P}_8\text{O}_{28}$	S42	4.0%	43.6
$\text{Li}_2\text{Ge}_4\text{O}_9$	COD	2019177	$\text{Li}_{16}\text{Ge}_{32}\text{O}_{72}$	S43	4.7%	189.1
$\text{Li}_1\text{Au}_1\text{F}_4$	ICSD	33953	$\text{Li}_8\text{Au}_8\text{F}_{32}$	S44	11.9%	58.2
$\text{Li}_2\text{Se}_1\text{O}_4$	ICSD	67234	$\text{Li}_{12}\text{Se}_6\text{O}_{24}$	S45	5.3%	116.3
$\text{Li}_1\text{Al}_1\text{Se}_2$	COD	4321118	$\text{Li}_{16}\text{Al}_{16}\text{Se}_{32}$	S46	3.1%	218.1
$\text{Li}_1\text{In}_1\text{P}_2\text{O}_7$	ICSD	60935	$\text{Li}_4\text{In}_4\text{P}_8\text{O}_{28}$	S47	6.3%	436.3
$\text{Li}_4\text{Ti}_1\text{O}_4$	ICSD	75164	$\text{Li}_{24}\text{Ti}_6\text{O}_{24}$	S48	1.4%	436.3
$\text{Li}_6\text{Si}_2\text{O}_7$	COD	1539516	$\text{Li}_{24}\text{Si}_8\text{O}_{28}$	S49	1.9%	445.2
$\text{Li}_2\text{In}_2\text{Si}_1\text{Se}_6$	COD	4329225	$\text{Li}_{16}\text{In}_{16}\text{Si}_8\text{Se}_{48}$	S50	5.5%	218.1
$\text{Li}_1\text{B}_1\text{S}_2\text{O}_8$	ICSD	425174	$\text{Li}_8\text{B}_8\text{S}_{16}\text{O}_{64}$	S51	6.9%	218.1

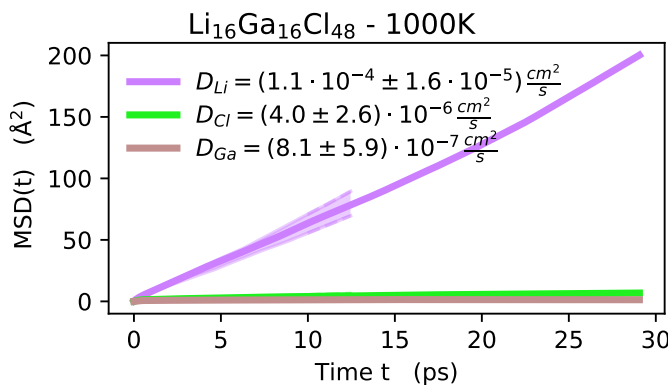


**Fig. S31** MSD(t) for  $\text{Li}_{16}\text{Ga}_{16}\text{Cl}_{48}$  from FPMD at 1000 K.

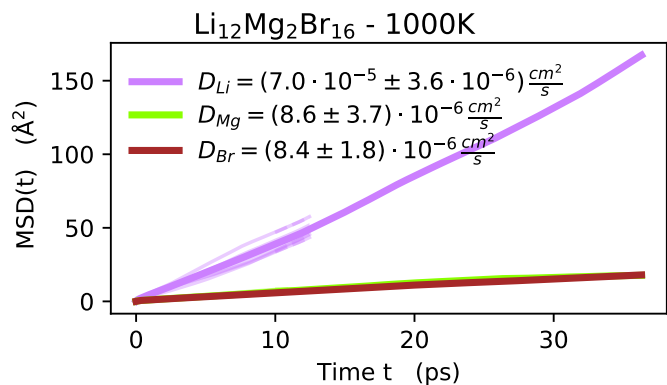


**Fig. S33** MSD(t) for  $\text{Li}_{12}\text{Mg}_2\text{Br}_{16}$  from FPMD at 1000 K.

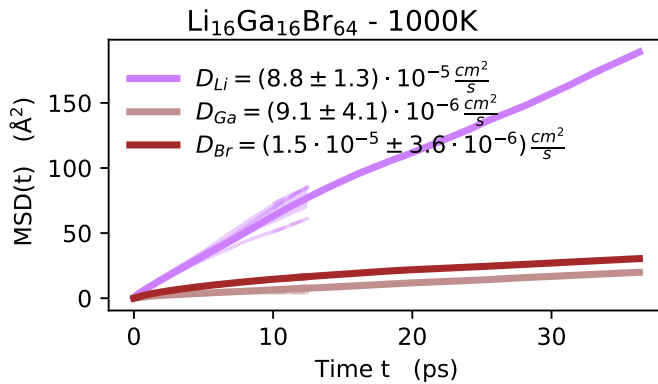


**Fig. S32** MSD(t) for  $\text{Li}_{16}\text{Ga}_{16}\text{Br}_{64}$  from FPMD at 1000 K.

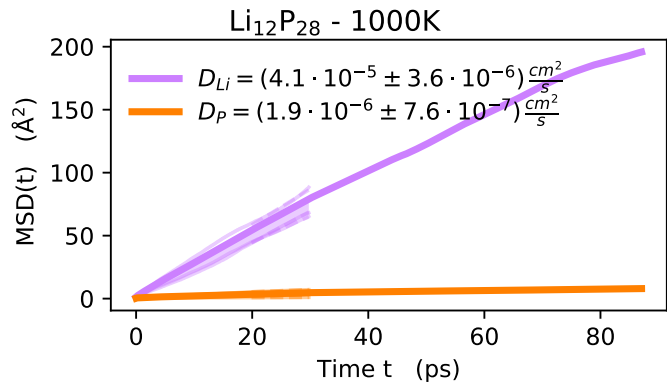


**Fig. S34** MSD(t) for  $\text{Li}_{12}\text{P}_{28}$  from FPMD at 1000 K.

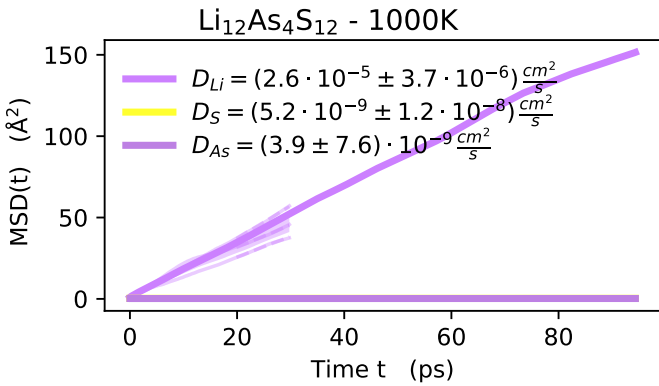


**Fig. S35** MSD(t) for Li<sub>12</sub>As<sub>4</sub>S<sub>12</sub> from FPMD at 1000 K.

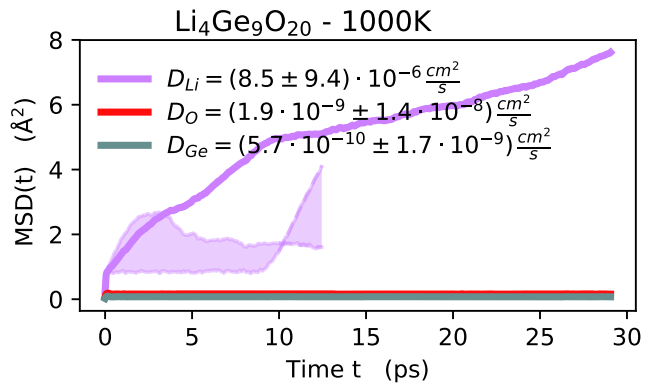


**Fig. S38** MSD(t) for Li<sub>4</sub>Ge<sub>9</sub>O<sub>20</sub> from FPMD at 1000 K.

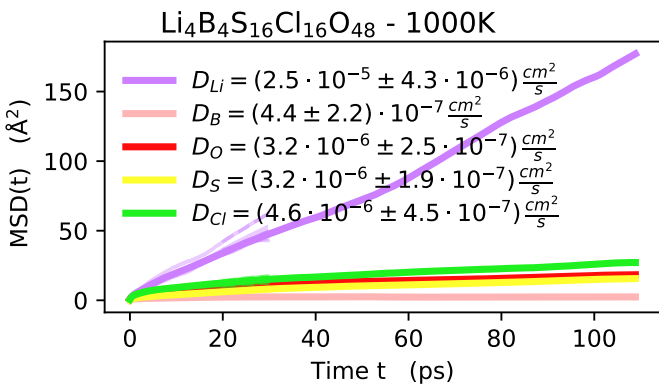


**Fig. S36** MSD(t) for Li<sub>4</sub>B<sub>4</sub>S<sub>16</sub>Cl<sub>16</sub>O<sub>48</sub> from FPMD at 1000 K.

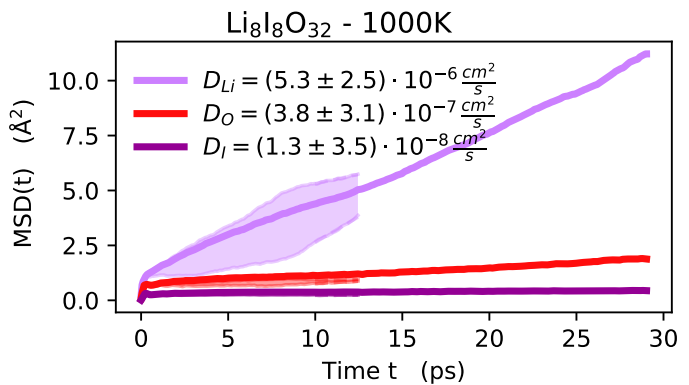


**Fig. S39** MSD(t) for Li<sub>8</sub>I<sub>8</sub>O<sub>32</sub> from FPMD at 1000 K.

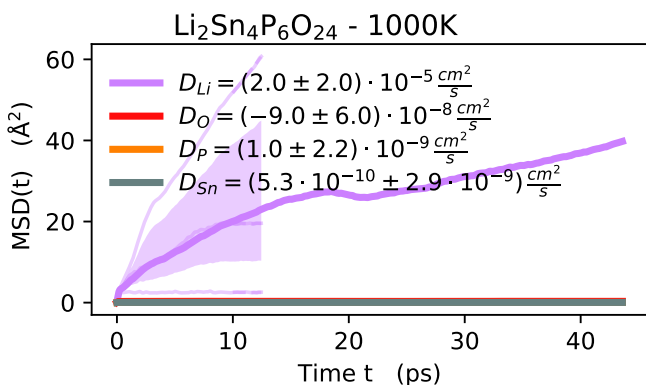


**Fig. S37** MSD(t) for Li<sub>2</sub>Sn<sub>4</sub>P<sub>6</sub>O<sub>24</sub> from FPMD at 1000 K.

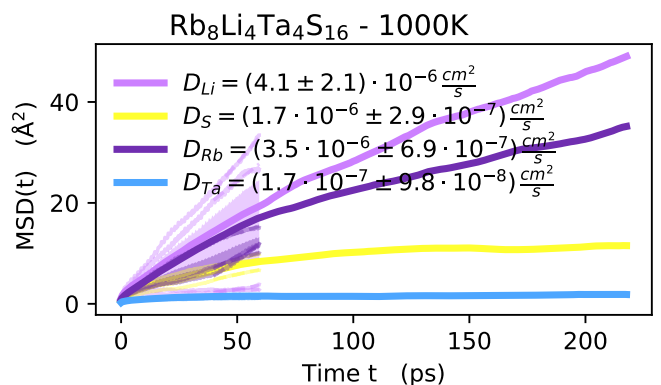


**Fig. S40** MSD(t) for Rb<sub>8</sub>Li<sub>4</sub>Ta<sub>4</sub>S<sub>16</sub> from FPMD at 1000 K.

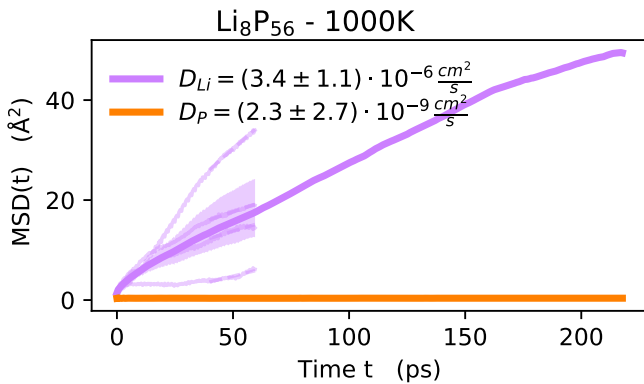


**Fig. S41** MSD(t) for Li<sub>8</sub>P<sub>56</sub> from FPMD at 1000 K.

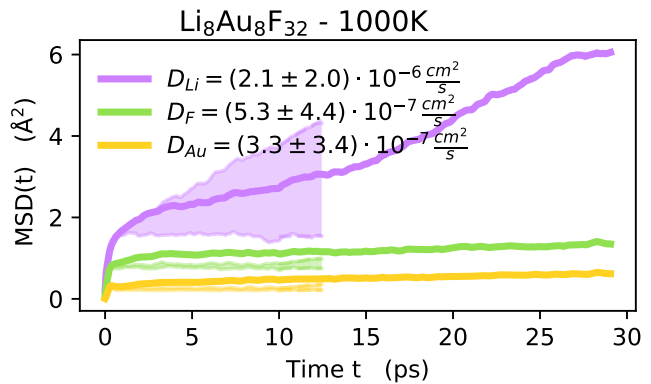


**Fig. S44** MSD(t) for Li<sub>8</sub>Au<sub>8</sub>F<sub>32</sub> from FPMD at 1000 K.

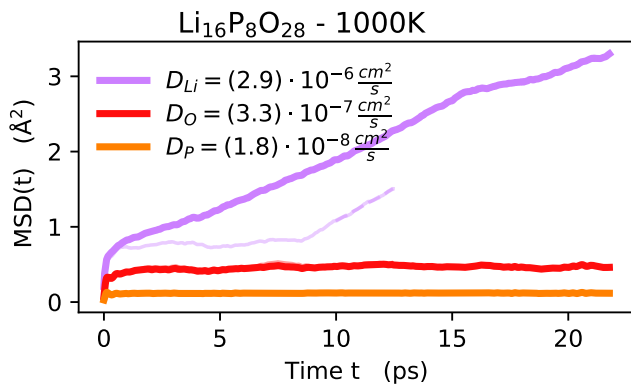


**Fig. S42** MSD(t) for Li<sub>16</sub>P<sub>8</sub>O<sub>28</sub> from FPMD at 1000 K.

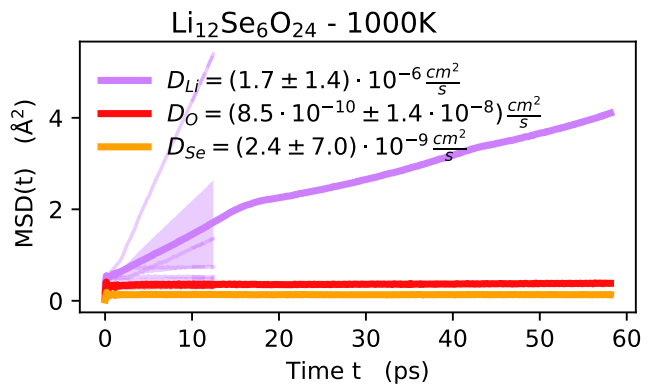


**Fig. S45** MSD(t) for Li<sub>12</sub>Se<sub>6</sub>O<sub>24</sub> from FPMD at 1000 K.

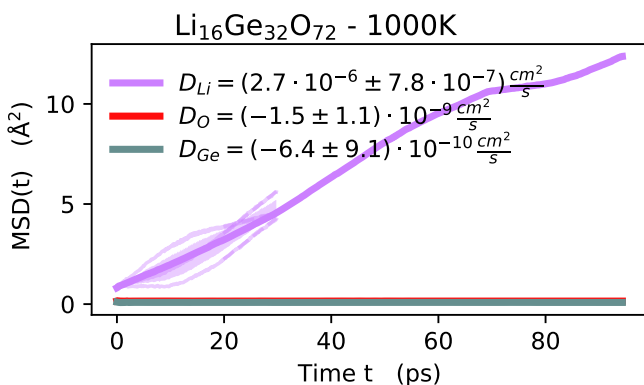


**Fig. S43** MSD(t) for Li<sub>16</sub>Ge<sub>32</sub>O<sub>72</sub> from FPMD at 1000 K.

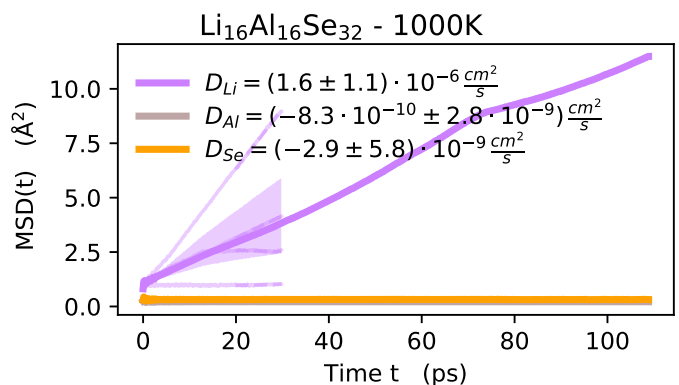


**Fig. S46** MSD(t) for Li<sub>16</sub>Al<sub>16</sub>Se<sub>32</sub> from FPMD at 1000 K.

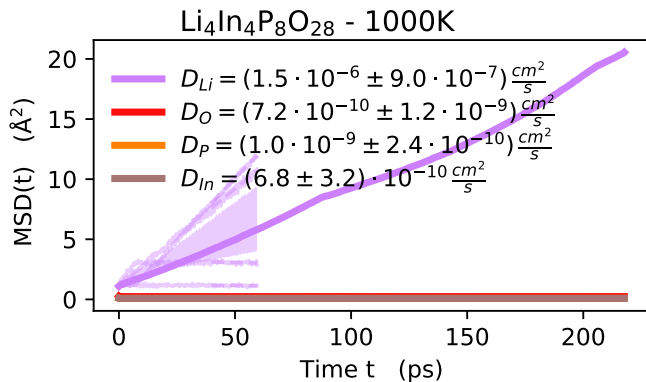


**Fig. S47** MSD(t) for Li<sub>4</sub>In<sub>4</sub>P<sub>8</sub>O<sub>28</sub> from FPMD at 1000 K.

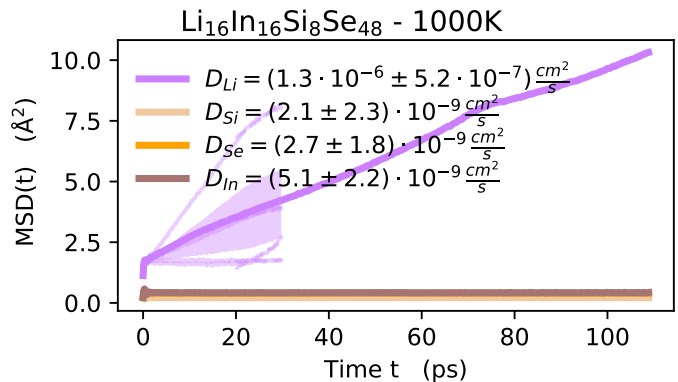


**Fig. S50** MSD(t) for Li<sub>16</sub>In<sub>16</sub>Si<sub>8</sub>Se<sub>48</sub> from FPMD at 1000 K.

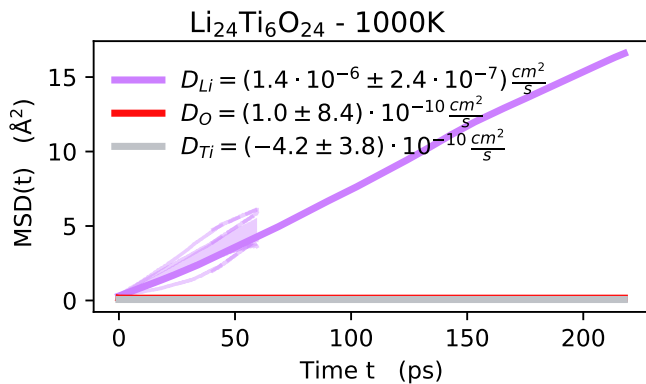


**Fig. S48** MSD(t) for Li<sub>24</sub>Ti<sub>6</sub>O<sub>24</sub> from FPMD at 1000 K.

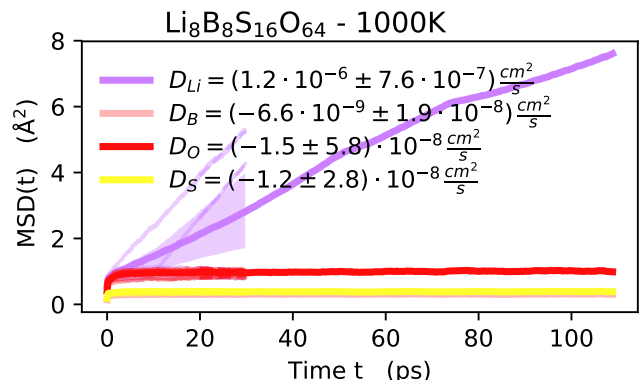


**Fig. S51** MSD(t) for Li<sub>8</sub>B<sub>8</sub>S<sub>16</sub>O<sub>64</sub> from FPMD at 1000 K.

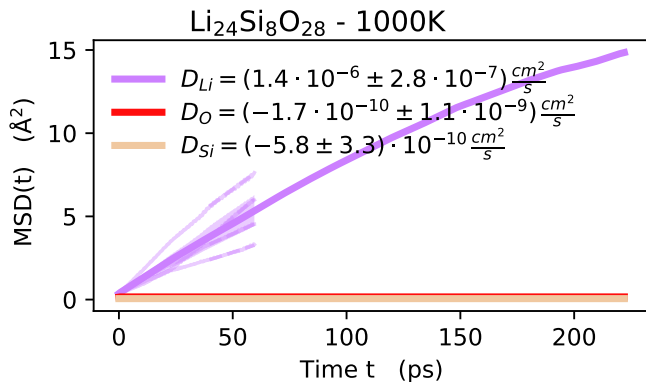


**Fig. S49** MSD(t) for Li<sub>24</sub>Si<sub>8</sub>O<sub>28</sub> from FPMD at 1000 K.

## 5 Non-diffusive structures (group C)

**Table S3** We list the structures that we find to be non-diffusive structures. We only calculated the diffusion at 1000 K. This is the first of two tables

Structure	DB	DB-id	Supercell	Figure	Volume change	T <sup>sim</sup> <sub>1000</sub>
Li <sub>2</sub> Ce <sub>1</sub> N <sub>2</sub>	ICSD	34003	Li <sub>16</sub> Ce <sub>8</sub> N <sub>16</sub>	S52	1.1%	334.5
Li <sub>6</sub> Sr <sub>3</sub> Ta <sub>2</sub> O <sub>11</sub>	COD	4306193	Li <sub>24</sub> Sr <sub>12</sub> Ta <sub>8</sub> O <sub>44</sub>	S53	2.0%	218.1
Li <sub>5</sub> Re <sub>1</sub> N <sub>4</sub>	ICSD	92468	Li <sub>20</sub> Re <sub>4</sub> N <sub>16</sub>	S54	0.2%	160.0
Li <sub>6</sub> Zn <sub>1</sub> O <sub>4</sub>	ICSD	62137	Li <sub>24</sub> Zn <sub>4</sub> O <sub>16</sub>	S55	1.6%	407.2
Li <sub>4</sub> K <sub>1</sub> Al <sub>1</sub> O <sub>4</sub>	ICSD	65260	Li <sub>64</sub> K <sub>16</sub> Al <sub>16</sub> O <sub>64</sub>	S56	1.9%	87.3
Li <sub>2</sub> Al <sub>1</sub> B <sub>5</sub> O <sub>10</sub>	COD	2012178	Li <sub>8</sub> Al <sub>4</sub> B <sub>20</sub> O <sub>40</sub>	S57	4.9%	72.7
Li <sub>2</sub> Cs <sub>3</sub> Br <sub>5</sub>	ICSD	245978	Li <sub>8</sub> Cs <sub>12</sub> Br <sub>20</sub>	S58	-12.5%	72.7
Na <sub>1</sub> Li <sub>2</sub> B <sub>1</sub> P <sub>2</sub> O <sub>8</sub>	ICSD	291512	Na <sub>4</sub> Li <sub>8</sub> B <sub>4</sub> P <sub>8</sub> O <sub>32</sub>	S59	4.7%	101.8
Li <sub>1</sub> La <sub>1</sub> C <sub>2</sub> O <sub>6</sub>	ICSD	174533	Li <sub>4</sub> La <sub>4</sub> C <sub>8</sub> O <sub>24</sub>	S60	3.2%	72.7
Li <sub>1</sub> Au <sub>1</sub> F <sub>4</sub>	COD	1510140	Li <sub>16</sub> Au <sub>16</sub> F <sub>64</sub>	S61	14.8%	43.6
Li <sub>1</sub> Si <sub>2</sub> B <sub>1</sub> O <sub>6</sub>	COD	1511474	Li <sub>16</sub> Si <sub>32</sub> B <sub>16</sub> O <sub>96</sub>	S62	2.7%	101.8
Li <sub>2</sub> Cd <sub>1</sub> P <sub>4</sub> O <sub>12</sub>	COD	1008009	Li <sub>8</sub> Cd <sub>4</sub> P <sub>16</sub> O <sub>48</sub>	S63	5.3%	116.3
Li <sub>2</sub> Si <sub>3</sub> O <sub>7</sub>	COD	1501470	Li <sub>16</sub> Si <sub>24</sub> O <sub>56</sub>	S64	3.5%	72.7
Li <sub>2</sub> Te <sub>1</sub> O <sub>3</sub>	ICSD	4317	Li <sub>32</sub> Te <sub>16</sub> O <sub>48</sub>	S65	10.3%	72.7
Li <sub>3</sub> Au <sub>1</sub> O <sub>3</sub>	COD	1510224	Li <sub>36</sub> Au <sub>12</sub> O <sub>36</sub>	S66	2.9%	58.2
Sr <sub>1</sub> Li <sub>2</sub> Si <sub>2</sub> N <sub>4</sub>	COD	4002768	Sr <sub>12</sub> Li <sub>24</sub> Si <sub>24</sub> N <sub>48</sub>	S67	-0.4%	72.7
Li <sub>1</sub> Y <sub>1</sub> Mo <sub>3</sub> O <sub>8</sub>	ICSD	28526	Li <sub>3</sub> Y <sub>3</sub> Mo <sub>9</sub> O <sub>24</sub>	S68	2.5%	72.7
Li <sub>2</sub> Mo <sub>1</sub> O <sub>4</sub>	COD	7024042	Li <sub>12</sub> Mo <sub>6</sub> O <sub>24</sub>	S69	3.8%	48.5
Li <sub>2</sub> Pd <sub>1</sub> O <sub>2</sub>	ICSD	61199	Li <sub>24</sub> Pd <sub>12</sub> O <sub>24</sub>	S70	2.0%	72.7
Li <sub>3</sub> Sc <sub>1</sub> B <sub>2</sub> O <sub>6</sub>	COD	2218562	Li <sub>24</sub> Sc <sub>8</sub> B <sub>16</sub> O <sub>48</sub>	S71	1.7%	218.1
Li <sub>1</sub> Nb <sub>3</sub> In <sub>1</sub> Cl <sub>9</sub>	ICSD	75071	Li <sub>2</sub> Nb <sub>6</sub> In <sub>2</sub> Cl <sub>18</sub>	S72	7.3%	334.5
Li <sub>6</sub> W <sub>1</sub> N <sub>4</sub>	ICSD	153620	Li <sub>24</sub> W <sub>4</sub> N <sub>16</sub>	S73	0.1%	72.7
Li <sub>1</sub> Zn <sub>1</sub> As <sub>1</sub> O <sub>4</sub>	ICSD	86184	Li <sub>6</sub> Zn <sub>6</sub> As <sub>6</sub> O <sub>24</sub>	S74	6.4%	226.5
Li <sub>4</sub> Ta <sub>1</sub> N <sub>3</sub>	COD	1535987	Li <sub>32</sub> Ta <sub>8</sub> N <sub>24</sub>	S75	0.1%	72.7
Li <sub>3</sub> Sc <sub>1</sub> N <sub>2</sub>	COD	1532734	Li <sub>24</sub> Sc <sub>8</sub> N <sub>16</sub>	S76	-0.5%	43.6
Li <sub>3</sub> Al <sub>1</sub> Mo <sub>2</sub> As <sub>2</sub> O <sub>14</sub>	COD	2220995	Li <sub>9</sub> Al <sub>3</sub> Mo <sub>6</sub> As <sub>6</sub> O <sub>42</sub>	S77	3.2%	174.5
Li <sub>1</sub> P <sub>1</sub> O <sub>3</sub>	COD	9014879	Li <sub>24</sub> P <sub>24</sub> O <sub>72</sub>	S78	5.3%	130.9
Li <sub>7</sub> P <sub>1</sub> N <sub>4</sub>	ICSD	642182	Li <sub>56</sub> P <sub>8</sub> N <sub>32</sub>	S79	0.2%	72.7
Li <sub>1</sub> Y <sub>1</sub> Si <sub>1</sub> O <sub>4</sub>	ICSD	34079	Li <sub>8</sub> Y <sub>8</sub> Si <sub>8</sub> O <sub>32</sub>	S80	3.0%	101.8
Li <sub>2</sub> Si <sub>2</sub> O <sub>5</sub>	COD	2003027	Li <sub>16</sub> Si <sub>16</sub> O <sub>40</sub>	S81	4.1%	72.7
Li <sub>16</sub> Nb <sub>2</sub> N <sub>8</sub> O <sub>1</sub>	ICSD	174443	Li <sub>64</sub> Nb <sub>8</sub> N <sub>32</sub> O <sub>4</sub>	S82	-1.7%	58.2
Li <sub>9</sub> Mg <sub>3</sub> P <sub>4</sub> O <sub>16</sub> F <sub>3</sub>	ICSD	426103	Li <sub>36</sub> Mg <sub>12</sub> P <sub>16</sub> O <sub>64</sub> F <sub>12</sub>	S83	3.4%	72.7
Li <sub>8</sub> Pt <sub>1</sub> O <sub>6</sub>	ICSD	61218	Li <sub>32</sub> Pt <sub>4</sub> O <sub>24</sub>	S84	2.2%	87.3
Li <sub>3</sub> Ga <sub>1</sub> B <sub>2</sub> O <sub>6</sub>	COD	1511740	Li <sub>24</sub> Ga <sub>8</sub> B <sub>16</sub> O <sub>48</sub>	S93	7.1%	58.2
Li <sub>3</sub> Al <sub>1</sub> Si <sub>1</sub> O <sub>5</sub>	COD	7224138	Li <sub>48</sub> Al <sub>16</sub> Si <sub>16</sub> O <sub>80</sub>	S86	3.1%	58.2
Li <sub>8</sub> Be <sub>5</sub> B <sub>6</sub> O <sub>18</sub>	COD	4337787	Li <sub>32</sub> Be <sub>20</sub> B <sub>24</sub> O <sub>72</sub>	S87	2.2%	145.4
Li <sub>4</sub> K <sub>1</sub> Nb <sub>1</sub> O <sub>5</sub>	ICSD	73124	Li <sub>32</sub> K <sub>8</sub> Nb <sub>8</sub> O <sub>40</sub>	S88	3.3%	58.2
Li <sub>4</sub> Te <sub>1</sub> O <sub>5</sub>	COD	1530934	Li <sub>16</sub> Te <sub>4</sub> O <sub>20</sub>	S89	7.2%	72.7
Li <sub>4</sub> Ge <sub>5</sub> O <sub>12</sub>	COD	9007843	Li <sub>16</sub> Ge <sub>20</sub> O <sub>48</sub>	S90	5.1%	72.7
Li <sub>7</sub> Nb <sub>1</sub> N <sub>4</sub>	COD	2000944	Li <sub>56</sub> Nb <sub>8</sub> N <sub>32</sub>	S91	-0.7%	58.2
Li <sub>3</sub> Al <sub>1</sub> N <sub>2</sub>	COD	1537475	Li <sub>24</sub> Al <sub>8</sub> N <sub>16</sub>	S92	0.4%	72.7
Li <sub>3</sub> Ga <sub>1</sub> B <sub>2</sub> O <sub>6</sub>	COD	2242045	Li <sub>24</sub> Ga <sub>8</sub> B <sub>16</sub> O <sub>48</sub>	S93	2.2%	58.2
Li <sub>2</sub> Al <sub>1</sub> B <sub>1</sub> O <sub>4</sub>	ICSD	50612	Li <sub>32</sub> Al <sub>16</sub> B <sub>16</sub> O <sub>64</sub>	S94	3.5%	72.7
Li <sub>4</sub> Zn <sub>1</sub> P <sub>2</sub> O <sub>8</sub>	COD	1544389	Li <sub>16</sub> Zn <sub>4</sub> P <sub>8</sub> O <sub>32</sub>	S95	3.7%	72.7
K <sub>1</sub> Li <sub>1</sub> Zn <sub>1</sub> O <sub>2</sub>	ICSD	49022	K <sub>6</sub> Li <sub>6</sub> Zn <sub>6</sub> O <sub>12</sub>	S96	3.1%	72.7
Li <sub>6</sub> Te <sub>1</sub> O <sub>6</sub>	ICSD	40247	Li <sub>48</sub> Te <sub>8</sub> O <sub>48</sub>	S97	13.8%	58.2
Li <sub>2</sub> W <sub>1</sub> O <sub>4</sub>	ICSD	67236	Li <sub>12</sub> W <sub>6</sub> O <sub>24</sub>	S98	3.6%	87.3
Sr <sub>1</sub> Li <sub>4</sub> P <sub>2</sub>	ICSD	416888	Sr <sub>4</sub> Li <sub>16</sub> P <sub>8</sub>	S99	0.5%	72.7
Li <sub>3</sub> B <sub>7</sub> O <sub>12</sub>	COD	9007831	Li <sub>12</sub> B <sub>28</sub> O <sub>48</sub>	S100	4.1%	145.4
Sr <sub>1</sub> Li <sub>2</sub> Ta <sub>2</sub> O <sub>7</sub>	ICSD	246277	Sr <sub>4</sub> Li <sub>8</sub> Ta <sub>8</sub> O <sub>28</sub>	S101	2.4%	72.7
Cs <sub>2</sub> Li <sub>3</sub> B <sub>5</sub> O <sub>10</sub>	COD	7213712	Cs <sub>8</sub> Li <sub>12</sub> B <sub>20</sub> O <sub>40</sub>	S102	0.0%	218.1
Li <sub>3</sub> Ba <sub>2</sub> Ta <sub>1</sub> N <sub>4</sub>	ICSD	75031	Li <sub>24</sub> Ba <sub>16</sub> Ta <sub>8</sub> N <sub>32</sub>	S103	0.8%	58.2
Li <sub>2</sub> Si <sub>2</sub> O <sub>5</sub>	ICSD	69300	Li <sub>32</sub> Si <sub>32</sub> O <sub>80</sub>	S104	3.5%	72.7

**Table S4** We list the structures that we find to be non-diffusive structures. This is the second of two tables

Structure	DB	DB-id	Supercell	Figure	Volume change	$T_{1000}^{\text{sim}}$
$\text{Li}_6\text{Be}_3\text{B}_4\text{O}_{12}$	COD	4337786	$\text{Li}_{24}\text{Be}_{12}\text{B}_{16}\text{O}_{48}$	S105	2.2%	72.7
$\text{Li}_1\text{In}_1\text{Ge}_1\text{O}_4$	ICSD	167518	$\text{Li}_{16}\text{In}_{16}\text{Ge}_{16}\text{O}_{64}$	S106	-0.1%	58.2
$\text{Cs}_2\text{Li}_2\text{B}_2\text{P}_4\text{O}_{15}$	ICSD	424281	$\text{Cs}_8\text{Li}_8\text{B}_8\text{P}_{16}\text{O}_{60}$	S107	5.9%	58.2
$\text{Li}_2\text{Te}_1\text{W}_1\text{O}_6$	COD	4330276	$\text{Li}_{16}\text{Te}_8\text{W}_8\text{O}_{48}$	S108	3.0%	72.7
$\text{Li}_4\text{Al}_3\text{Ge}_3\text{Br}_1\text{O}_{12}$	ICSD	87991	$\text{Li}_8\text{Al}_6\text{Ge}_6\text{Br}_2\text{O}_{24}$	S109	2.5%	72.7
$\text{Li}_2\text{Mo}_4\text{O}_{13}$	ICSD	4155	$\text{Li}_6\text{Mo}_{12}\text{O}_{39}$	S110	5.9%	72.7
$\text{Li}_2\text{Ta}_2\text{O}_3\text{F}_6$	ICSD	405777	$\text{Li}_{24}\text{Ta}_{24}\text{O}_{36}\text{F}_{72}$	S111	4.5%	101.8
$\text{Li}_2\text{Mg}_1\text{Si}_1\text{O}_4$	COD	7222190	$\text{Li}_{16}\text{Mg}_8\text{Si}_8\text{O}_{32}$	S112	2.7%	72.7
$\text{Li}_3\text{Ba}_2\text{Nb}_1\text{N}_4$	ICSD	75516	$\text{Li}_{24}\text{Ba}_{16}\text{Nb}_8\text{N}_{32}$	S113	0.4%	58.2
$\text{Rb}_2\text{Li}_3\text{B}_1\text{P}_4\text{O}_{14}$	ICSD	424352	$\text{Rb}_8\text{Li}_{12}\text{B}_4\text{P}_{16}\text{O}_{56}$	S114	5.8%	116.3
$\text{Li}_6\text{Zr}_1\text{Be}_1\text{F}_{12}$	COD	1528861	$\text{Li}_{24}\text{Zr}_4\text{Be}_4\text{F}_{48}$	S115	0.0%	58.2
$\text{Li}_1\text{B}_1\text{O}_2$	COD	2310701	$\text{Li}_{32}\text{B}_{32}\text{O}_{64}$	S116	6.4%	72.7
$\text{Li}_2\text{B}_3\text{P}_1\text{O}_8$	COD	7031897	$\text{Li}_{16}\text{B}_{24}\text{P}_8\text{O}_{64}$	S117	7.3%	218.1
$\text{Li}_3\text{Al}_1\text{B}_2\text{O}_6$	COD	1100060	$\text{Li}_{24}\text{Al}_8\text{B}_{16}\text{O}_{48}$	S118	3.7%	87.3
$\text{Li}_1\text{Re}_1\text{O}_4$	COD	1535227	$\text{Li}_{12}\text{Re}_{12}\text{O}_{48}$	S119	8.2%	145.4
$\text{K}_1\text{Li}_1\text{Y}_1\text{F}_5$	ICSD	187751	$\text{K}_{16}\text{Li}_{16}\text{Y}_{16}\text{F}_{80}$	S120	1.8%	105.3
$\text{Li}_1\text{Nb}_1\text{O}_3$	ICSD	182033	$\text{Li}_{16}\text{Nb}_{16}\text{O}_{48}$	S121	2.5%	58.2

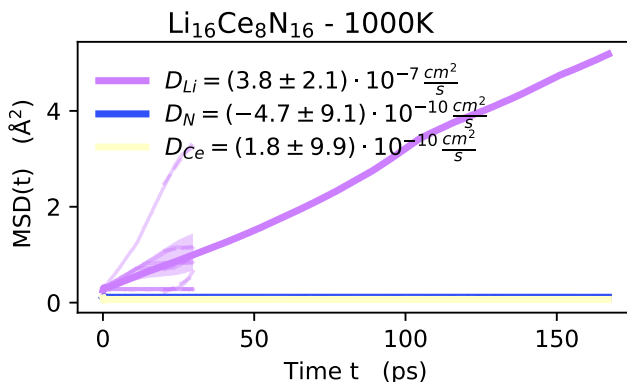


Fig. S52 MSD(t) for  $\text{Li}_{16}\text{Ce}_8\text{N}_{16}$  from FPMD at 1000 K.

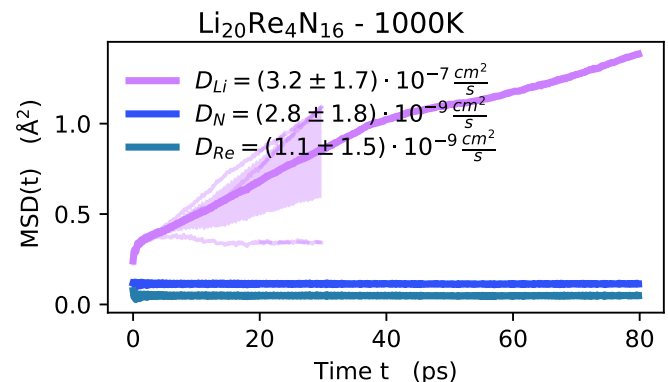


Fig. S54 MSD(t) for  $\text{Li}_{20}\text{Re}_4\text{N}_{16}$  from FPMD at 1000 K.

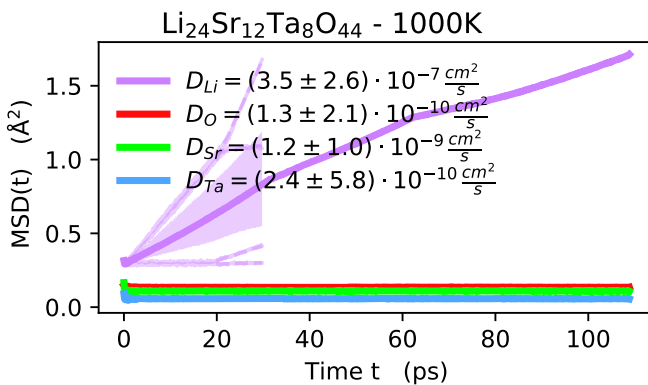


Fig. S53 MSD(t) for  $\text{Li}_{24}\text{Sr}_{12}\text{Ta}_8\text{O}_{44}$  from FPMD at 1000 K.

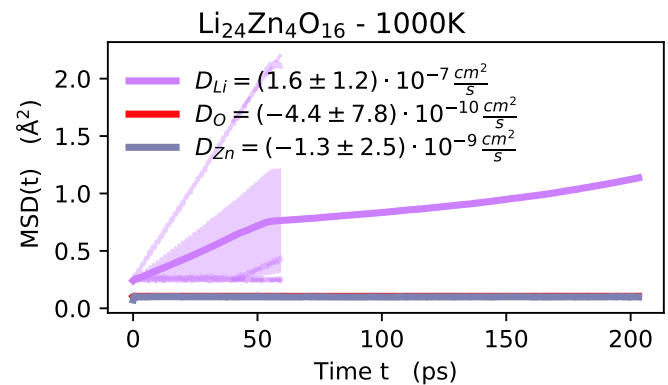


Fig. S55 MSD(t) for  $\text{Li}_{24}\text{Zn}_4\text{O}_{16}$  from FPMD at 1000 K.

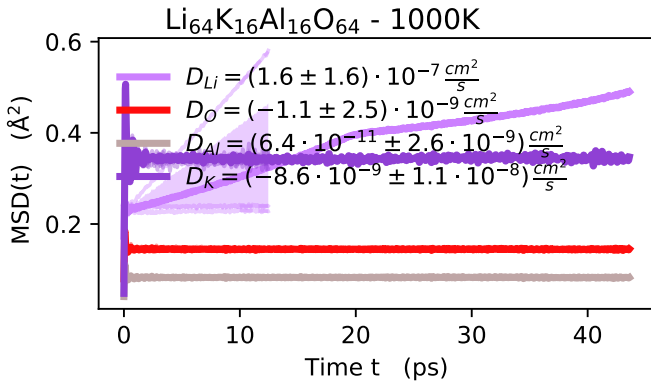


Fig. S56 MSD(t) for Li<sub>64</sub>K<sub>16</sub>Al<sub>16</sub>O<sub>64</sub> from FPMD at 1000 K.

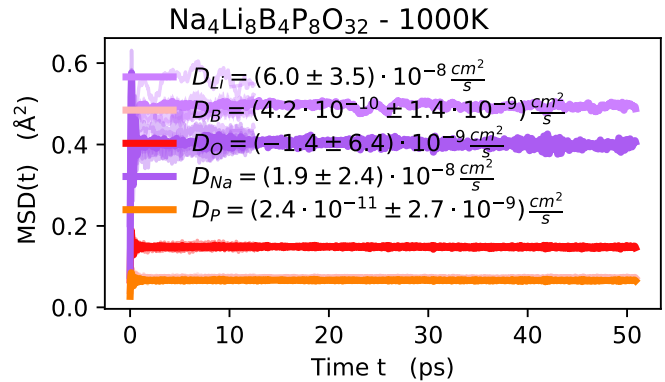


Fig. S59 MSD(t) for Na<sub>4</sub>Li<sub>8</sub>B<sub>4</sub>P<sub>8</sub>O<sub>32</sub> from FPMD at 1000 K.

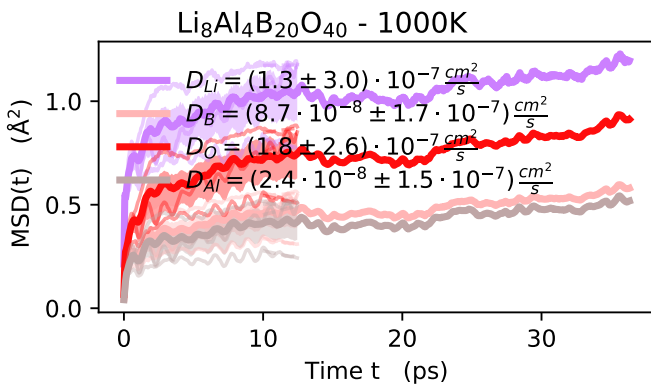


Fig. S57 MSD(t) for Li<sub>8</sub>Al<sub>4</sub>B<sub>20</sub>O<sub>40</sub> from FPMD at 1000 K.

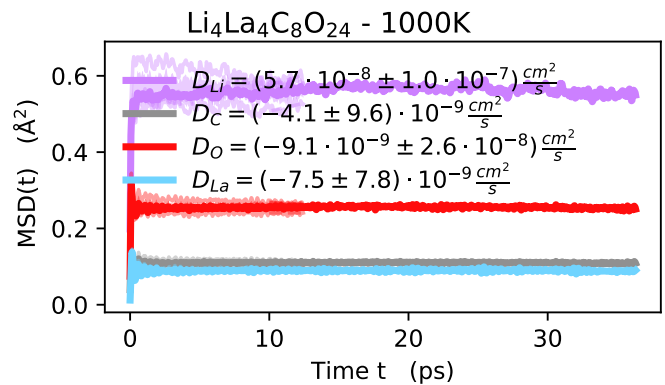


Fig. S60 MSD(t) for Li<sub>4</sub>La<sub>4</sub>C<sub>8</sub>O<sub>24</sub> from FPMD at 1000 K.

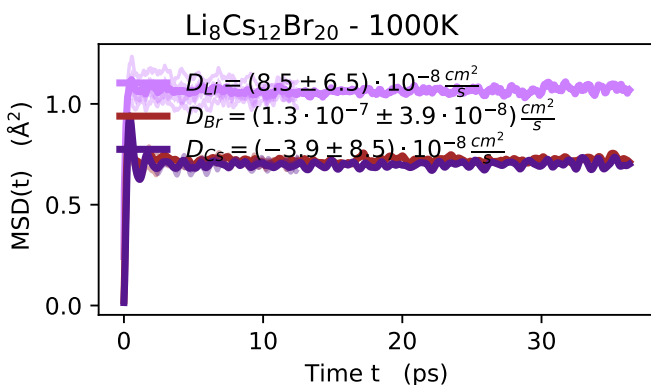


Fig. S58 MSD(t) for Li<sub>8</sub>Cs<sub>12</sub>Br<sub>20</sub> from FPMD at 1000 K.

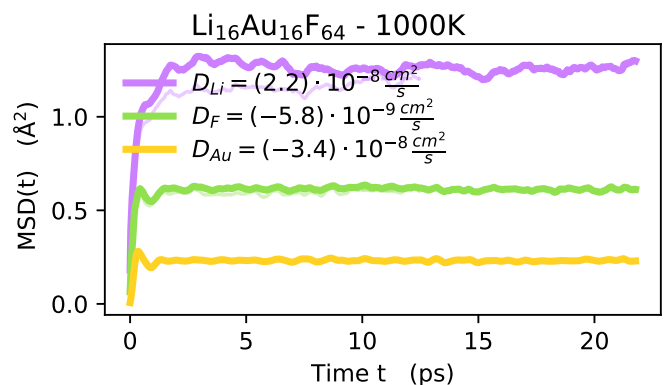
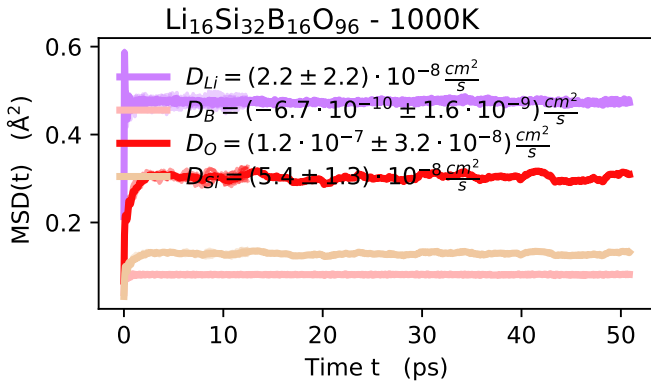
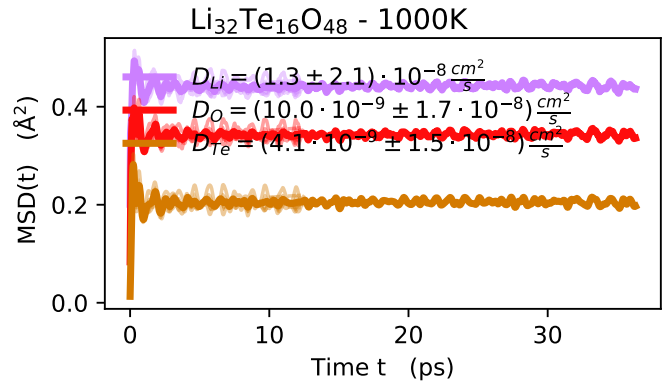


Fig. S61 MSD(t) for Li<sub>16</sub>Au<sub>16</sub>F<sub>64</sub> from FPMD at 1000 K.



**Fig. S62** MSD(t) for Li<sub>16</sub>Si<sub>32</sub>B<sub>16</sub>O<sub>96</sub> from FPMD at 1000 K.



**Fig. S65** MSD(t) for Li<sub>32</sub>Te<sub>16</sub>O<sub>48</sub> from FPMD at 1000 K.

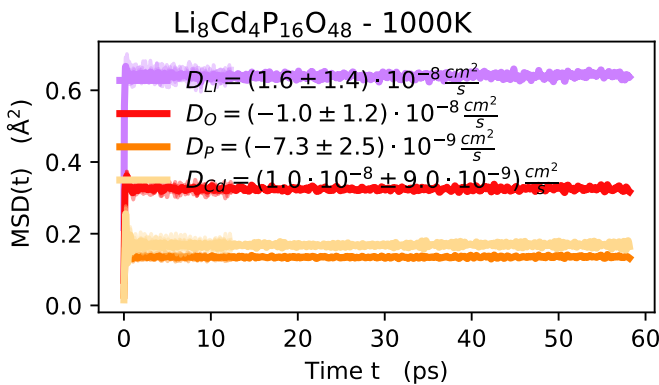


**Fig. S63** MSD(t) for Li<sub>8</sub>Cd<sub>4</sub>P<sub>16</sub>O<sub>48</sub> from FPMD at 1000 K.

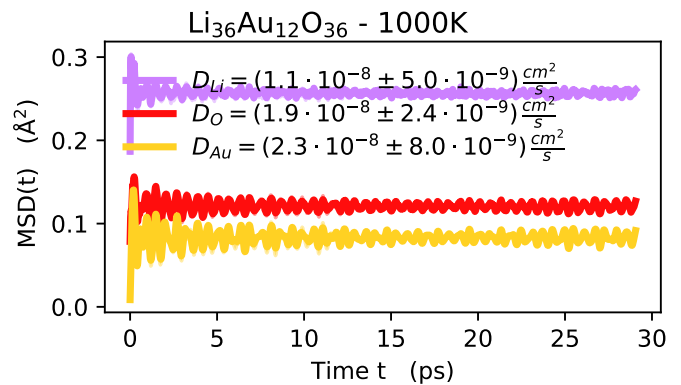


**Fig. S66** MSD(t) for Li<sub>36</sub>Au<sub>12</sub>O<sub>36</sub> from FPMD at 1000 K.

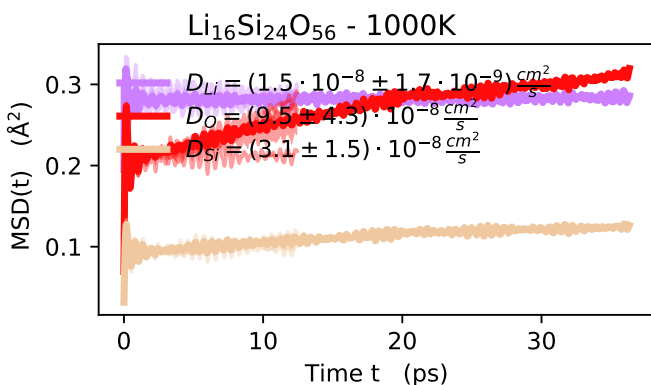


**Fig. S64** MSD(t) for Li<sub>16</sub>Si<sub>24</sub>O<sub>56</sub> from FPMD at 1000 K.

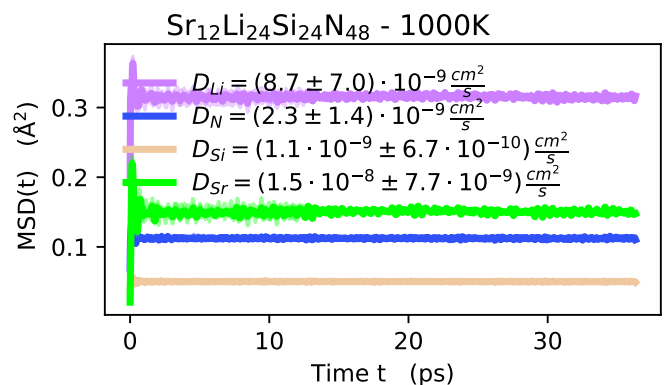


**Fig. S67** MSD(t) for Sr<sub>12</sub>Li<sub>24</sub>Si<sub>24</sub>N<sub>48</sub> from FPMD at 1000 K.

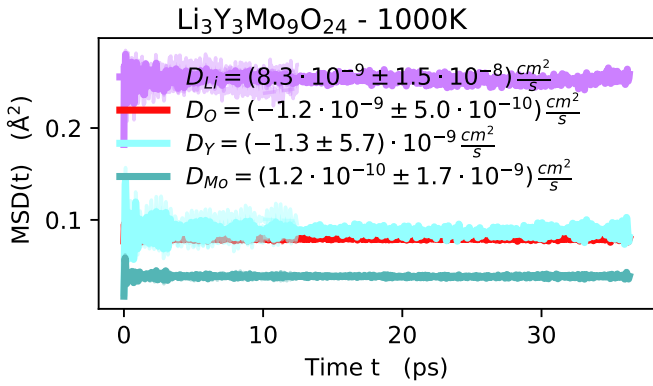


**Fig. S68** MSD(t) for Li<sub>3</sub>Y<sub>3</sub>Mo<sub>9</sub>O<sub>24</sub> from FPMD at 1000 K.

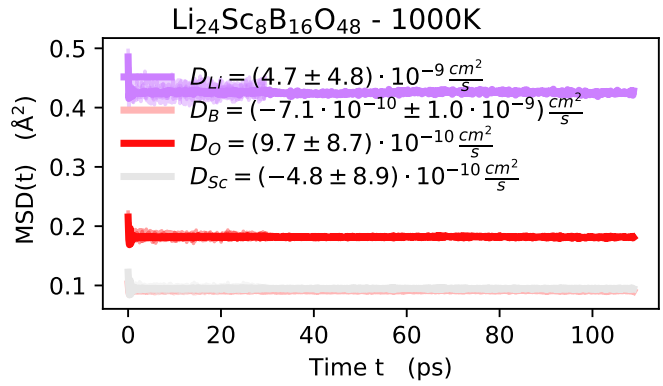


**Fig. S71** MSD(t) for Li<sub>24</sub>Sc<sub>8</sub>B<sub>16</sub>O<sub>48</sub> from FPMD at 1000 K.

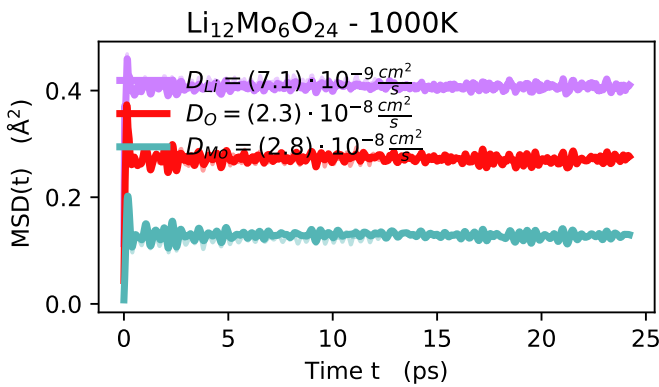


**Fig. S69** MSD(t) for Li<sub>12</sub>Mo<sub>6</sub>O<sub>24</sub> from FPMD at 1000 K.

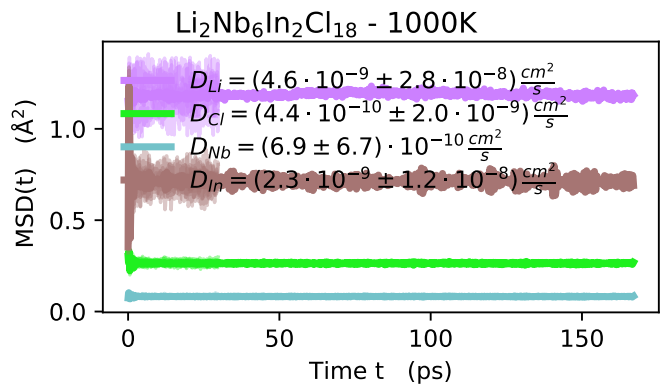


**Fig. S72** MSD(t) for Li<sub>2</sub>Nb<sub>6</sub>In<sub>2</sub>Cl<sub>18</sub> from FPMD at 1000 K.

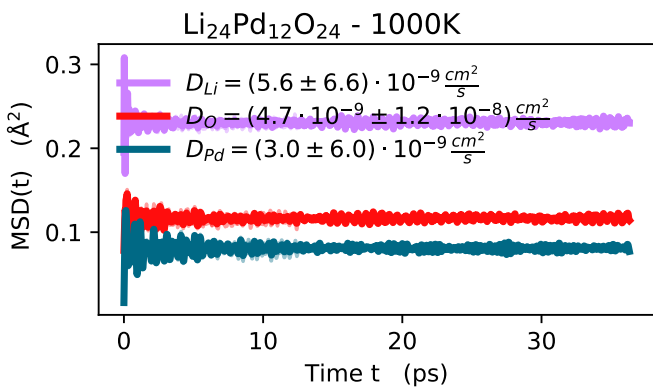


**Fig. S70** MSD(t) for Li<sub>24</sub>Pd<sub>12</sub>O<sub>24</sub> from FPMD at 1000 K.

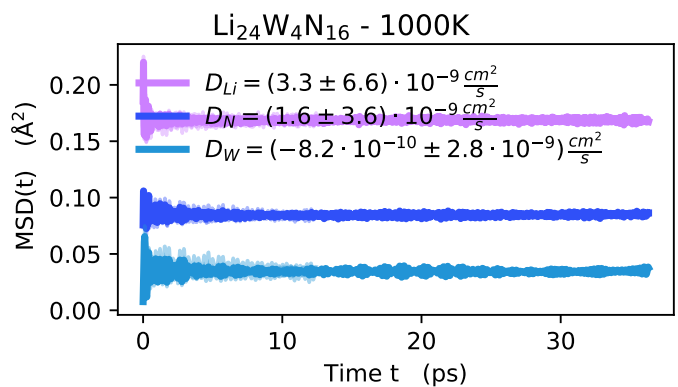


**Fig. S73** MSD(t) for Li<sub>24</sub>W<sub>4</sub>N<sub>16</sub> from FPMD at 1000 K.

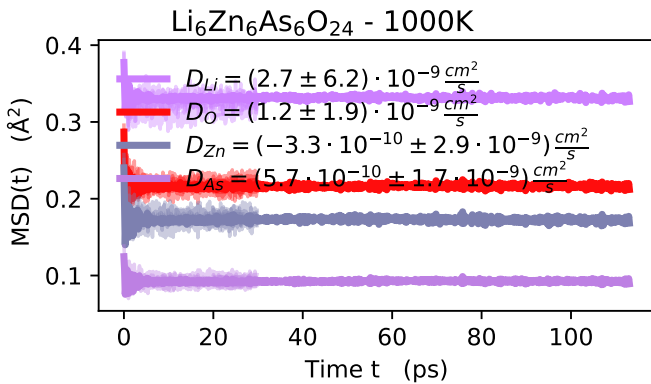


Fig. S74 MSD(t) for Li<sub>6</sub>Zn<sub>6</sub>As<sub>6</sub>O<sub>24</sub> from FPMD at 1000 K.

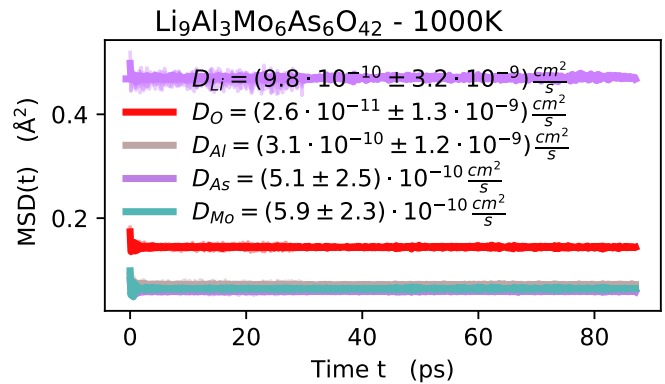


Fig. S77 MSD(t) for Li<sub>9</sub>Al<sub>3</sub>Mo<sub>6</sub>As<sub>6</sub>O<sub>42</sub> from FPMD at 1000 K.

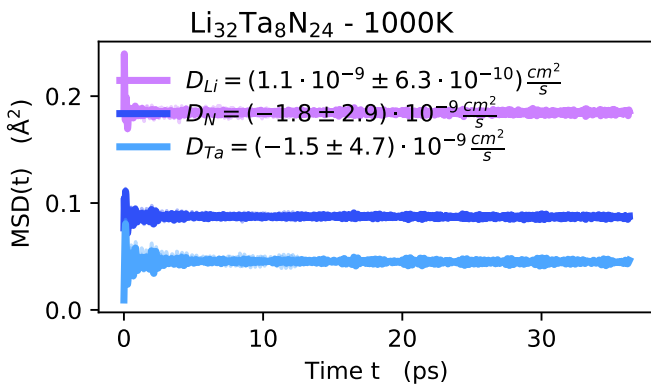


Fig. S75 MSD(t) for Li<sub>32</sub>Ta<sub>8</sub>N<sub>24</sub> from FPMD at 1000 K.

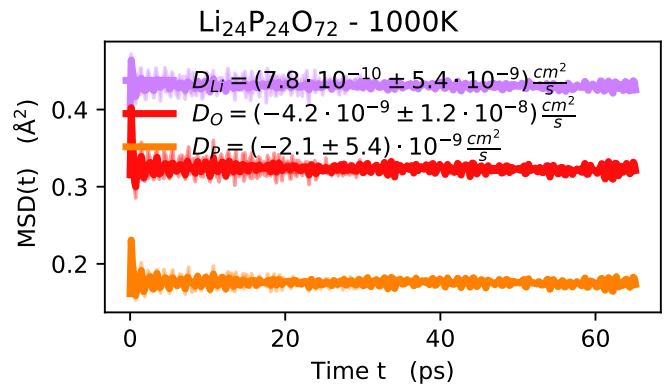


Fig. S78 MSD(t) for Li<sub>24</sub>P<sub>24</sub>O<sub>72</sub> from FPMD at 1000 K.

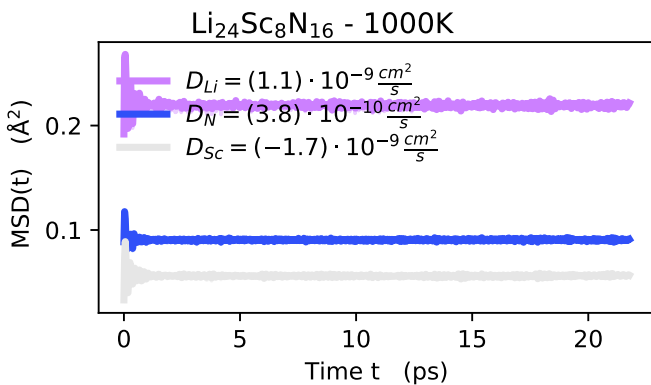


Fig. S76 MSD(t) for Li<sub>24</sub>Sc<sub>8</sub>N<sub>16</sub> from FPMD at 1000 K.

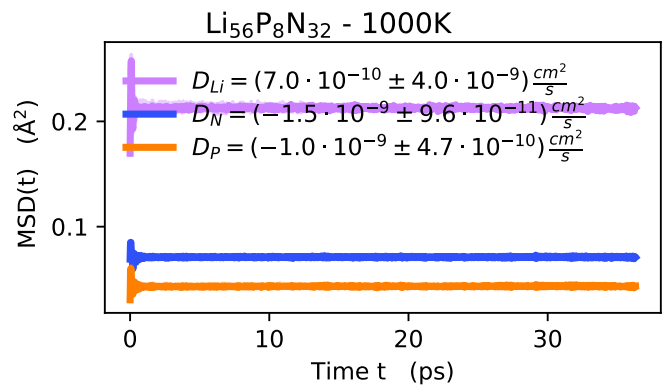


Fig. S79 MSD(t) for Li<sub>56</sub>P<sub>8</sub>N<sub>32</sub> from FPMD at 1000 K.

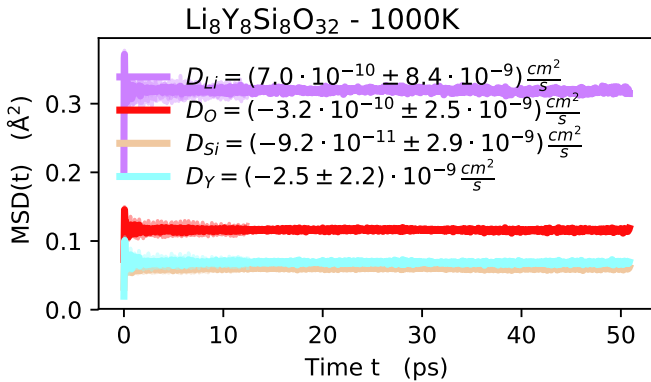


Fig. S80 MSD(t) for Li<sub>8</sub>Y<sub>8</sub>Si<sub>8</sub>O<sub>32</sub> from FPMD at 1000 K.

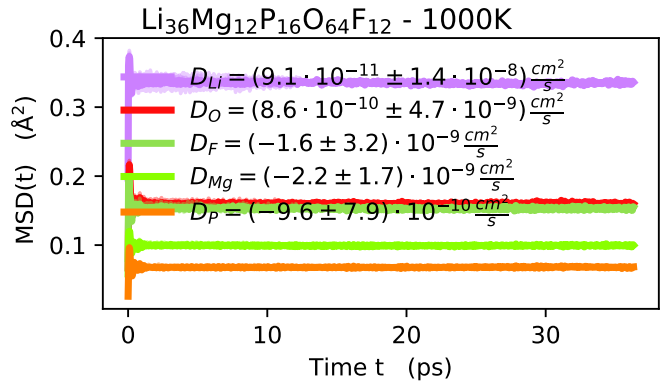


Fig. S83 MSD(t) for Li<sub>36</sub>Mg<sub>12</sub>P<sub>16</sub>O<sub>64</sub>F<sub>12</sub> from FPMD at 1000 K.

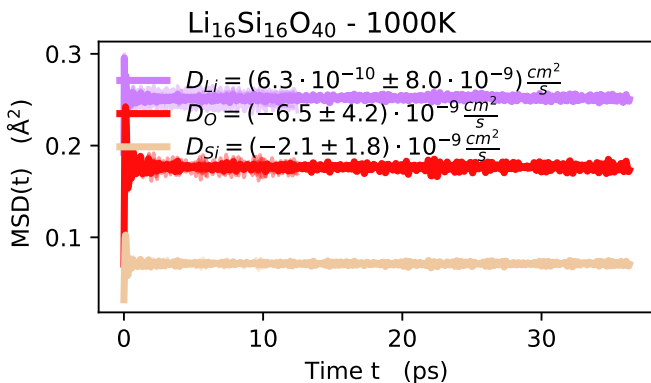


Fig. S81 MSD(t) for Li<sub>16</sub>Si<sub>16</sub>O<sub>40</sub> from FPMD at 1000 K.

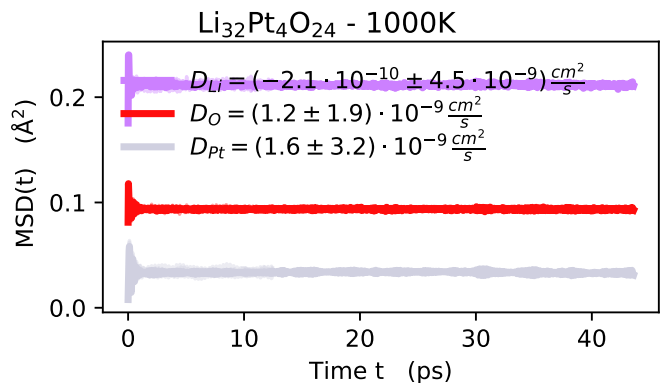


Fig. S84 MSD(t) for Li<sub>32</sub>Pt<sub>4</sub>O<sub>24</sub> from FPMD at 1000 K.

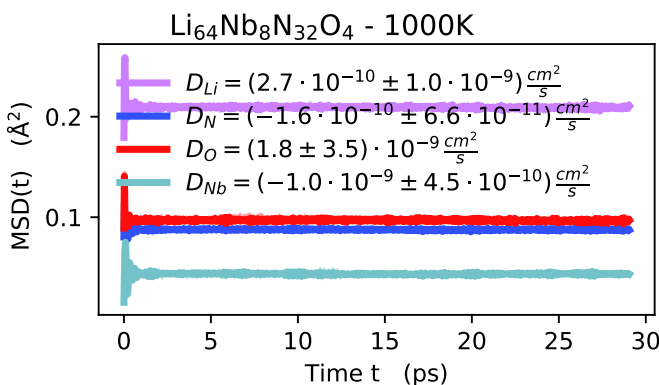


Fig. S82 MSD(t) for Li<sub>64</sub>Nb<sub>8</sub>N<sub>32</sub>O<sub>4</sub> from FPMD at 1000 K.

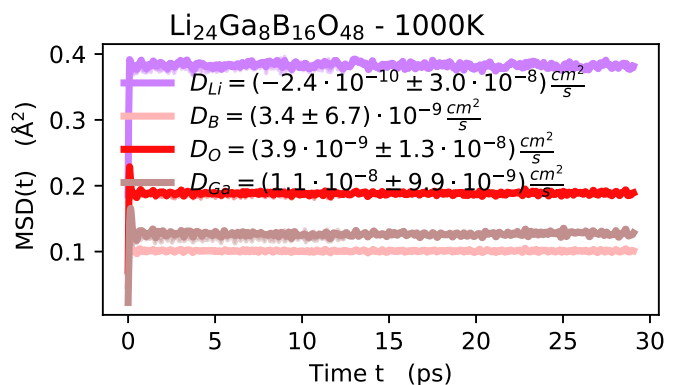
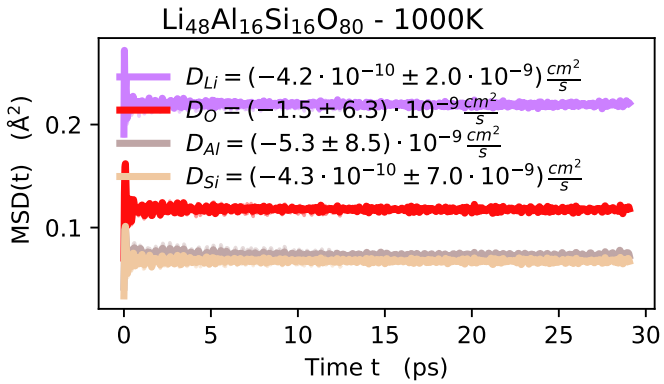
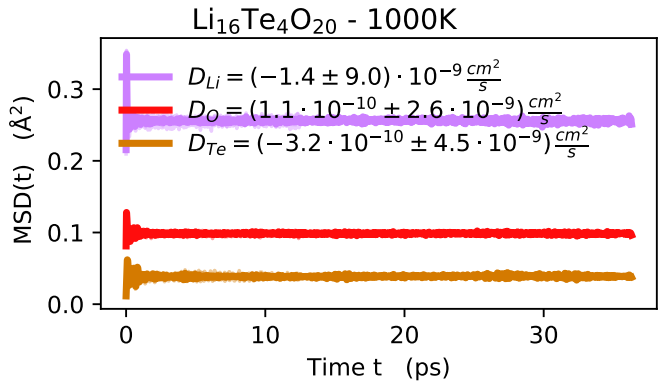


Fig. S85 MSD(t) for Li<sub>24</sub>Ga<sub>8</sub>B<sub>16</sub>O<sub>48</sub> from FPMD at 1000 K.



**Fig. S86** MSD(t) for Li<sub>48</sub>Al<sub>16</sub>Si<sub>16</sub>O<sub>80</sub> from FPMD at 1000 K.



**Fig. S89** MSD(t) for Li<sub>16</sub>Te<sub>4</sub>O<sub>20</sub> from FPMD at 1000 K.

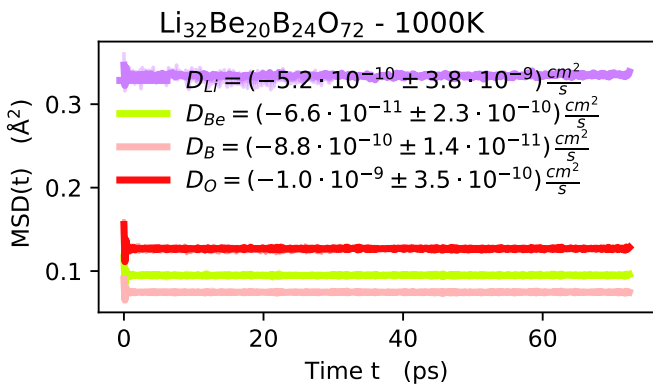


**Fig. S87** MSD(t) for Li<sub>32</sub>Be<sub>20</sub>B<sub>24</sub>O<sub>72</sub> from FPMD at 1000 K.

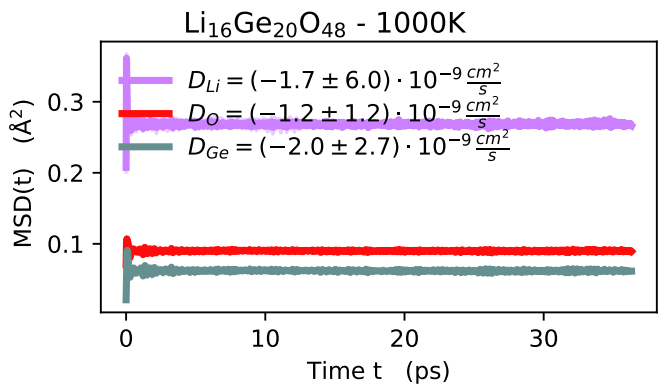


**Fig. S90** MSD(t) for Li<sub>16</sub>Ge<sub>20</sub>O<sub>48</sub> from FPMD at 1000 K.

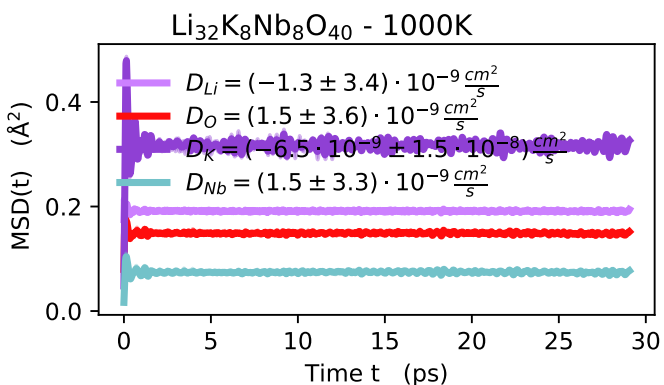


**Fig. S88** MSD(t) for Li<sub>32</sub>K<sub>8</sub>Nb<sub>8</sub>O<sub>40</sub> from FPMD at 1000 K.

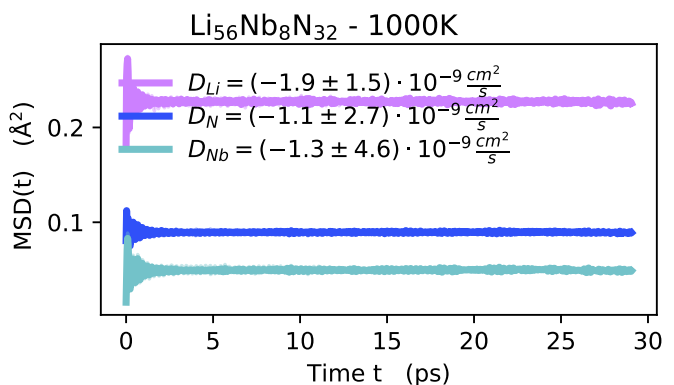


**Fig. S91** MSD(t) for Li<sub>56</sub>Nb<sub>8</sub>N<sub>32</sub> from FPMD at 1000 K.

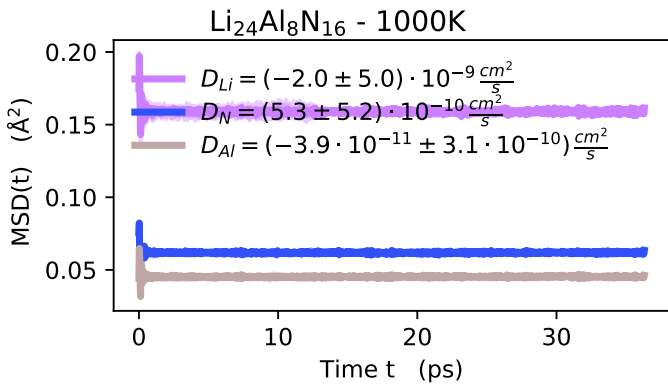


Fig. S92 MSD(t) for Li<sub>24</sub>Al<sub>8</sub>N<sub>16</sub> from FPMD at 1000 K.

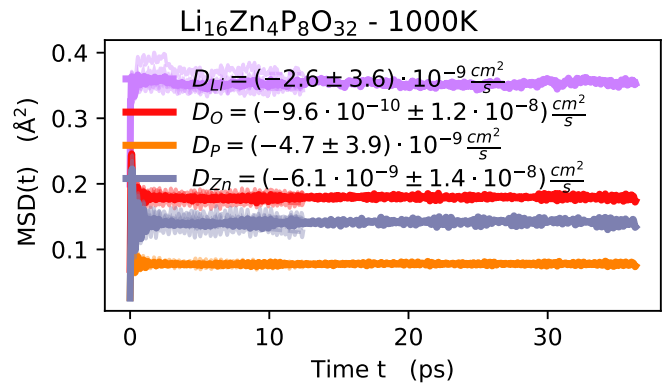


Fig. S95 MSD(t) for Li<sub>16</sub>Zn<sub>4</sub>P<sub>8</sub>O<sub>32</sub> from FPMD at 1000 K.

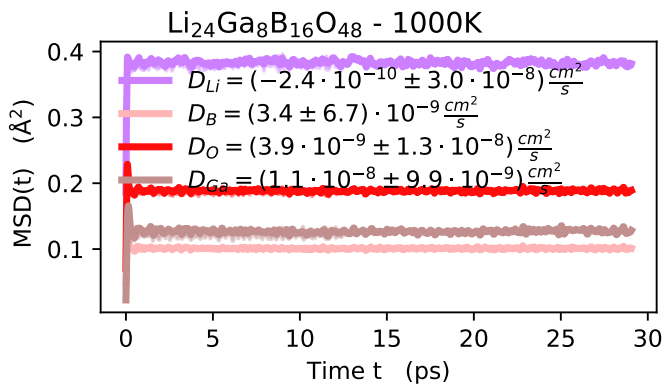


Fig. S93 MSD(t) for Li<sub>24</sub>Ga<sub>8</sub>B<sub>16</sub>O<sub>48</sub> from FPMD at 1000 K.

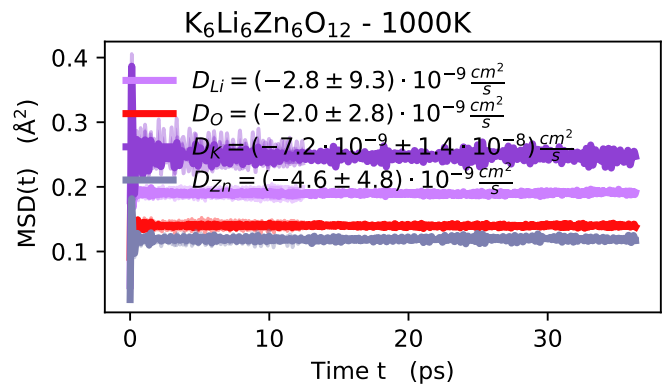


Fig. S96 MSD(t) for K<sub>6</sub>Li<sub>6</sub>Zn<sub>6</sub>O<sub>12</sub> from FPMD at 1000 K.

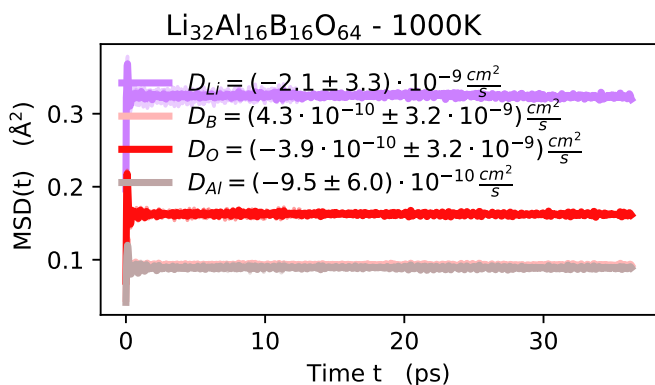


Fig. S94 MSD(t) for Li<sub>32</sub>Al<sub>16</sub>B<sub>16</sub>O<sub>64</sub> from FPMD at 1000 K.

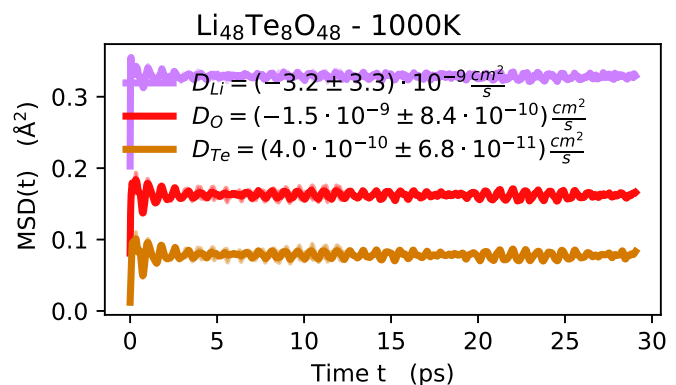
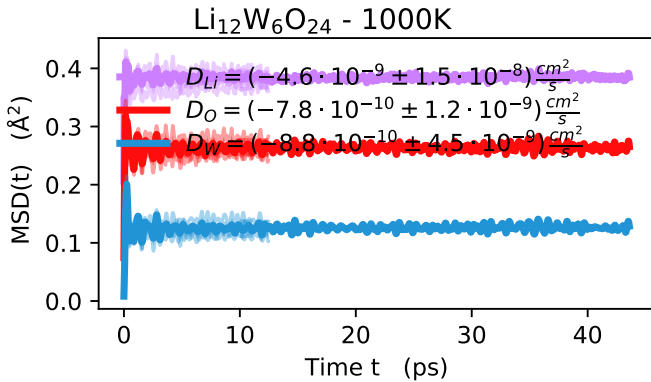
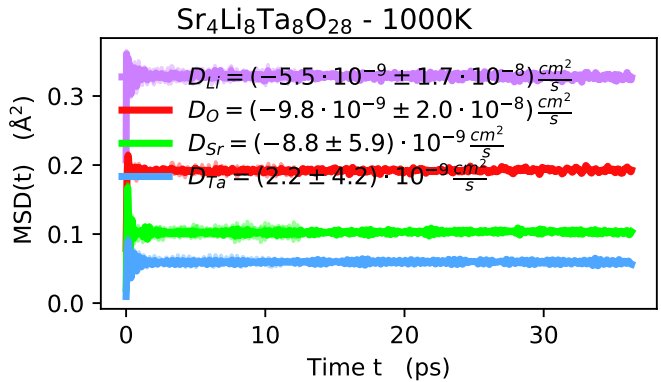


Fig. S97 MSD(t) for Li<sub>48</sub>Te<sub>8</sub>O<sub>48</sub> from FPMD at 1000 K.



**Fig. S98** MSD(t) for Li<sub>12</sub>W<sub>6</sub>O<sub>24</sub> from FPMD at 1000 K.



**Fig. S101** MSD(t) for Sr<sub>4</sub>Li<sub>8</sub>Ta<sub>8</sub>O<sub>28</sub> from FPMD at 1000 K.

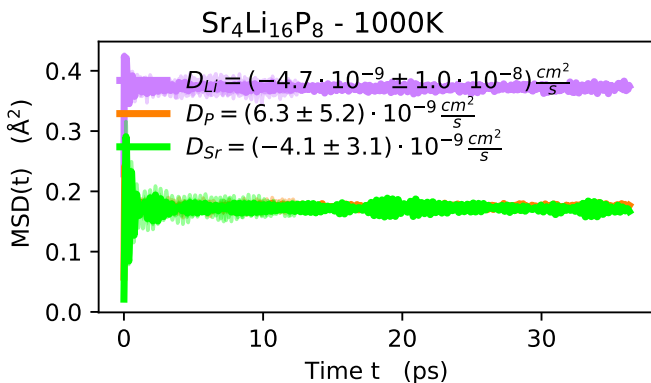


**Fig. S99** MSD(t) for Sr<sub>4</sub>Li<sub>16</sub>P<sub>8</sub> from FPMD at 1000 K.

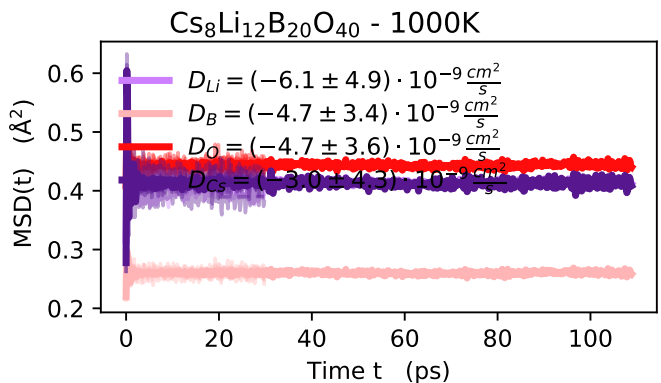


**Fig. S102** MSD(t) for Cs<sub>8</sub>Li<sub>12</sub>B<sub>20</sub>O<sub>40</sub> from FPMD at 1000 K.

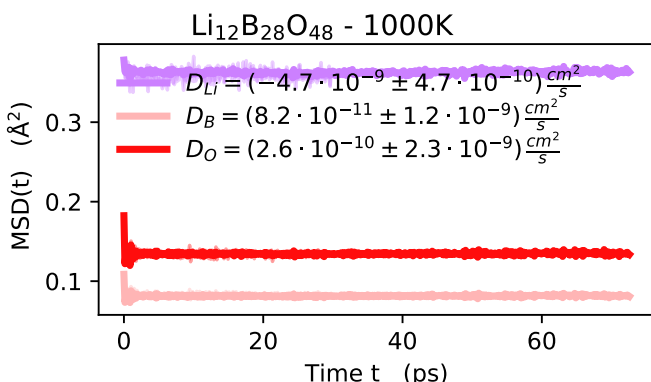


**Fig. S100** MSD(t) for Li<sub>12</sub>B<sub>28</sub>O<sub>48</sub> from FPMD at 1000 K.

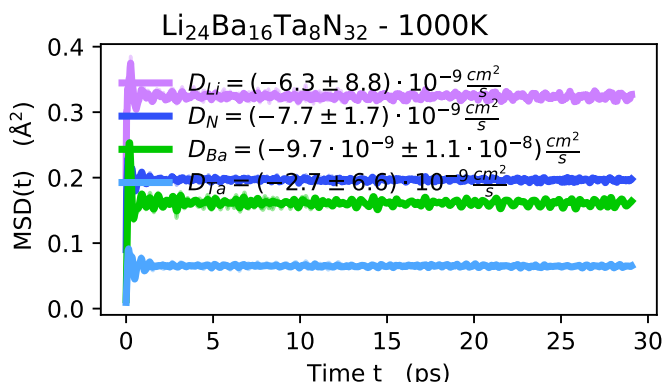


**Fig. S103** MSD(t) for Li<sub>24</sub>Ba<sub>16</sub>Ta<sub>8</sub>N<sub>32</sub> from FPMD at 1000 K.

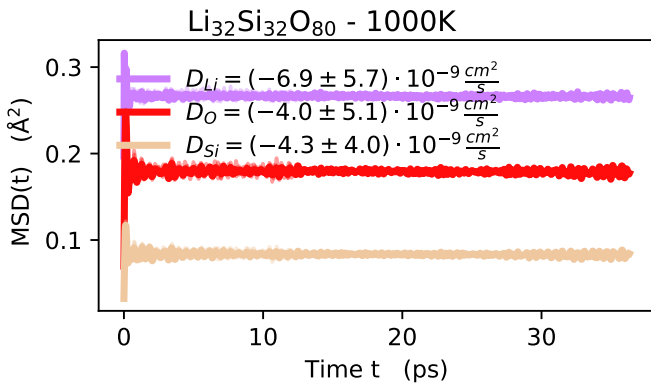


Fig. S104 MSD(t) for Li<sub>32</sub>Si<sub>32</sub>O<sub>80</sub> from FPMD at 1000 K.

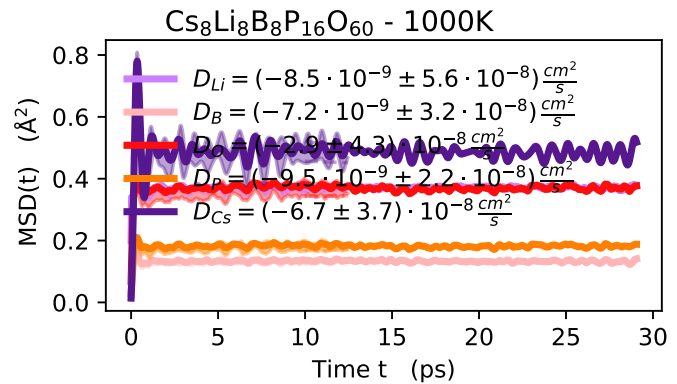


Fig. S107 MSD(t) for Cs<sub>8</sub>Li<sub>8</sub>B<sub>8</sub>P<sub>16</sub>O<sub>60</sub> from FPMD at 1000 K.

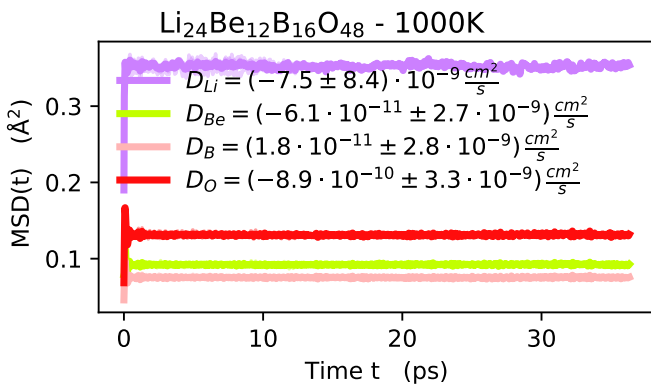


Fig. S105 MSD(t) for Li<sub>24</sub>Be<sub>12</sub>B<sub>16</sub>O<sub>48</sub> from FPMD at 1000 K.

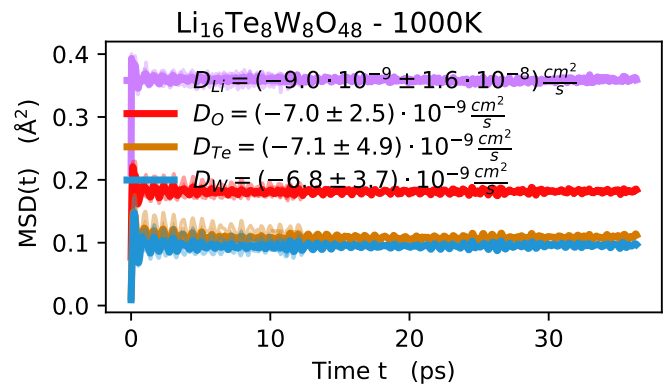


Fig. S108 MSD(t) for Li<sub>16</sub>Te<sub>8</sub>W<sub>8</sub>O<sub>48</sub> from FPMD at 1000 K.

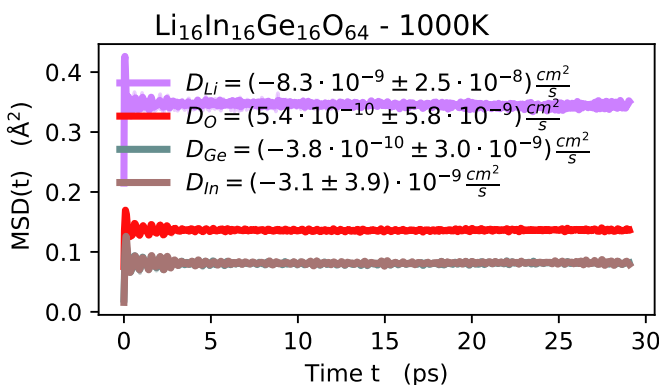


Fig. S106 MSD(t) for Li<sub>16</sub>In<sub>16</sub>Ge<sub>16</sub>O<sub>64</sub> from FPMD at 1000 K.

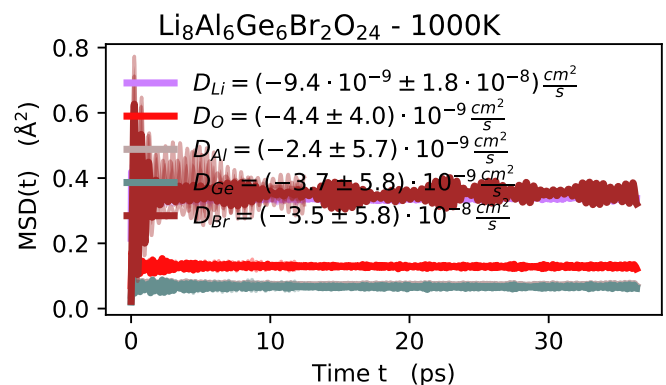


Fig. S109 MSD(t) for Li<sub>8</sub>Al<sub>6</sub>Ge<sub>6</sub>Br<sub>2</sub>O<sub>24</sub> from FPMD at 1000 K.

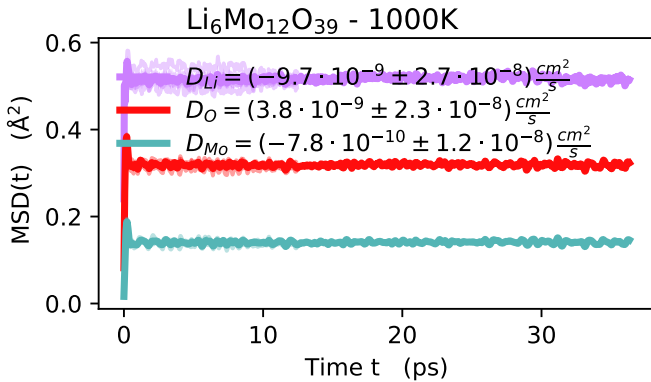


Fig. S110 MSD(t) for Li<sub>6</sub>Mo<sub>12</sub>O<sub>39</sub> from FPMD at 1000 K.

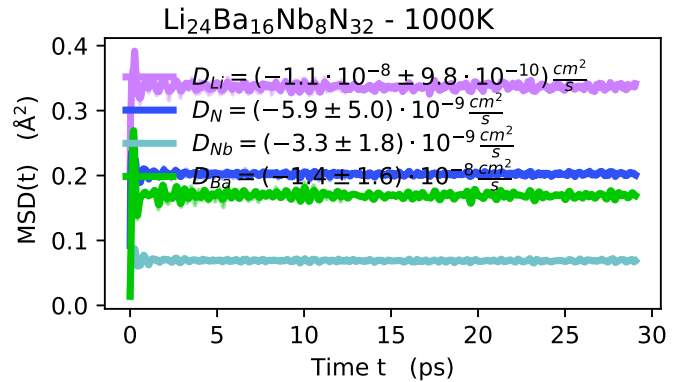


Fig. S113 MSD(t) for Li<sub>24</sub>Ba<sub>16</sub>Nb<sub>8</sub>N<sub>32</sub> from FPMD at 1000 K.

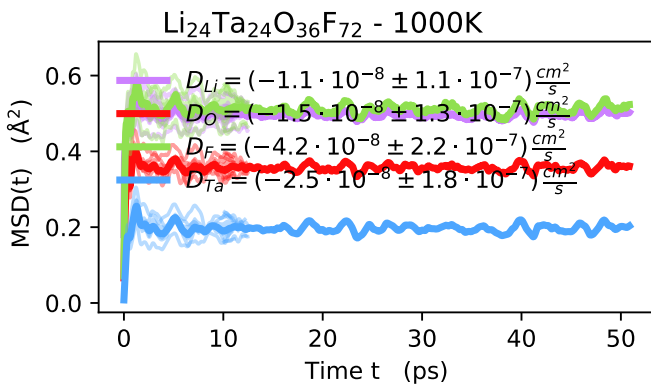


Fig. S111 MSD(t) for Li<sub>24</sub>Ta<sub>24</sub>O<sub>36</sub>F<sub>72</sub> from FPMD at 1000 K.

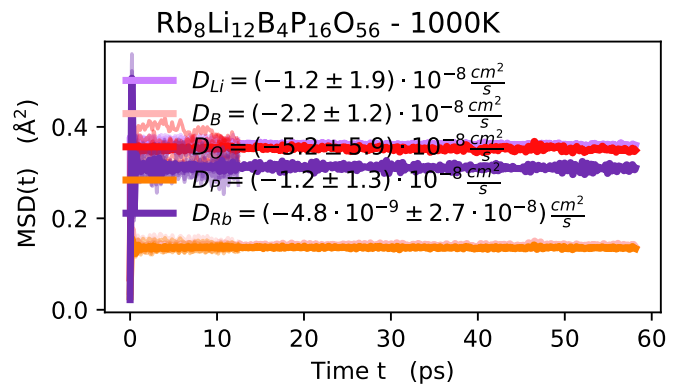


Fig. S114 MSD(t) for Rb<sub>8</sub>Li<sub>12</sub>B<sub>4</sub>P<sub>16</sub>O<sub>56</sub> from FPMD at 1000 K.

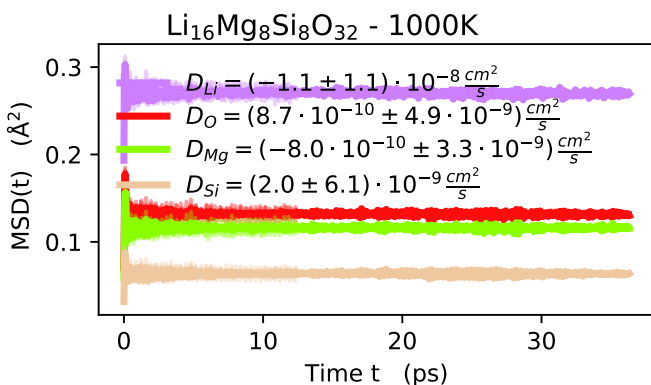


Fig. S112 MSD(t) for Li<sub>16</sub>Mg<sub>8</sub>Si<sub>8</sub>O<sub>32</sub> from FPMD at 1000 K.

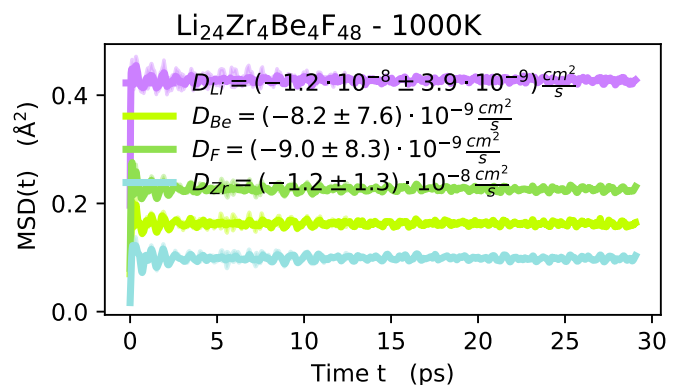


Fig. S115 MSD(t) for Li<sub>24</sub>Zr<sub>4</sub>Be<sub>4</sub>F<sub>48</sub> from FPMD at 1000 K.

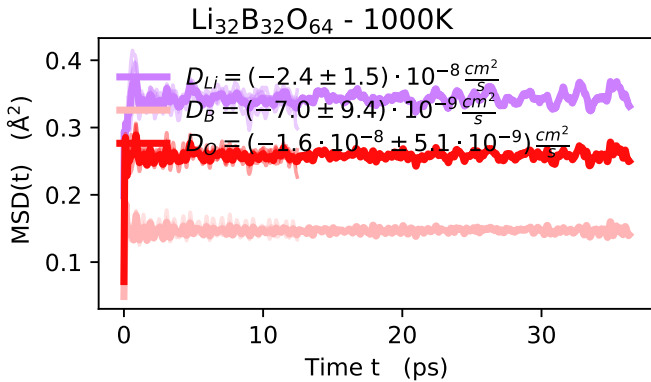


Fig. S116 MSD(t) for Li<sub>32</sub>B<sub>32</sub>O<sub>64</sub> from FPMD at 1000 K.

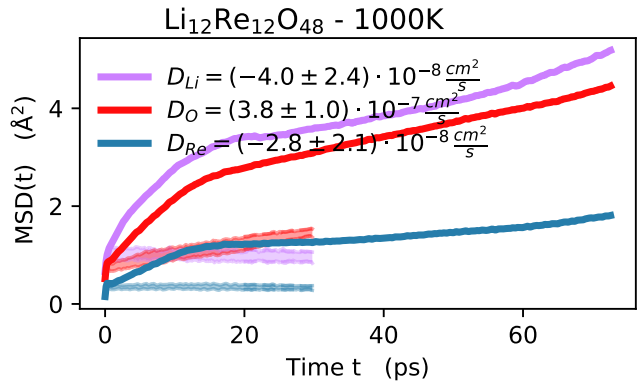


Fig. S119 MSD(t) for Li<sub>12</sub>Re<sub>12</sub>O<sub>48</sub> from FPMD at 1000 K.

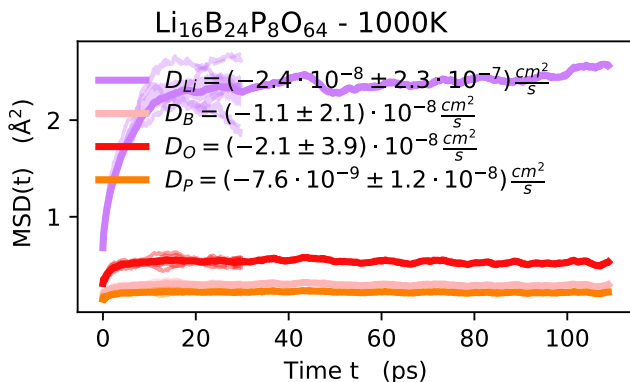


Fig. S117 MSD(t) for Li<sub>16</sub>B<sub>24</sub>P<sub>8</sub>O<sub>64</sub> from FPMD at 1000 K.

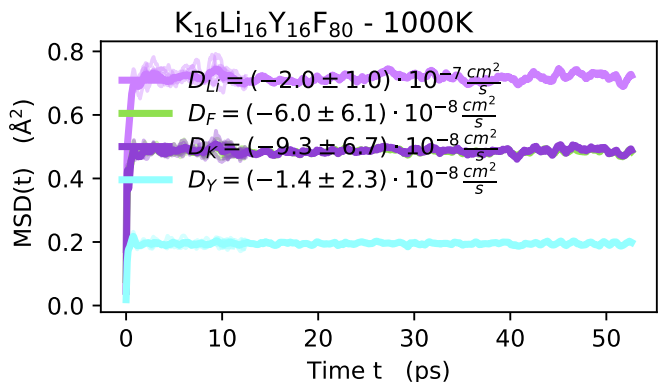


Fig. S120 MSD(t) for K<sub>16</sub>Li<sub>16</sub>Y<sub>16</sub>F<sub>80</sub> from FPMD at 1000 K.

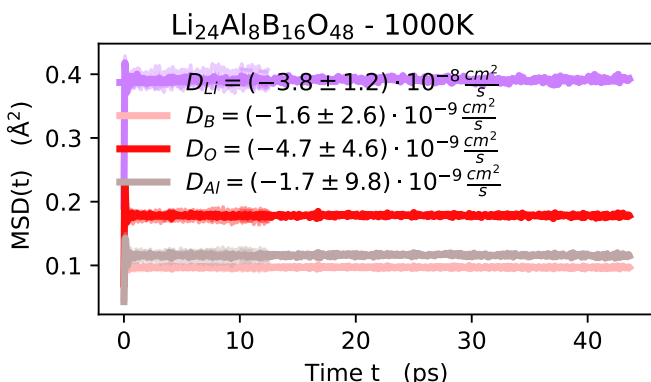


Fig. S118 MSD(t) for Li<sub>24</sub>Al<sub>8</sub>B<sub>16</sub>O<sub>48</sub> from FPMD at 1000 K.

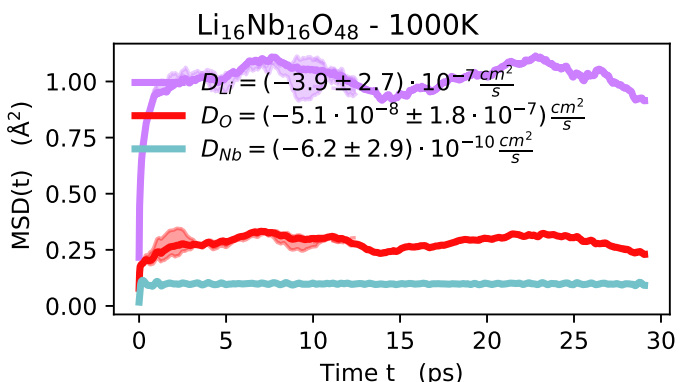


Fig. S121 MSD(t) for Li<sub>16</sub>Nb<sub>16</sub>O<sub>48</sub> from FPMD at 1000 K.

## 6 Structures diffusive in pinball model (group D)

**Table S5** Structures that are diffusive in the pinball model, but where we could not estimate the diffusion from FPMD ( group D)

Structure	DB	DB-id	Supercell	Volume change
$\text{Li}_4\text{Mo}_3\text{O}_8$	ICSD	84602	$\text{Li}_{24}\text{Mo}_{18}\text{O}_{48}$	5.8%
$\text{Li}_1\text{Ta}_1\text{Si}_1\text{O}_5$	COD	1534486	$\text{Li}_4\text{Ta}_4\text{Si}_4\text{O}_{20}$	3.1%
$\text{Li}_2\text{P}_2\text{Pd}_1\text{O}_7$	COD	1000333	$\text{Li}_8\text{P}_8\text{Pd}_4\text{O}_{28}$	14.9%
$\text{Na}_1\text{Li}_2\text{P}_1\text{O}_4$	COD	9004248	$\text{Na}_8\text{Li}_{16}\text{P}_8\text{O}_{32}$	3.9%
$\text{Ba}_1\text{Na}_1\text{Li}_3\text{B}_6\text{O}_{12}$	ICSD	423774	$\text{Ba}_2\text{Na}_2\text{Li}_6\text{B}_{12}\text{O}_{24}$	2.9%
$\text{Na}_1\text{Li}_1\text{B}_4\text{O}_7$	ICSD	416956	$\text{Na}_4\text{Li}_4\text{B}_{16}\text{O}_{28}$	4.2%
$\text{Na}_1\text{Li}_2\text{B}_1\text{O}_3$	COD	1511223	$\text{Na}_{16}\text{Li}_{32}\text{B}_{16}\text{O}_{48}$	2.8%
$\text{Li}_1\text{Au}_1\text{S}_4\text{O}_{14}$	COD	4326716	$\text{Li}_4\text{Au}_4\text{S}_{16}\text{O}_{56}$	22.1%
$\text{Li}_{10}\text{B}_{14}\text{Cl}_2\text{O}_{25}$	COD	1530960	$\text{Li}_{10}\text{B}_{14}\text{Cl}_2\text{O}_{25}$	1.8%
$\text{Li}_1\text{Au}_1\text{I}_4$	COD	1510187	$\text{Li}_8\text{Au}_8\text{I}_{32}$	8.4%
$\text{Li}_5\text{La}_3\text{Nb}_2\text{O}_{12}$	ICSD	68251	$\text{Li}_{20}\text{La}_{12}\text{Nb}_8\text{O}_{48}$	2.4%
$\text{Li}_1\text{Zr}_2\text{As}_3\text{O}_{12}$	ICSD	190656	$\text{Li}_2\text{Zr}_4\text{As}_6\text{O}_{24}$	4.0%
$\text{Li}_1\text{Al}_1\text{Ge}_1\text{O}_5$	COD	1526845	$\text{Li}_8\text{Al}_8\text{Ge}_8\text{O}_{40}$	-6.3%
$\text{Li}_3\text{Sc}_1\text{F}_6$	COD	1535801	$\text{Li}_{18}\text{Sc}_6\text{F}_{36}$	4.0%
$\text{Li}_1\text{Nb}_3\text{Cl}_8$	ICSD	50232	$\text{Li}_4\text{Nb}_{12}\text{Cl}_{32}$	5.8%